Until September 2016, a 1990 draft was on the web site, with Figures in a separate file. This final, 1992 version has the Figures attached.

RE-ESTIMATING THE NOBLE GAS RELEASES FROM THE THREE MILE ISLAND ACCIDENT

Jan Beyea and John DeCicco*

National Audubon Society
950 Third Avenue
New York, NY 10022

October 1, 1992

Prepared for the
Three Mile Island Public Health Fund
1622 Locust Street
Philadelphia, PA 19103

*John DeCicco
ACEEE
1001 Connecticut Avenue, N.W.
Suite 801
Washington, D.C. 20036

ABSTRACT

Radiation dosimetry data for Three Mile Island are re-analyzed in order to obtain revised estimates of the noble gas releases and attendant population doses during the March 1979 accident. A statistical treatment, distinctive to the present analysis, of the field dosimetry data and their uncertainties, enables the extraction from sparse data of maximal information about the release rates and projected doses. The release pattern giving a best fit to the dosimeter data yields an estimate of 820 (-310 +220) PBq for the noble gas activity released over the first day and a half of the accident. The corresponding estimate of population dose is 37 (-9 +7) person-Sv within 50 miles of the plant. The major uncertainties reflected in these estimates are due to the unknown venting temperature of the release (which affects the plume rise), possible errors in the wind direction measurements, less than fully resolved release timing, and calibration errors for TLD response. These uncertainties are more precisely stated as well as greatly narrowed in comparison with previous assessments of the accident.

The meteorological dispersion and dosimetry model applied for this analysis includes refinements--for plume rise, changing wind direction, full terrain effects, plant-site building and cooling tower effects, finite cloud dose integration, and ground correction--which had not been collectively incorporated in previous analyses of the accident. A new method is developed to enable the estimation of time-dependent rates of radioactivity release by utilizing dose measurements accumulated through time by thermoluminescent dosimeters distributed in the area surrounding the plant. The meteorological model is used to project the possible doses to locations in the vicinity of the plant. A constrained, weighted, multivariate regression procedure is used to estimate the time pattern of releases that best fits the data from all of the dosimeters. The meteorological model is then used to project doses to surrounding populations on the basis of the estimated release rates.

Sensitivity analyses are performed to determine the effects of the assumptions regarding plume rise, wind direction, energy dependence of the dosimeters. A probabilistic analysis is used to quantify the uncertainty due to inability to fully resolve to timing of the releases. The results are compared to previous analyses of the accident, including dose assessments based on the use of the area radiation monitor data. It was found that doses based on fits to the dosimeters correlate well with doses based on the area monitor data, thereby serving to validate the use of the latter in the exposure model for a concurrent study of cancer epidemiology in the vicinity of Three Mile Island.

Table of Contents

List of Tables

List of Figures

In this draft, all figures are located at the end of the document.

List of Figures (continued)

Re-estimating *the* Noble Gas Releases from the Three Mile Island Accident

SUMMARY

One of the major concerns following the 1979 accident at the Three Mile Island nuclear power plant was the release of radioactive gases blown by the wind over the surrounding populated area. The gases which escaped the reactor in largest quantities were xenon and krypton, which are known as noble gases. Because of inadequate monitoring, it was uncertain how much radioactivity escaped the plant and how large a radiation dose was received by people in the affected area. This report gives a re-assessment of the noble gas releases and resultant radiation doses from the accident. The underlying research was carried out for the Three Mile Island Public Health Fund.

The background of this study is as follows: Although studies by the government and others concluded that the radiation doses from Three Mile Island were too small to have a significant health effect, the adequacy of those studies was questioned during legal proceedings regarding the accident. One result of the litigation was the establishment in 1981 of the Three Mile Island Public Health Fund. The purpose of the Fund includes investigating possible detrimental consequences of the accident and carrying out other projects to improve the protection of public health in the area around Three Mile Island (TMI). The Fund commissioned an independent review of the published studies of the radiation doses from the TMI accident, which resulted in the *Review of Dose Assessments* report (Beyea 1984). This review was followed by the *TMI Dosimetry Workshop* (November 1984, proceedings edited by Goldberg 1985), which brought together the principal investigators of previous TMI studies, critics, and the independent scientific advisory board of the Public Health Fund. The Fund concluded that the earlier studies of the accident were too ambiguous to be regarded as final. It was recommended that the published results be re-examined along with any unpublished data that had bearing on the doses assessment and that a more refined statistical analysis be used to obtain release and dose estimates of greater accuracy.

2.1 The amount of radioactivity released

The noble gases which escaped the reactor contained isotopes of xenon and krypton. Noble gases are chemically inert and are not metabolized or accumulated in plants, animals, or humans. Some isotopes of these gases emit radiation which can be harmful if a person inhales them or is close to an airborne cloud of the gases. (The present study does not examine radioactive iodine, a possible release

from nuclear accidents which is metabolized. Radioiodine releases from TMI appear to have been very small and are addressed in a separate study.) The quantity and timing of a radioactive release from a nuclear accident is called a source term. A source term is measured in curies, a unit of radioactivity equal to 37 billion nuclear disintegrations per second. Previous studies of the TMI accident reported noble gas source term estimates ranging from 0.6 to 30 million curies, depending on the data and assumptions used in making the estimate. The present study (using the methods described below) has narrowed the uncertainty, obtaining a mean estimate for the noble gas released of 22 million curies, with an uncertainty ranging from 14 to 28 million curies.

2.2 Doses to the population around TMI

The health effects of radiation from noble gases is determined by the gamma ray energy which penetrates a person's body and its likely impact on human tissues. This is known as the whole-body (as opposed to a specific organ) dose equivalent, measured in units called rem, or for the relatively low doses from an accident such as TMI, millirem (1/1000 rem). Gamma radiation doses are considered "low" if they amount to less than 20 rem for an individual. The dose collectively received by a population is termed the population dose and is measured in person-rem. For example, if a population of 1000 individuals receives an average dose equivalent of 1 millirem each, their population dose is I person-rem. The risk of health effects from radiation, such as increased cancer mortality in the population, depends on the population dose; it is estimated by using risk factors extrapolated from studies of past radiation exposures (such as the atomic bombings of Japan). For the TMI accident, dose assessments were made for the population of approximately 2 million people living within 50 miles of the power plant. Previous studies reported population doses ranging from 300 to 63,000 person-rem due to the noble gas releases from TMI. The present study has reduced this uncertainty, obtaining a mean estimate of 3700 person-rem, with an uncertainty range of from 2900 to 4400 person-rem.

2.3 Shortcomings of past assessments of the accident

The divergence among the earlier estimates of the source term and the population dose resulted from the different assumptions and methods used by different analysts. Some assumed the noble gas release was proportional to readings on indirect monitors in the plant. These "area radiation monitor" readings were converted to a source term using a scale factor obtained either from the single monitor capable of directly measuring the releases, which went off-scale early on, or from a few "grab" samples

taken at the stack later during the release. Other approaches to estimating the doses were based on extrapolations from the standard field radiation monitoring network surrounding the power plant. These instruments are thermoluminescent dosimeters (TLDs), which were situated at 8 locations on the plant grounds (on-site) and another 12 locations (off-site), sparsely scattered up to 13 miles from the plant. A TLD does measure the dose at the site where it is located. However, different analysts judged that only some of readings should be used, uncertainty resulted from the calibrations and corrections needed, and in any case, the coverage of the surrounding populated area was so sparse that added uncertainties were introduced during the process of extrapolation. Most analysts used a meteorological model to estimate the dose received in locations around the plant. Some took an approach which combined elements of the above methods. However, no attempt was made to reconcile the various approaches in a systematic manner, leaving it difficult to judge what the more critical assumptions were and how the divergent estimates could be understood.

2.4 Methodology used for this study

The work reported here examined all available data, including information not used in earlier dose assessments, and applied a consistent methodology to obtain best estimates of the noble gas source term and resultant population doses from the TMI accident. Four major aspects of this dose assessment methodology are: (1) the meteorological dispersion model, which determines where and when the released noble gases were blown over the area surrounding the plant; (2) radiation dosimetry model, which determines the dose received by persons on the ground below the dispersed gases; (3) analysis of the TLD data, including information about the exact locations and collection times of the dosimeters and possible errors and corrections needed in their readings; (4) the statistical method for estimating the releases based on the TLD data and allowing incorporation of the area radiation monitor data. Refinements were made in all four aspects of the dose assessment. While some of the refinements may have been used in previous studies, this is the first that incorporates all of them in a comprehensive fashion.

The analysis was performed for a "base case," using a set of parameters determined to best represent the conditions that occurred during the accident. The most significant parameter in our base case that differs from earlier assessments is the division of the release period into several time segments, estimating a separate release rate for each segment. This time-varying representation of the source term revealed a distinct peak in the noble gas releases, late in the evening of the first day of the accident, during which a larger quantity of gas escaped than previously estimated. Another significant parameter

is the value of "plume rise," generally chosen to be zero in earlier studies. A plume lofted above ground (due to its warmth) must contain more curies than a ground-level release to give the same radiation doses to detectors. Other base case conditions, detailed in the report, have a less critical bearing on the results. The base case results are a source term of 22 million curies and an attendant population dose of 3700 person-rem within 50 miles of TMI.

A comprehensive set of sensitivity analyses was carried to determine the uncertainty of our estimates and to examine how the results would be affected by different assumptions about the conditions during the accident. In all, fourteen variations of the modeling assumptions were considered. These were the base case, as described above, lower and higher plume rise, westward and eastward wind shifts, energy correction of TLD response, a higher value of the most uncertain TLD reading, changes in the TLD data weighting, straight line plume with and without plume rise, and three cases based on fits using the area monitor data. In addition, since there are insufficient data to fully resolve the timing of the releases, there is an added uncertainty not reflected in the sensitivity analyses. To estimate this uncertainty, releases at randomly assigned times were fit to the TLD data and we computed the standard deviations of the resulting estimates. These sensitivity analyses and randomized fits are the basis for our estimated uncertainty ranges of 14 to 28 million curies for the source term and 2900 to 4400 person-rem for the 50-mile population dose.

2.5 Implications of our results

Based on our re-assessment, the mean estimate of 3700 person-rem for the population within 50 miles of TMI implies an average dose of 1.8 millirem. This is about 3% of the 65 millirem average annual dose from background radiation in the TMI area. Many portions of the population received little or no dose from the accident; several thousand persons received doses as large as the background dose. The population dose resulting from TMI is therefore quite small. There is, however, no known safe level of radiation. The lifetime radiation risk factor published by the National Academy of Sciences is approximately 800 excess cancer deaths per million person-rem. Using this risk factor, our estimate implies 3 excess cancer deaths in the population of 2 million persons within 50 miles of TMI. Otherwise put, for an average member of this population, there is roughly a one in a million chance of cancer death over and above the one in five chance of cancer death that is typical in the United States.

The population dose assessment provided here indicates that the public health risk from the TMI accident is quite small. Our estimates are consistent with the conclusion that there would be no observable health effects in the general population around TMI, which was reached by government reports regarding the accident. The dose assessments suggest that finding cancers linked to the accident would be like finding a needle in a haystack, given that the estimated one in a million risk from the accident is a very small increment to the typical cancer risk of one in five. Nevertheless, there had been no scientific test as to whether or not cancers associated with such low radiation doses are observable. Therefore, in addition to this dose assessment project, the Three Mile Island Public Health Fund also commissioned a study of the cancer incidence in the vicinity of TMI.

The methods used here for estimating the doses in different parts of the population were also used in the TMI cancer Epidemiology Study. This involved making estimates of the doses for 65 separate populated areas within about 10 miles of the plant. (This approach is like looking for the "needle" by dividing the haystack into small bales and carefully sifting through each one.) Such a finely resolved method had not been previously applied to examine the possible health effects in the vicinity of a nuclear facility. An added objective of our study was to validate the dose estimates used for the cancer study against the more extensive data and sensitivity analyses carried out here. We found that the dose estimates for the cancer study correlated well with doses based on the modeling variations we tested, indicating that the results of the cancer study would hold up very well in spite of the uncertainties regarding the doses received by various portions of the population.

In summary, this re-assessment of the releases and doses from the Three Mile Island accident has shown that, while the amount of noble gas radioactivity that escaped the plant is somewhat larger than reported by the President's Commission on Three Mile Island, the resulting population doses are still estimated to be quite small, making it unlikely that health effects traceable to noble gas releases from the accident will be observed in the area around TMI. The uncertainty surrounding these results has been greatly narrowed, due to an extensive examination of the effects of assumptions affecting the results. The modeling techniques, statistical methods, and error analyses applied for this study provide a prototype of a comprehensive methodology that can be applied to other situations involving public exposure to excess radiation, particularly when monitoring data are limited.

Re-estimating the Noble Gas Releases from the Three Mile Island Accident

Jan Beyea and John M. DeCicco

1 INTRODUCTION

Although the 1979 accident at the Three Mile Island (TMI) nuclear power plant was studied extensively,[1] it had not been possible to unambiguously ascertain the amount and timing of the noble gas activity release. Indirect methods had to be used because the stack monitor went off scale early in the accident. Moreover, the thermoluminescent dosimeters (TLDs) in place during the accident were of insufficient number to fully characterize the release and resultant doses.

Several analysts obtained noble gas release estimates (source terms) by assuming that area monitors in the reactor auxiliary building, which were far enough away from the radioactivity to generally remain on scale, were proportional to the stack release. With this assumption, the absolute scale of the release could be obtained by calibrating the area monitors either against grab sample measurements taken in the exhaust stack or against TLD dose measurements. The most detailed source term estimate was obtained by adjusting the trends of the area radiation monitors to match nearby TLD readings when projected via a meteorological model (Pickard, Lowe, and Garrick 1979; Woodard and Potter 1979). However, the adjustments were made by using rough scale factors for different time periods of the release, rather than statistically estimated adjustment factors. Moreover, not all of the TLD data were considered when adjusting the area monitor trends. The resulting source term is therefore not entirely consistent with the doses indicated by the TLDs. Being the best available, however, this source term based on adjusted area monitor data has been used in several dose assessments, including an epidemiological study performed concurrently with the work reported here (Hatchet *al.* forthcoming).

[1] Rogovin (1979); Kemeny (1979); Pickard, Lowe, and Garrick (1979); Knight *et al.* (1981).

Various other methods have been used to estimate the releases from the TMI accident. A comprehensive review of the literature on TMI releases and doses has been given previously by one of the authors and will not be repeated here. By way of summary, the accident assessments reported to date give estimates of released activity ranging from 20 PBq (20×10^{15} Bq, 0.6×10^{6} Curies) to 1100 PBq (30 MCi). These studies did not, moreover, provide sensitivity analyses sufficient to evaluate their comparative accuracy or explain the reasons for the divergence of the estimates.

Corresponding to the range of source term estimates, there is a range of estimates for the resulting population dose. At issue is the whole-body gamma dose received by the population of approximately 2 million persons residing within 80 km (50 miles) of TMI. The published estimates range from 3 to 630 person-Sv (300 to 63,000 person-rem). The population dose reported by the President's Commission on the Accident at Three Mile Island was 20 person-Sv (2000 person-rem; Kemeny 1979). These estimates is are on the order of 1% to 10% of annual background radiation doses in the area, but were delivered in a few days rather than spread over a year. Also, previous studies (Rogovin 1979; Kemeny 1979; Pickard, Lowe, and Garrick 1979) also reported estimates of the maximum likely dose to individuals of not more than I mSv (100 mrem). Gur *et al.* (1983), who used source term estimates based on Pickard, Lowe, and Garrick (1979), and Pasciak *et al.* (1981) calculated the dose distribution pattern to individuals, both basing their results on sector-averaged doses and both limited to a 8 km (5 mile) radius from the plant. As for the source term estimates, there was insufficient sensitivity analysis reported to fully evaluate the dose estimates and to clarify the apparently wide range of values.

1.1 Objectives

The primary objective of the work reported here was to provide a re-assessment of the noble gas radioactivity releases from Three Mile Island using full statistical treatment of all available data regarding the releases and the resulting doses: This work was performed as a public charge

[2] See Beyea (1984), Tables 3 and A-3, for summaries of the published estimates and a review of the methods used to obtain them; further discussion is given in Goldberg (1984).

initiated by the Three Mile Island Public Health Fund[3] in order to address the uncertainties that remained in previous assessments of the TMI accident. As needed for this re-assessment, an implied objective has been to develop a methodology that allows one to vary explicitly the assumptions about accident conditions and data. A further goal has been to provide error analyses based on the known data and sensitivity analyses regarding the modeling assumptions so that the certainty of the resulting estimates can be more clearly stated. It is hoped that public interest is better served by reporting estimates with stated uncertainties rather than a collection of seemingly disparate point estimates.

An epidemiological study of cancer incidence around TMI is being performed concurrently and so another. goal of this work has been to validate the accident exposure model used for that investigation (Hatch *et* al. forthcoming). It has been concluded by many that the radiation releases from TMI were too small to result in detectable cancers (Kemeny 1979; Rogovin 1979). Nonetheless, when a survey conducted by area residents found an apparent cluster of cancer deaths, there was concern in the community that accident releases had been inadequately estimated (Aamodt and Aamodt 1984). In fact, dose assessment and epidemiological methods sufficient to test such hypotheses had not been demonstrated at the time of the accident and the subsequent governmental investigations. Our objective in this regard has been the refinement and validation of methods that provide an improvement over previously existing nuclear accident assessment techniques in terms of the geographic resolution of dose estimates. It is hoped that the present work will demonstrate analytic methods, both for dose assessment and in support of epidemiological studies, applicable to other occurrences of airborne radioactivity releases that might threaten public health.

[3] The Three Mile Island Public Health Fund was established in 1981 as a result of a legal settlement regarding the Three Mile Island accident. The purpose of the Fund is to investigate possible detrimental consequences of the accident, to improve radiation monitoring and emergency planning in the TMI area, to investigate the health effects of low level radiation, and to develop a program of public education on the operation of the TMI facility. The Fund is supervised by Judge Sylvia H. Rambo, U.S. Middle District of Pennsylvania, and administered by David Berger, Attorney at Law, Philadelphia, PA, chief counsel for the Fund.

1.2 Overview

The first major section of this paper describes an analytic framework which serves the dual purposes of release estimation and dose projection. The method entails meteorological dispersion modeling and least-squares estimation of the time-dependent radioactivity release using data on time-integrated doses measured at spatially distributed locations. Section 3 reports the analysis for a set of base case assumptions, describing in detail how the source term and population doses estimates were obtained using the described method. Section 4 presents the results of sensitivity analyses and discusses our estimates in the context of previous assessments of the TMI accident. The sensitivity of the release and dose estimates to the plume rise is shown to be a major contributor to the uncertainty of the results. The inability to fully resolve the timing of the release causes a further uncertainty, which is addressed by a probabilistic analysis to determine how source term and dose estimates are affected. Finally, section 5 compares our findings to those reported previously and summarizes the implications of the present work.

Further details are provided in the report-length version of this paper (Beyea and DeCicco 1990). Appendices in the report include details of the airborne radioactivity dispersion and exposure models, analysis of TLD data, dose pattern correlation analyses related to the validation of the TMI epidemiology study, tabulations of lengthier data sets, and details of the error analyses.

2 METHODOLOGY

The most general problem treated here is the estimation of the dose at collection of locations (termed receptors) in the vicinity of TMI due to gamma radiation from the radioactive noble gases released during the accident[4]. The receptors may be grid points within geographic blocks, such as the population groupings used in the concurrent epidemiology study (these blocks are shown in

[4] Note that this paper addresses only the whole-body gamma doses from noble gases released during the accident and dispersed by the wind over the area surrounding the plant. The method used here is not applicable for assessing doses such as thyroid doses from inhaled short-lived radioiodine or organ doses from long-lived radionuclides.

Figure 1). Available are data from area radiation monitors inside the plant, data from thermo-luminescent dosimeters (TLDs) in the vicinity of plant, and data on atmospheric conditions (wind and temperature) from the weather station at the plant. A Gaussian puff atmospheric dispersion algorithm is used to relate airborne releases from the plant to noble gas concentrations as a function of time in the vicinity of receptor points. A dosimetric algorithm is then used to calculate doses at the receptors. The doses to a population in a block are calculated by summing over the grid points in a block and the total population dose in a region is found by summing the product of population and dose over the blocks. The dispersion and dosimetric models were originally developed by one of the authors for nuclear accident assessment work at Princeton University (Beyea 1978, 1980). The core algorithms were tested as part of the International Exercise in Reactor Accident Consequence Modelling and were found to give results in the middle of the range of the various models tested (NEA 1983).

The regions considered for dose assessment are a 16 km (10 mile) radius from the TMI plant (population 160,000) and a 80 km (50 mile) radius (population 2 million), for comparison to earlier published results. Figure 1 shows block number assignments on polar grids around the plant, for blocks (a) within the 16 km radius and (b) between 16 km and 80 km. Figure 2 shows the detail of the block boundaries for the 16 km area. Blocks were laid out based on the availability of health and population statistics and made as small as possible given the accuracy limits of the dispersion model. Inside the 16 km area, a 10° lower limit on angular size was used, based on the ±5° uncertainty associated with wind direction data. Grid points inside the blocks were separated by 500 m to 1000 m, with points taken closer together in regions of greater dose variability and a minimum of 10 per block. Blocks from 16 to 80 km are bounded by circles of 16 km radius and sectors of 22.5° angular widths as shown in Figure 1(b). Note that, for epidemiological investigations which examine the relationship of a pattern of health effects to a pattern of environmental exposures, it is the relative exposure levels that are significant for statistical purposes. While uncertainty may remain in the absolute value of estimated doses, it is possible to provide a

greater certainty in the relative values of the geographically distributed doses.

2.1 Relating releases to doses

A primary requirement for projecting doses using a dispersion model is a source term, that is, a representation of the radioactivity release from the site. By way of example, Figure 3 shows noble gas source terms based on data from auxiliary building area radiation monitors (these data will be discussed in more detail shortly). For our purposes, a source term is represented as a time series, $\{q_k\}$, where k is an index running over 15-minute time intervals into which the whole time period is broken. Each q_k, therefore, has a dimension of activity (e.g., Bq or Curies) for some estimated radioisotope composition, being the integral of the instantaneous release rate (e.g., Ci/s) over a 15-minute interval. The use of 15-minute time intervals is dictated by the recording frequency of the weather data, which also sets the time resolution of the dispersion model.

Consider a unit puff of radioactivity released at a given time, represented by qk = 1 for some interval k. The dose at receptor location i due to this quasi-instantaneous unit release is called a dose factor, designated by r_{ik} and having a dimension of absorbed dose per unit release. Dose factors are obtained by (1) using the meteorological model to track the puff as it is dispersed, taking into account information on the wind, atmospheric stability conditions, and topographic features, and (2) using an exposure model to calculate the dose from the passing puff, taking into account information on the energy spectrum of the radiation, the geometry, and the response of the receptor.

The dose factors, r_{ik}, can be organized as a matrix, designated by R when the receptors are TLDs and by S when the receptors are population blocks. Vector designations of q for the source term, T for the doses measured by the TLDs, and B for the doses to population blocks are used. Relating the releases to the doses algebraically, the source term estimation problem is to determine q in the equation

$$T = R\,q\,. \qquad (1)$$

Then, given an estimate of q, population doses are calculated by

$$\mathbf{B} = \mathbf{S}\,\mathbf{q}\,. \qquad (2)$$

Thus, doses are linear functions of the releases--the complexities of the dispersion and dosimetry models are incorporated into the construction of the R and S matrices.

2.2 **Representing the source term**

In implementing the above formulation of the dose assessment problem, one of the challenges faced is how to extract maximal information from the rather sparse measured dose coverage provided by the TLDs. The information content on dosage is limited by the number of measurements (there are 20 distinct TLD sites relevant to the early releases of concern here), which sets an upper bound on the number of degrees of freedom that can be meaningfully estimated. In practice, this number is further restricted by the uncertainties in the measured data and in the dispersion model. Nevertheless, one can hope to obtain some time resolution of the release rather than having to assume a constant average release over the whole period (as done by Pasciak *et al.),* which gives a source term with but one degree of freedom.

To this end, the release period is partitioned into time segments, each comprised of one or more 15-minute intervals. The partitioning method is illustrated in Figure 3(c), where the source term given in Figure 3(b) is replotted with its reduction to a sequence of constant releases over seven time segments. The times at which one segment ends and the next segment begins may be chosen to incorporate prior knowledge about the releases and their dispersion or to help fit the TLD data. A combined approach is taken, in which a set of segment boundary times, based on an inspection of the meteorological data, is specified *a priori* to any fitting and then the algorithm successively selects the boundary times which yield the greatest increase in goodness of fit for a given set of modeling assumptions. The possible segment boundaries (15-minute intervals which can terminate a time segment) are chosen in advance so that the meteorological conditions within a time segment are kept as uniform as possible.

To represent a segmented source term, time segments are indexed by j so that Q; designates the average activity release over a time segment. That is to say, Q; is the average of q_k for the intervals k comprising segment j. The source term estimation problem is thereby implemented as the estimation of a step function, designated by the vector Q, comprised of elements Q;. In order to transform a source term represented as releases over time segments (a Q-vector) to releases per 15-minute interval (a q-vector), define a matrix, W, such that

$$\mathbf{q} = \mathbf{W}\,\mathbf{Q}. \qquad (3)$$

A W matrix maps a coarse representation of a source term to a fine representation, with an element w_{kj} of W representing the portion of the aggregate release over time segment j that is released in interval k. Thus, estimating the release as a 7-segment step function over 160 intervals (a 40 hour time period) involves a 160-by-7 W matrix in which w_{kj} is 1 when interval k is in segment j and is 0 otherwise. Such an assignment of the elements of W corresponds to the release being constant over each time segment. Note that W is non-dimensional, that is, its elements represent relative releases within a time segment and are normalized so as to have no effect on the total quantity of activity released.

Given the previously mentioned limit on the number of degrees of freedom which can be meaningfully estimated, the actual pattern of the release cannot be fully resolved. The effect of more highly unsteady release patterns on dose estimates are examined through a probabilistic analysis. This is done by assigning random values to the w_{kj} within each segment and then normalizing the values to meet the constraint that the quantity of the activity released over a time segment remains unchanged (discussed further in Section 4). Thus, a deterministic or probabilistic formulation of dose assessment problem is permitted in this framework, depending on whether constant values or random values (sampled from some probability distribution), respectively, are assigned to the elements of W.

2.3 Release estimation and dose projection

Substitution of WQ for q according to Equation (3) yields expressions for the release estimation and dose projection analysis. If TLD data are given, the regression problem

$$\mathbf{T = R\ W\ Q + e} \qquad (4)$$

is solved to estimate the source term, Q, where e is a vector of measurement errors. The number of time segments comprising Q is increased by splitting a segment at the boundary which causes the greatest reduction in the sum of squared residual errors, thereby increasing the dimension of Q in the regression model. As discussed above, the set of possible segment boundaries is specified in advance based on the meteorological data. The number of time segments is increased until a further increase in dimension is no longer meaningful, as determined by a statistical test on the residual errors.

Given a source term estimated as above or in some other fashion) population doses are computed as

$$B = S\ W\ Q \qquad (5)$$

For a fixed S, varying Q permits one to examine the sensitivity of population doses to uncertainties in the source term. Varying W (randomly assigning its. elements) permits one to probabilistically determine the range of population doses consistent with the estimated source term; this approach is taken up in Section 4.

3 BASE CASE ANALYSIS

A base case assessment was done to obtain the estimated source term and population doses for a specific set of exposure modeling and TLD data analysis assumptions. The results given in this section are our best assessment of the noble gas releases. and attendant population doses during the first day and a half of the TMI accident. The effects of varying the modeling assumptions and the uncertainties due to limited resolution. of the source term will be discussed in Section 4-

3.1 Dispersion modeling assumptions

A number of refinements, which had not been collectively included in previous assessments of the TMI accident, are incorporated in the base case dispersion model. These include the modeling of flow over terrain features out to ten miles, the effects of wind direction changes, flow disturbance by the plant buildings and cooling towers, and plume buoyancy. Sensitivity tests showed that the assumptions regarding plume rise have the greatest effect on the estimates of noble gas releases and attendant doses. Plume rise assumptions are discussed here; further details on this and the other aspects of the dispersion model are provided in Beyea and DeCicco (1989).

A key factor in determining the dispersion of a pollutant from a stack is the plume rise, which is governed by atmospheric conditions as well as the temperature and momentum of the effluent (G.A. Briggs, Chapter 8 in Randerson 1984). For TMI, while the initial momentum of vented gases is known except for apparently brief periods when the ventilation.system was turned off, no data have been found on the actual effluent temperature. The gases were vented from the auxiliary building; the temperature sensors there were not functioning properly, however, and so auxiliary building air temperature measurements during the accident are not available.[5] Some data on air temperatures in the reactor building are available based on the sensors analyzed by Mock (1982). Reactor building air temperatures averaged 35±3°C over 12 hours prior to the accident and rose to an average of 45±4°C over the first day of the accident, with peaks averaging 56±9°C during the hydrogen conflagration that occurred around 2:00 PM. Outdoor temperatures in the vicinity of TMI on March 28, 1979 ranged from -2°C to 12°C (based on National Weather Service records for Harrisburg, PA). The fact that hot water from the reactor building entered the auxiliary building suggests that the auxiliary building air may have been warmer than outdoor air.

In light of the considerable uncertainty about the noble gas effluent conditions, we analyzed a range of plume rise parameters. The lowest case assumes zero momentum flux and zero temperature difference between the effluent and ambient air. For all other cases, the effluent momentum

[5] A.H. Wilcox (Pepper, Hamilton, and Scheetz, Philadelphia, PA), pers. comm., May 16, 1989.

assumed an exit velocity of 9.1 m/s from the stack, based on exhaust fan data (Pickard, Lowe, and Garrick, p. F-3). The highest case assumed an exit temperature 100°C higher than ambient. For our base case, we assume an effluent temperature 10°C higher than ambient, giving a moderate degree of buoyant plume rise.

3.2 Radiation modeling assumptions

Doses of gamma radiation absorbed at a receptor from a passing radioactive plume were calculated as the sum of doses from the series of puffs used to represent the plume. A separate finite-cloud integration was used rather than the sector-average method which is standard for regulatory analyses. Doses to receptors up to 6 km from the puff path centerline were integrated for each puff position out to 100 km as propagated by the dispersion model. Puffs were treated as moving in a straight line during each 15-minute time step. The exposure from each point accounted for radiation attenuation through air, buildup from scattering in air, and gamma ray interactions with the ground. Exposures were calculated assuming a single 80 keV energy, the dominant radiation that would be received from ^{133}Xe. It was unnecessary to correct for decay in transit because the 5-day half-life of ^{133}Xe is much longer than transit times. These assumptions become progressively better after the early hours of the accident: To ease comparisons with earlier assessments, the whole-body dose estimates are not corrected for building shielding. Buildings in the area are predominantly made of wood and are estimated to reduce the stated doses by approximately 25% (Auxier *et al.,* Appendix C; Knight *et al.,* Appendix D).

3.3 TLD data

The doses recorded by the thermoluminescent dosimeters (TLDs) located around TMI have been used as a key source for most dose assessments of the accident. A comprehensive review and error analysis of the TLD measurements was performed in order to obtain a set of corrected net dose estimates for the 20 monitoring sites that were in operation at the beginning of the accident. The TLD monitoring sites are indicated in Figure 4, marked on a map showing terrain elevations

surrounding TMI. New information was obtained at the authors' request from Metropolitan Edison's dosimetry contractor to correct inaccuracies in the locations and collection times of the TLDs. Table 1 lists the net doses and their standard errors for the first period following the accident along with TLD site designators, site locations, and times of collection from the field. The exact TLD collection times--spanning a period of over ten hours--had not been considered in previous TMI dose assessments, which assumed single, fixed exposure periods for all TLDs. The exact exposure times and net doses are used here as the input data for source term estimation.

The gross TLD readings utilized here are the same as those given by the reports subsequent to the accident , but the treatment of the data differs from the earlier analyses in several ways. Background doses are based on five years of data prior to the accident, rather than a few readings from 1978, and the variation of recorded background is included in the error analysis. At locations where more than one dosimeter was in place, a weighted average of the readings is used to compute the dose. This results in a significant reduction in net dose at one location, 16A1, for which previous analysts had discarded the lower of two readings which differed by a factor of two, and incidentally improves the quality of source term estimation fit. An order-of-magnitude understatement of the net dose for location 14S1 was corrected; apparently, a typographical error resulted in loss of the most significant digit and the mistake was perpetuated--Appendix B of Beyea and DeCicco (1989) gives further details. Otherwise, differences in dose values are minor.

In addition to the corrections and refinements just mentioned, it should be noted that this analysis includes all of the TLD readings when fitting the source term, rather than discarding readings that some might deem insignificant. The inclusion of zero or near-zero net doses along with their standard error estimates (which provide the certainty at which they are judged to be not significantly different from zero) is important because it provides information about where doses were not likely to have occurred, constraining the source term estimation accordingly.

[6] Auxier *et al.;* Battist *et al.;* Pickard, Lowe, and Garrick.

TABLE 1. TLD doses for the first collection period during the accident

Dosimeter	location	Sector	Distance (km)	Azimuth (deg)	Coordinates X (m)	Y	Time (3/29)	Dose (mrad)	StdErr (mrad)
1	1S1	N	0.694	357.5	-30	693	16:40	81.5	4.1
2	2S2	NNE	0.989	21.5	363	920	17:15	29.4	4.6
3	4S2	ENE	0.343	60.4	298	169	17:07	18.5	5.8
4	5S2	E	0.310	76.0	301	75	17:05	15.3	4.1
5	9S1	S	1.150	180.0	1	-1150	16:55	8.3	3.2
6	11S1	SW	0.190	264.3	-189	-19	16:50	198.4	24.3
7	14S1	WNW	0.621	296.1	-558	273	12:15	112.3	20.6
8	16S1	NNW	0.385	336.2	-155	352	16:45	1025.7	128.2
9	4A1	ENE	0.908	51.4	709	567	9:20	4.4	1.9
10	5A1	E	0.661	91.6	661	-19	9:10	2.8	2.0
11	16A1	NNW	0.800	331.6	-381	704	12:10	516.8	321.5
12	IOBI	SSW	1.799	201.7	-664	-1672	12:25	2.6	4.8
13	12B1	WSW	2.101	258.0	-2055	-437	11:50	2.6	2.0
14	ICI	N	4.365	357.0	-230	4359	14:45	6.1	1.9
15	8C1	SSE	3.503	159.9	1202	-3290	9:30	0.5	4.8
16	7F1	SE	15.526	127.8	12264	-9521	10:00	0.8	3.0
17	4G1	ENE	17.337	64.4	15632	7498	18:10	0.0	3.6
18	7G1	SE	23.053	125.7	18710	-13468	10:20	0.0	9.7
19	9G1	S	20.201	-183.1	-1083	-20172	10:50	2.5	2.5
20	15G1	NW	21.558	309.0	-16746	13577	13:25	0.8	3.8

NOTES:

Geographic coordinates are referenced. with respect to the TMI auxiliary building vent stack (Pennsylvania UTM coordinates 530.6, 459.8).

Time column gives the time of day on March 29, 1979 when the dosimeters were collected from the field.

Doses are given in mrad (10 Gy) net of background radiation for the first collection. period (4 am March 28 to each dosimeter's collection time on March 29, 1979).

Values for locations having redundant dosimeters are based on weighted averages (including that for location 16A1).

Standard errors are based on combining the error estimates due to the TLD reading, background subtraction, and calibration uncertainties.

3.4 Source term estimation results

The rate of noble gas release over the time period from 4:00 March 28 to 18:00 March 29, 1979 is estimated by regressing measured TLD doses against dose factors computed by the dispersion model. The regression model is Equation (4), given above, using an R matrix generated under the assumptions of the base case dispersion and dosimetry model. The specific collection times for each dosimeter location are used to specify the cutoff times for dose integration. The observations (T vector) are given by the measured TLD doses in Table 1 and are weighted inversely to their. estimated standard errors to permit statistical interpretation of the results. The dimension of the source term vector, Q, is successively increased until dimension 7, after which there is no further improvement in the fit. The resulting estimated source term, designated source term A, is given Table 2 and is plotted in Figure 5.

Table 3 lists data and parameters regarding the fitting process used to obtain our base case source term estimate. Part (a) of the table lists the set of possible segment boundaries over which we refined the fit. This set was chosen *a priori* so that consistent wind directions were maintained

TABLE 2. Source term estimation results for base case assumptions

Segment number	Segment boundary	Times of day (March 28-29)	Length (hours)	Release rate (10 Ci/h)	Standard error (10 Ci/h)
1	31	4:00 - 11:45	7.75	67	23
2	40	11:45 - 14:00	2.25	287	117
3	76	14:00 - 23:00	9.00	1040	253
4	81	23:00 - 0:15	1.25	6600	2220
5	86	0:15 - 1:30	1.25	38	146
	110	1:30 - 7:30	6.00	398	85
7	149	7:30 - 17:15	9.75	106	53

Total release (4:00 March 28 - 17:15 March 29): 22 ±2 MO (820 ±70 PBq)

Note: Release rate is effective ^{133}Xe activity for an assumed 80 keV energy.

within a time segment.. When iteratively fitting to an increasing dimension, the order in which the time segmentation is refined affects the segments finally selected, but does not affect the general shape of the estimated release pattern. Use of equal-length segments yielded fits that were not quite as good; however, there was little effect on the shape of the release pattern through time.

Table 3(b) lists the sequence of regression statistics and the estimated total released activity as the dimension of Q is increased. (Also listed are the estimated population doses within 10 and within 50 miles--these will be discussed shortly.) Part (c) of the table lists the sequence in which the solution was obtained by successively refining the time segmentation of the estimated release. According to an F-test (Draper and Smith 1981, p. 101.) at the 0.05 significance level, there is no improvement in fit beyond a dimension of 7, when an r^2 of 0.953 is obtained. Table 3(b) shows

TABLE 3. Summary of the source term fitting process over the first TLD collection period for base case assumptions

(a) Times (15-minute interval numbers) from which segment boundaries were chosen:

5	15	20	24	31	40	52	62	68	76
81	86	94	103	110	118	127	132	138	149

(b) Source term estimation statistics as solution dimension (N) is increased by splitting segments at added interval boundaries:

N	Segment boundary	X^2 (1)	r^2 (1)	F-test	Sig (2)	Total Release (3)	10-mile, 50-mile population doses (person-Sv)	
1	149	35.26	0.547	22.93	yes	220	3	8
2	31	21.81	0.720	11.11	yes	390	6	15
3	110	12.60	0.838	12.41	yes	420	8	19
4	81	12.08	0.845	0.69	no	430	8	18
5	76	5.65	0.927	17.06	yes	770	18	38
6	40	5.01	0.936	1.80	no	790	18	38
7	86	3.68	0.953	4.70	yes	820	18	37
8	20	2.65	0.966	4.66	no	820	18	37
9	94	1.89	0.976	4.39	no	860	19	40
10	24	1.51	0.981	2.55	no	860	19	40

NOTES:
(1) X^2 is the sum of squared residuals and r^2 is the percent variation explained.
(2) Whether or; not the added dimension of the estimated source term is significant at a 0.05 confidence level according to the F-test statistic.
(3) Release is the estimated cumulative noble gas activity in PBq (10^{15} Bq = 27,000 Curies) for the first 38 hours of the TMI accident, based on dose factors of (grad/h) per (Ci/h) computed on 15-minute intervals.

(c) Estimated release rates (10^{-} Ci/h) for successive temporal refinements of the solution by increasing the number of time segments:

Solution dimension	Segment boundaries (15-minute interval number): 31	40	76	81	86	110	149
N = 1	156	156	156	156	156	156	156
N = 2	40	340	340	340	340	340	340
N = 3	68	492	492	492	492	492	96
N = 4	15	576	576	576	420	420	100
N = 5	64	432	432	9604	344	344	100
N = 6	72	304	*724*	*4364*	308	308	92
N = 7	67	287	1040	6600	38	398	106

the effect of continuing the iteration out to dimension 10, illustrating how further refinements yield little improvement in fit; neither do they change the estimated release pattern in any significant way.

Carrying out the solution procedure with ordinary least squares (OLS) results in a segmentation scheme that gives negative estimated release rates at dimension 4, violating the physical constraint that releases are non-negative. Therefore a non-negative least squares (NNLS) algorithm (Lawson and Hanson 1974, Chapter 23) is used to impose a constraint that all parameter estimates be greater than or equal to zero. Fitting with NNLS enforces a time segmentation that gives physically meaningful parameter estimates but has the disadvantage that standard errors cannot be directly obtained. A solution for the variance of constrained least-squares parameter estimates is known only for the single parameter case (Judge and Takayama 1985), which is moot for the problem considered here.

For the base case, it turns out that the NNLS solution yields release estimates that are all strictly positive. The OLS and NNLS solutions are therefore identical and so it is fortuitously possible to estimate the releases and their standard errors by using OLS with the time segmentation obtained by using NNLS. The fact that release estimates are strictly positive means that the non-negativity constraint is non-binding for this particular solution. The constraint was, however, employed in earlier iterations that determined how the time segmentation was refined. Strictly speaking, the resulting regression error statistics reflect neither the use of the non-negativity constraint for choosing the time segments nor the use of wind information for specifying the set of possible time segments. The effect of these two factors on the estimation errors for the releases in each time segment is indeterminate because, while the non-negativity constraint would tend to reduce the errors, the uncertainty in the segment boundary times would tend to increase the errors. It is necessary, therefore, to turn to a probabilistic analysis in order to provide information on the further uncertainties due to these restrictions on the source term estimation. This is done as part of the general sensitivity studies discussed in Section 4.

TABLE 4. Observed, predicted, and residual values from source term fits

(a) For base case fit (as given in Table 2)

		UNWEIGHTED DATA			WEIGHTED FOR FIT		
	TLD	Observed	Predicted	Residual	Observed	Predicted	Residual
1	151	81.5	70.3	11.16	3.2874	2.8371	0.4503
2	2S2	29.4	28.9	0.45	2.9555	2.9105	0.0451
3	4S2	18.5	21.3	-2.84	2.3045	2.6586	-0.3540
4	5S2	15.3	15.5	-0.20	2.4860	2.5184	-0.0325
5	9S1	8.3	7.8	0.53	2.0470	1.9157	0.1314
6	11S1	198.4	242.6	-44.17	3.0860	3.7732	-0.6871
7	14S1	112.3	90.2	22.14	2.8438	2.2832	0.5607
8	16S1	1025.7	966.5	59.23	3.0770	2.8993	0.1777
9	4A1	4.4	2.6	1.81	1.9019	1.1203	0.7815
10	5A I	2.8	1.3	1.46	1.2908	0.6162	0.6746
11	16A1	516.8	544.5	-27.67	1.4479	1.5254	-0.0775
12	10131	2.6	0.0	2.56	0.5347	0.0090	0.5257
13	12B1	2.6	3.3	-0.69	1.2112	1.5303	-0.3191
14	1C1	6.1	6.7	-0.56	2.3124	2.5260	-0.2136
15	8C1	0.5	0.0	0.50	0.1041	0.0000	0.1041
16	7F1	0.8	0.0	0.80	0.2658	0.0000	0.2658
17	4G1	0.0	0.0	0.00	0.0000	0.0000	0.0000
18	7G1	0.0	0.0	0.00	0.0000	0.0000	0.0000
19	9G1	2.5	0.0	2.50	0.9578	0.0000	0.9578
20	15G1	0.8	0.3	0.50	0.2101	0.0779	0.1322

(b) For adjusted area monitor source term (Pickard, Lowe, and Garrick)

		UNWEIGHTED DATA			WEIGHTED FOR FIT		
	TLD	Observed	Predicted	Residual	Observed	Predicted	Residual
I	I S 1	81.5	64.2	17.29	3.2874	2.5900	0.6974
2	2S2	29.4	32.2	-2.75	2.9555	3.2315	-0.2760
3	4S2	18.5	28.7	-10.24	2.3045	3.5797	--1.2751
4	5S2	15.3	21.9	-6.56	2.4860	3.5519	-1.0659
5	9S1	8.3	4.4	3.89	2.0470	1.0873	0.9597
6	11S1	198.4	117.4	80.98	3.0860	1.8265	1.2596
7	14S1	112.3	48.5	63.78	2.8438	1.2287	1.6151
8	16S1	1025.7	509.0	516.70	3.0770	1.5269	1.5500
9	4A I	4.4	4.5	-0.07	1.9019	1.9309	-0.0290
10	5A1	2.8	1.9	0.91	1.2908	0.8710	0.4197
11	16A1	516.8	212.9	303.89	1.4479	0.5965	0.8514
12	10131	2.6	0.1	2.50	0.5347	0.0207	0.5140
13	12B1	2.6	0.3	2.33	1.2112	0.1235	1.0877
14	ICI	6.1	7.2	-1.09	2.3124	2.7251	-0.4127
15	8C1	0.5	0.0	0.50	0.1041	0.0008	0.1033
16	7F1	0.8	0.0	0.80	0.2658	0.0003	0.2655
17	4G1	0.0	0.0	-0.04	0.0000	0.0116	-0.0116
18	7G1	0.0	0.0	0.00	0.0000	0.0001	-0.0001
19	9G1	2.5	0.0	2.46	0.9578	0.0137	0.9441
20	15G 1	0.8	1.7	-0.92	0.2101	0.4528	-0.2427

Unweighted values are in mrad (10^{-}Gy); weighted values are dimensionless.

To evaluate the fit to the TLD data, the residuals (observed TLD doses minus the doses predicted by the fit) are examined and compared with residuals from source terms estimated according to other methods. Table 4 lists observations, predicted values, and residuals for (a) the base case fit and (b) a fit to the adjusted area monitor data as derived by Pickard, Lowe, and Garrick. Listed are unweighted values (in mrad) as well as the weighted values (dimensionless, doses divided by standard errors) which were used for fitting. Figure 6(a) and (b) show plots of the residuals versus predicted values for the same respective cases in Table 4. Note the improvement in fit for the 16A1 TLD, as well as for several of the TLDs having lower readings, for this estimated source term compared to that derived from the adjusted area monitor data. The unadjusted area monitor data shown in Figure 3(a) fit the TLDs rather poorly. Figure 6(c) shows the residuals from a source term given as a constant release rate over the whole period, based on the doses and meteorological dispersion factors given in Table 1 of Pasciak *et al.* (1981). In this case the fit is quite poor ($r = 0.63$) in comparison with source terms that allow for a time-varying release rate; note that the scale of the residuals axis in part (c) of Figure 6 is five times the scale in parts (a) and (b).

3.5 Population doses

Given the estimated source term obtained above, the doses received by-individuals in the vicinity of the plant can be calculated according to Equation 5. For the area within 16 km of the plant, the population data and block groupings established by the TMI epidemiologic study (Hatch *et al.)* are used. For 16 km to 80 km, 22.5° angular by 16-km radial sectors are used, with population data based on the TMI Final Safety Analysis Report (as tabulated by Battist *et al.).* Dose factors for grid points within population blocks are calculated using the same base case dispersion assumptions as specified above. The dose factors are summed over the grid points in each block and then, given an estimated source term, the doses to each block are computed as described in Section 2.3.

Figure 7 shows the resulting block doses (a) within 16 km and (b) within 80 km. As previously reported, the highest doses were received in the NNW sector. Figure 8 shows the estimated doses in the 16 km radius area as an elevation plot (excluding locations on the Susquehanna River) for (a) the source term estimated using the base case assumptions and (b) the source term based on the adjusted area monitor data by Pickard, Lowe, and Garrick. The correlation coefficient between the block doses for the two cases is 0.97, reflecting the similarity of dose distribution patterns apparent in the figure. The refinement in the source term that enables a better fit to all of the TLDs has, therefore, an insignificant effect on the relative pattern of doses to the population blocks. Nevertheless, the fact that data from all of the TLDs are incorporated, rather than just a subset as used to adjust the area monitor source term, provides added credibility to the results in that it leaves less chance that part of the release went undetected.

Figure 9 shows the distribution of doses by population, obtained by cumulatively averaging the doses to blocks out to 80 km resulting from noble gas releases over the first 38 hours of the accident. The estimated population dose totals to 18 person-Sv (1800 person-rem) for the 0-16 km area and 37 person-Sv (3700 person-rem) for the 0-80 km area, over which it averages 0.017 mSv (1.7 mrem) per person, since many areas received little or no dose. Exposures were concentrated in the areas lying to the north and west, with the NNW sector averaging 0.28 mSv (28 mrem). The population estimated to have received 1 mSv (100 mrem, the value cited by Rogovin as the maximum likely offsite dose to an individual) is on the order of 6000 persons. The highest study area block (number 74, with 1700 persons, in the NNW sector about 7.4 km or 4½ miles from the plant) received an average dose of 1.1 mSv and the peak dose in this block is estimated at 2.1 mSv. The highest projected doses to persons in the vicinity of TMI are this far from the plant because the plume bearing the highest releases was over the river until it reached land around blocks 71, 73, and 74 (refer back to Figure 2b). As noted earlier, these dose estimates do not include a correction factor for building shielding, which would reduce doses by about 25%.

4 SENSITIVITY ANALYSES

A series of sensitivity analyses is carried out by varying parameters relating to the dispersion and dose models, the TLD data, and the error assumptions. Then, in order to obtain better information on the possible uncertainties remaining in the analysis (due to the limited time resolution possible when estimating the source term from the limited number of TLD measurements), a probabilistic analysis is performed by simulating the effect of sampling from a distribution of release patterns within the time segments.

4.1 Effects of varying key assumptions

Table S lists the variations in assumptions tested for their effect on the results from the base case analysis, which is listed first in the table (Case A). The remaining cases are listed in terms of the assumption by which they differ from Case A. The sensitivity analysis includes examinations of the variations in plume rise, wind direction, TLD data used, energy dependence of TLD response, and residual error weighting of the TLD data. Table 6 summarizes the results of these sensitivity tests, showing the total estimated noble gas release and the attendant dose estimates. The X^2 and r^2 statistics are indications of the goodness of fit for the source term estimation.

TABLE 5. Variations in modeling, data, and estimation assumptions

Case	Description of assumptions
A	Base case: meandering puff model with nominal wind direction and 10°C thermal plume buoyancy, nominal TLD data with weighted averages for all duplicates, 30% redundancy error.
•	No plume rise.
C	100°C thermal plume buoyancy.
•	Wind direction shift +5° (eastward).
•	Wind direction shift -5° (westward).
F	TLD response energy correction.
•	Higher value of TLD 16A1 (rather than weighted average).
•	Reduce redundancy error to 10%.
I	Straight line plume.
J	Straight line plume, no plume rise.
K	Straight line plume, fitting to all TLDs to estimate a constant scale factor for source term P.
•	Straight plume, no rise, source term P scaled as case K.
M	Straight plume, no rise, source term P scaled by a constant estimated by fitting to only the 4 highest TLDs.

Case A is fully discussed in Section 3 of the text. Other cases are described in terms of the assumption by which they differ from case A; see the text of this section for further details.

The results are most sensitive to the assumption regarding plume rise. Figure 10(a) shows the plume rise during the time of estimated peak release (11:00 pin March 28) for cases B, A, and C. Final rise above the top of the vent stack for these cases is estimated to be 0 m, 51 m, and 90 m, respectively. For the sake of the analysis, we take cases B and C as the endpoints of the range of plume rise and perform a logarithmic interpolation about the base case (case A). The

TABLE 6. Estimated radioactivity releases, doses, and solution statistics for the modeling variations tested.

Case (description)	Release (PBq)	Person-Sv: 16 km	80 km	Max (mSv)	N	χ^2	r^2
A (base 10° rise)	820	18	37	2.1	7	3.68	0.953
B (no plume rise)	320	11	20	1.0	7	2.74	0.965
C (100° plm rise)	1680	20	45	3.8	6	7.39	0.905
D (+5° wind shft)	720	14	31	1.6	6	4.26	0.945
E (-5° wind shft)	800	19	41	2.3	6	9.85	0.874
F (TLD energy)	580	13	27	2.1	8	3.33	0.957
G (high '16A1)	840	18	36	2.2	8	3.18	0.960
H (10% err wght)	860	19	40	2.3	10	1.53	0.980
I (strt 10° rise)	850	16	28	1.9	7	2.66	0.966
J (strt 0 rise)	370	11	18	1.0	6	3.00	0.961
K (adj st10°rise)	530	10	16	1.2	1	12.99	0.833
L (adj st0 rise)	210	6	9	0.5	1	14.39	0.815
M (adj st0 4TLDs)	440	12	19	1.1	1		

NOTES:

See Table 5 and the text for full descriptions of the assumptions for each case.

Conversions: 1 PBq (10^{15} Bq) = 0.027 MCi (27,000 Curies); 1 Sv = 100 rem.

Max column is the estimated maximum dose to a grid point within any populated block. Values for cases G to M are based on the ratios of maximum dose to 16 km population dose for similar earlier cases.

N is the dimension (degrees of freedom) of the estimated source term.

The X^2 and r^2 statistics are, respectively, sum of squared residuals and percent variation explained for weighted regression of TLD data against modeled dose factors (not shown for case M, which is based on a much different weighting than the others).

lower.[7] Lacking any measurements of the vent stack temperature, we assume a log-normal distribution with mean 10°C and standard deviation 10°C for the temperature difference. Using the sensitivity curves plotted in Figure 10 yields one standard deviation equivalent intervals of 560 to 970 (mean 820) PBq for the activity released during the first day and a half of the accident and 32 to 38 (mean 36) person-Sv for the attendant 80 km population dose. (Further details on these calculations are given in Appendix E of Beyea and DeCicco).

Given that some buoyant rise was very likely, these sensitivity curves and the likely temperature difference distribution suggest that the release and dose estimates for 10°C plume rise are quite robust. Most of the plume rise effect occurs over the lower temperature differences, since the sensitivity curves level off with increasing temperature difference. We therefore take the results for our base case 10°C plume buoyancy, with the error bounds implied by a ±10°C log-normal standard deviation, as our best estimates.

The cases of ±5° wind direction show the effect of possible errors in the wind direction data, from the weather station on site at TMI, which is used by the dispersion model. An uncertainty of ±5° is generally considered acceptable for wind direction measurement equipment (Randerson 1984, Ch. 4, p. ;140). A counterclockwise shift increases the population dose estimates because the dominant plume direction is shifted toward the more populated areas near Harrisburg, but the increase is small, about 10% for the 80 km population dose. A positive direction shift decreases the estimated 80 km population dose by about 15%. In either case, the quality of fit to the TLDs decreases, suggesting that the nominal wind direction is more consistent with the measured doses.

As discussed in Appendix B, the $CaSO_4$:Dy (Teledyne) dosimeters may have over-responded to the dominant ^{133}Xe radiation present in the release. Applying a correction factor (Woodard and Potter, July 1979, Appendix G) for the TLD energy response results in decreases in the estimated source term and 80 km population dose of about 30% and a slight decrease in the goodness of fit.

[7] Outdoor temperature data for the accident period analyzed here are given in Beyea and DeCicco (1990).

The effects of other assumptions regarding the TLD data are generally small. There is a factor of two discrepancy in two readings at the TLD location recording the. second highest doses (16A1). The base case fit uses a weighted average of the two readings; use of the only the higher reading (as done in dose assessments by Auxier *et al.* and Battist *et al.)* has no significant effect on the results. As discussed in Section 3, source term estimation was done with TLD data weighted inversely to their estimated error. In addition to TLD dose. uncertainties estimated from known sources of measurement error, we considered an additional overall error, assumed proportional to dose, due to unknown causes. A reason to suspect additional uncertainty in the TLD readings is that the data show an average discrepancy of 30% over the three locations having redundant dosimeters. This and other aspects of TLD error analysis are further discussed in Appendix B of Beyea and DeCicco (1989). The nominal proportional error added for the purpose of weighting is 30%; neither increasing this to 50% nor decreasing it to 10%. results in an appreciable change in the parameter estimates.

The last three cases (K, L, M) listed in Tables 5 and 6 represent fits performed for the purpose of comparing the present results with those based on the source term derived from the area monitor data. In each of these cases, the relative time pattern of releases is assumed to follow the adjusted area monitor trend given in Table 4-1 of Woodard and Potter (July 1979), plotted here in Figure 3b. A single parameter is estimated to represent the factor by which the adjusted area monitor values must be multiplied to match the TLD data used in the fit. A straight-line plume dispersion model is used for these three cases, with plume rise assumptions as noted. *Case* M scales the term to fit only the four highest TLDs; this is accomplished by heavily de-weighting all other TLDs and assigning minimal error to the four TLDs. Because the error weighting is significantly different for case **M, its** X^2 and r^2 statistics are not comparable to those for the other cases and are not listed in the table. These cases are further discussed in Section 5.2.

4.2 Probabilistic analyses

In representing the source term using few enough parameters to estimate it from the limited TLD data, the releases are represented as constant averages over time segments. It is reasonable to ask what would be the effect of non-constant releases in a segment, since the actual release pattern is not likely to have conformed to the constant rate per segment pattern introduced to make the analysis tractable. Non-constant releases can make a difference in dose estimates because of the unsteady nature of the plume dispersion process. In particular, we wish to determine the likelihood of the noble gas activity releases having been timed such that a large release may have gone undetected given the spatial distribution of the TLDs and the dispersion conditions at.the time of the accident.

In order to determine how much of a difference is possible within the information constraints given by the TLD data, a probabilistic analysis is used to simulate the effects of non-constant releases. The method for performing such an analysis is to assign the W matrix (see Equation 3) with random values. The simplest randomization scheme would be to assign all elements of W with a randomly varying relative release rate in each interval. (Recall that elements of W are normalized so,, that they average to 1 over the whole release period.) A release pattern more concentrated in time can be simulated by letting non-zero releases occur only in some fraction of the intervals. The most extreme case is to have all of the release concentrated in a single 15-minute time interval in each segment. This would correspond to the activity being released in a discrete bursts, as simulated by assigning a non-zero element of W (w_{kJ}) for only one randomly chosen 15-minute interval in each time segment.

We define a parameter, termed the release time fraction, to be the average fraction of 15-minute intervals within a time segment having non-zero releases. The randomization schemes just described would have release time fractions ranging from 0, representing the limiting case with all of a release concentrated in a single time interval per segment, to 1, representing releases

of varying magnitude spread uniformly through each time segment. The effect of non-constant releases is examined by estimating a source term and then projecting the resultant population doses by running random trials for release time fractions of 0 (limiting case), 0.2, 0.4, and 1.

Using a release time fraction of 1 results in very tight distributions, having a coefficient of variation (CV, i.e., ratio of standard deviation to mean) of less than 5% for total released activity and less than 10% for 80 km population dose. Simulation with releases concentrated in a single randomly assigned interval per segment gives a distribution having an enormous range, including some results that are physically unreasonable (the CV of simulated released activity exceeded 400% due to clumps of trials yielding estimates two orders of magnitude higher than the mean). Examination of. the extreme cases, which gave release estimates exceeding the total noble gas activity content of the reactor, showed that they all occurred when the release burst fell in one particular interval late in time period considered (hour 33). Extending the period of analysis by including TLD readings from March 29 to 31 would eliminate these extremes by constraining the fit to the low measured doses in the area where the releases from that time interval are carried by the winds at that time. Simulations using release time fractions of 0.2 and 0.4 give results with somewhat broader distributions than the fraction 1 case but which remain physically reasonable. So as not to overstate the confidence level of our release and dose estimates, results are presented here for the time fraction 0.2 case, using 2000 random trials. This case gives the largest range of variation that does not result in estimates that can be excluded on physical grounds.

Figure 11 shows the resulting distributions for (a) the estimated total activity release over the first 38 hours of the accident, (b) the corresponding 80 km population dose, (c) the maximum block dose, and (d) the correlation of the block dose pattern with that of the TMI epidemiology study. Simulations were repeated for the lower and higher cases of plume rise, as summarized in Table 7. For our base case (10° plume buoyancy), the CVs of the simulation estimates around their mean values are 18% for the total released activity, 17% for the 80 km population dose, and 28% for the maximum block dose. These can be taken as measures of the additional uncertainty

in our release and dose estimates due to the possibility that noble gas releases occurred as isolated bursts rather than as constant rates over the time period considered. For the maximum block dose, the differences due to varying the plume rise are not statistically significant. On the other hand, for the release and population dose estimates, the uncertainty due to the unknown plume rise is comparable to that due to uncertainty the less than fully resolved timing of the releases.

TABLE 7. Probabilistic analysis of release and dose estimates

Estimated parameter:	Dispersion model used (by plume rise): A (10°)	B (no rise)	C (100°)
Noble gas activity release over first 38 hours, PBq (MCi)	850 ±150 (23 ±4)	330 ±70 (9 ±2)	2100 ±440 (56 ±12)
Population dose within 50 miles of TMI, person-Sv	36 ±6	22 ±4	45 ±9
Dose to block receiving highest projected dose (mSv)	1.5 ±0.4	1.0 ±0.3	1.2 ±0.4
Correlation of block doses to those of epidemiology study	0.80 ±0.19	0.88 ±0.12	0.82 ±0.17

The tabulated values are the means and standard deviations based on 2000 trials in which randomly apportioned non-constant releases occur in 0.2 of the 15-minute intervals in each segment. Note that mean parameter values from the random trials are not the same as the respective values for the non-random case, although the differences are minor.

There has been some concern regarding the possibility of releases during the very earliest hours of the accident. Such early releases would contain short half-life isotopes having more intense radioactivity from which exposures to β radiation could result. The simulations suggest that this is unlikely. The average estimated release rate during the first time segment (first 8 hours) is two orders of magnitude lower than the highest estimated release rate. The possible releases simulated during the. early period do not greatly deviate from the estimated average low level, particularly during the earliest hours when highly active isotopes might have been present.

4.3 Summary error analysis

The uncertainty in the key estimates presented here depends on a number of factors. The principal sources of error are:

1. Uncertainty of the plume rise.
2. Uncertainty in the exact timing of the releases.
3. Uncertainty remaining after the fit to the TLD data.
4. Uncertainty in wind direction measurements.

Table 8 shows a summary error calculation for the estimates of noble gas activity release and 80 km population dose for the period covered (first 38 hours of the accident). The error analysis is performed around the nominal estimates obtained using assumptions for our base case (case A in Tables 5 and 6).

TABLE 8. Summary error analysis for release and dose estimates

	Activity release (PBq)	Population dose (person-Sv)
Nominal estimate	820	37
Plume rise uncertainty	-260 +150	-4 +2
Uncertainty in release timing	±150	±6
Uncertainty from fit	±70	±0.4
Wind direction uncertainty	-60 +0	=6 +4
Total uncertainty	-310 +220	-9 +7
As percent of nominal	-36% +27%	-25% +20%

Error values are for one standard deviation. The lower-to-upper error range gives a 68% confidence interval if a normal distribution is assumed.
Conversions: 1 PBq = 0.027 MCi; 1 person-Sievert = 100 person-rem.

The plume rise uncertainty was discussed under cases B and C in Table 6. Using the sensitivity curves plotted in Figure 10 yields one standard deviation equivalent intervals of 560 to 970 (mean 820) PBq for the activity released during the first day and a half of the accident and 32 to 38 (mean 36) person-Sv for the attendant 80 km population dose. These ranges are the basis for the non-symmetric error' estimates shown in Table 8 for plume rise.

The uncertainty in release timing was summarized in Table 7. Although the mean estimates of released activity and population dose are somewhat different than the nominal (base case analysis) estimates used here, the standard deviations from the probabilistic analysis are used here as estimates of the error from unresolved aspects of the release timing. They are applied as symmetric errors of ±4 MCi (±150 PBq) and ±6 person-Sv about the nominal estimates of activity released and 80 km population dose, respectively.

The uncertainty remaining after the fit to TLD data is given by the covariance matrix resulting from the release estimation procedure. The square roots of the variance estimates (diagonal elements of the covariance matrix) were reported as the standard errors of the estimated release rates given. in Table 2. The covariance matrix was also used to calculate the standard error of the total activity release reported for the base case analysis as ±2 MCi (±70 PBq) about the estimate of 22 MCi (820 PBq).

Note that uncertainties in the TLD data (e.g., due to calibration errors, etc.) were used to calculate the weighting factors used in the source term estimation procedure. Their effect on the certainty of the results is propagated through the release estimation and dose projection procedure and is reflected in the uncertainty remaining after the fit, as just described. Therefore, no further accounting of this source of error is required.

As for the uncertainty in wind direction, we assume that the ±5° direction shifts (cases D and E in Tables 5 and 6) represent one standard error of the nominal wind direction. As reported in Table 6, these deviations result in a -20 PBq (-5° shift) and -100 PBq (+5° shift) deviations in estimated activity release. They result in +4 person-Sv (-5° shift) and -6 person-Sv (+5° shift) deviations in the 80 km population dose. While the effect of wind direction error on population dose is somewhat non-symmetric, this source of error always serves to lower the estimate of released activity. We take the average of the two deviations for activity release, which is -60 PBq, as the contribution towards the overall error.

As shown Table 8, not all of the uncertainties are symmetric around the nominal.(base case) estimates of release and dose. To propagate the errors asymmetrically, the squares of the standard error estimates are separately summed for negative and positive deviations about the nominal estimates and then the total error is calculated by taking the square root of the sum for each side. In other words, the overall error on each side of the mean estimate is taken as the geometric mean of the constituent errors, which are assumed to be independent. Therefore, the estimated activity release is 820 (-310 +200) PBq, or 510 to 1020 PBq (14 to 28 MCi), for an estimated one standard deviation interval. The estimated 80 km (50 mile) population dose is 37 (-9 +7) person-Sv, or 2800 to 4400 person-rem. Note that plume rise dominates the uncertainty for the released activity, while wind direction is the most important source of uncertainty for population dose. The uncertainty due to the inability to fully resolve the timing of the releases is significant in both cases.

5 DISCUSSION

The significance of the results presented here is twofold. First, a new assessment is provided of the amount of noble gas radioactivity released during the early part of the Three Mile Island accident and the resulting gamma radiation doses in the surrounding populated area. Second, the methods developed for this reassessment are an advance in the methodology available for estimating radiation releases and the attendant population doses based on limited radiological field data.

5.1 Comparisons with earlier work

Several analysts obtained estimates of noble gas releases from TMI by using data from the area monitors in the reactor auxiliary building which were far enough away from radioactivity to generally remain on scale. With an assumption that the area monitor readings were proportional to the stack release, the absolute scale of the release could be obtained, either by calibrating the area monitors against grab sample measurements taken in the exhaust stack or by calibrating them against dose readings in nearby off-site TLDs using the predictions of a meteorological model. Using the first approach, Auxier *et al.* obtained a value of 89 PBq (2.4 MCi) for.the noble gas

activity released during the period March 28 to April 15, 1979, which they estimated to be accurate within a factor of two. Using the second approach, Woodard and Potter obtained and estimate of 370 PBq (10 MCi) released from March 28 to April 6.

Pasciak *et al.* found a way to avoid relying on the area monitors, but only by assuming that the release rate was constant during the period considered. Although they did not explicitly report a value for activity released, the results of Pasciak *et al. imply* a noble gas release of 22 PBq to 81 PBq (0.6 to 2.2 MCi) depending on whether or not three distant TLDs are excluded from the analysis. Our analysis indicates that these estimates are so low because of the assumption of a constant activity release rate. Refering back to Table 3(b) shows how the estimated release increases by a factor of three in going from a single, constant release rate for the whole time period to multiple segments having different release rates.

Knight *et al.* performed two analyses. One used grab samples obtained later in the accident to calibrate the area monitor stripchart data, giving an estimated noble gas release of 260 PBq to 630 PBq (7 to 17 MCi). The second used measurements of ^{85}Kr to estimate the quantity of noble gas activity carried into the auxiliary building by the cooling water, giving a range of 200 PBq to 1100 PBq (5.5 to 30 MCi) escaping through the auxiliary building.

The only previously published information that specified the time pattern of noble gas releases, as opposed to a cumulative total, is that of Woodard and Potter (July 1979, September 1979). The available data are the area monitor "trends," an unspecified composite of readings from several area monitors. Woodard and Potter's analysis indicated that the fraction 66%, or 240 PBq, of their total estimate of 370 PBq was released during the first 38 hours of the accident (through the last TLD collection time on March 29, 1979). We performed the first period analysis using the exact times of collection for each TLD, so that the exposure period in effect for the TLDs varies from 27 to 38 hours, depending on location. Our base case estimate for this first collection period is higher, being 820 PBq (22 MCi) compared to 240 PBq (6.6 MCi).

Besides the differences in the specification of TLD exposure periods, the other important differences between our approach and that of Woodard and Potter are that we have a meandering puff model that calculates doses at specific locations (grid points and TLD sites) rather than a plume model giving sector-averaged doses, we account for plume rise, and we estimate the source term using data from 20 TLDs (as opposed to only the four TLDs having the highest readings) without using the area monitor data. Cases K, L, and M of our sensitivity analyses summarized in Table 6 address these points of comparison with Woodard and Potter. Cases K and L show the effect of the plume rise assumption, which increases the release estimate by a factor similar to that seen in our cases A and B. In case M, using a straight-line, no-rise plume model, we fit to only the four highest TLDs, which Woodard and Potter used in adjusting the area monitor data. This case should most closely approximate their assumptions, but results in estimate of 440 PBq (12 MCi) for released activity during the first period, which is larger than the 240 PBq (6.6 MCi) estimated reported by Woodard and Potter. Therefore, our plume rise assumption accounts for some but not all of the difference between our release estimate and that of Woodard and Potter.

The source term estimated by the base case fit to the TLDs shows a distinct peak at hour 19 (23:00 on March 28), with an estimated 310 ±100 PBq (8.3 ±2.8 MCi) being released during this 75-minute time segment alone. This relative magnitude of this estimated peak release is much larger than that of the corresponding peak indicated by the adjusted area monitor trend reported by Woodard and Potter. Otherwise, the time pattern of our release estimate (Figure 5) agrees roughly with that of Woodard and Potter (July 1979, Figure 3b) regarding the timing of the peak night release around hour 19. We also agree in indicating little appreciable release before hour 5 and after hour 28. We do not resolve the secondary peak during hours 10-14 that is indicated by the adjusted area monitor data but rather show a lower release rate over a broader time span from hours 10-19.

Because no absolute calibration of the areas monitors was possible, Woodard and Potter made several *ad hoc* adjustments to match the release pattern to the TLD measurements. Not all of the area monitors remained on-scale during the release period. Although they assume that the area monitors responded proportionally to the stack monitor (which remained off scale from early on), Woodard and Potter did not apply a uniform scaling to the area.monitor data, but rather made different adjustments during certain hours in order to better match the nearby TLD readings. Our estimated source term was obtained strictly by fitting _to the TLD data. Uncertainty remains, of course, as indicated by the standard errors of the estimated releases that were listed in Table 2. Nevertheless, the distinct peak estimated at hour 19 remains when the modeling assumptions are varied. Although the peak changes in magnitude, depending primarily on the plume rise assumed, its timing is little changed.

As noted earlier, our dosimetry model assumes a single energy level for the noble gas releases, namely, the dominant 80 keV gamma radiation of ^{133}Xe. The fact that the bulk of the estimated releases occurred some hours into the accident, as evidenced by both the area monitor trends and our estimated release time pattern, indicates that the more. energetic isotopes had significantly decayed by the.time of the peak releases. The resulting estimates for the total activity release and population dose are therefore insensitive to this dosimetry modeling assumption.

Comparisons can also be made with isotope inventory estimates obtained from measurements of the radionuclides remaining in the TMI unit 2 reactor building after the accident. Estimated quantities of fission products inside the reactor building were reported by Akers *et al.* (1989). Of the noble gases, only ^{85}Kr decays slowly enough to have been reported. However, the transport characteristics are essentially the same for other noble gases, in particular, for the xenon isotopes which comprised the larger part of the release. Akers *et al.* found that a fraction 0.91 (±0.07) of the initial ^{85}Kr inventory remained inside the reactor building, implying that a fraction 0.09 (±0.07)

[8] See Woodard and Potter (July 1979) and Woodard's remarks in Goldberg (ed. 1984, vol. 1, p. 47ff.) for further discussion.

escaped. Assuming this same fraction for all noble"gases and given the initial inventory of 5600 PBq (150 MCi) at shutdown yields an estimate of 480 (±440) PBq (13 ±12 MCi) for the noble gas source term.

To compare our estimate to that of Akers *et al.,* we need to extrapolate beyond the first TLD reading period for which we performed our fit. Woodard and Potter's first period fraction was 66%, implying a factor of 1.5 for such extrapolation. However, as pointed out above, an important difference in our source term is the strength of the main peak at 19 hours from the start of the accident. Other things being equal, this suggests that the first period accounted for more than 66% of the total. We treat this as introducing additional uncertainty and so assume an extrapolation factor of 1.5 (-0.2 +0.1). Applying this to our results yields 1200 (-500 +350) PBq, or about 34 MCi for the total release. Akers *et al.* estimate of 480 (±440) PBq is lower than ours, but the fairly broad error bounds around both estimates implies that neither can rule the other out with any statistical confidence. Attempting to combine these estimates derived from such different data involves assumptions that further increase the uncertainty. For the sake of argument, a combined estimate giving equal weight to ours and that of Akers *et al.* would be 860 (-670 +560) PBq, or 23 (-18 +15) MCi. This is essentially the same as our original base case estimate, only with greater error bounds.

The range of 80 km population dose estimates reported by other analysts is from 3 to 630 person-Sv. Estimates that relied most directly on early period TLD data range from 10 to 66 person-Sv. Our estimates are most comparable to-these, except that ours are for releases during the first TLD collection period only. Assuming doses proportional to the release, the population dose estimate would increase by a factor of about 1.5 as a result of releases during later periods of the accident. As noted earlier, building shielding would reduce the doses estimates by about 25%. The net effect of these two factors would„ be to increase the population dose estimate by about 12%. The estimated uncertainty of the population dose is about 25% (Table 8). While

The estimate of the source term as a function of time enabled a more finely resolved spatial projection of the population doses. The source term estimate given here agrees reasonably well with the stack release pattern recorded by the area monitors during nighttime. Agreement during the daytime is not as good, but this was found to have little affect on the population dose estimates, because atmospheric dispersion is so rapid during the day that doses are greatly reduced. Dose patterns projected from the two source terms compare quite well, providing confidence that the spatial distribution of population doses has been reliably characterized. This consistency validates the use of relative activity release rates based on the area monitor data in the TMI cancer epidemiology study (Hatch *et al.)* carried out concurrently with the present work.

The noble gas radioactivity release estimate given here is the first obtained by regressing measured environmental doses against the airborne release dispersion and exposure pattern calculated from weather data at the time of the accident. Under base case assumptions of a moderate plume rise and release transport by variable wind directions as measured at the TMI tower, it is estimated that 820 (-310 +220) PBq, or 22 (-8 +6) MG, of noble gas radioactivity was released during the first day and a half of the accident, when the bulk of releases occurred. The major uncertainty is the venting temperature of the release (which affects the plume rise). Other uncertainties result from the possible errors in the wind direction measurements, less than fully resolved release timing, and calibration errors for TLD response. Nevertheless, the remaining uncertainty has been more precisely stated as well as greatly narrowed in comparison with previous assessments of the accident.

Dose assignments to persons in the vicinity of TMI were made by projecting exposures onto geographic blocks having populations of 2300 persons on average. The aggregate dose to the population within 16 km (10 miles) of the TMI plant (160,000 persons) is estimated as 18 person-Sv (1800 person-rem). The estimated population dose within 80 km (50 miles, 2 million persons) is 37 (-9 +7) person-Sv, or 3700 (-900 +700) person-rem. Sensitivity analyses indicated that the dominant sources of uncertainty are unresolved aspects of the release timing and possible errors in the wind direction data, both of which affect the size of the exposed population. The unknown

plume rise is also as source of uncertainty. Our population dose estimate is therefore only slightly higher than the conclusions reported by the President's Commission on TMI and the Nuclear Regulatory Commission, who gave estimates of about 20 person-Sv (2000 person-rem). Our 2.1 mSv (210 mrem) estimate of the highest individual exposures is, however, higher than the official estimates of not more than 0.8 mSv (80 mrem), due to the finer resolution of our dose assessment method. The population estimated to have received doses of about I mSv (100 mrem) is on the order of 6000 persons.

A way to place these population dose estimates in context is to note that the accident dose was equivalent to about 3% of the annual background radiation dose in the TMI area. The population dose rate over the first two days of the accident was about five times the background dose rate of 21×10^{-7} Sv s^{-1} (0.18 mrem/day) when averaged over the 80 km radius area. Some portions of the population received 100 times the average dose, corresponding to a dose rate 500 times the background rate over the first two days of the accident, or about 16 times the dose of an average chest X-ray for a medical examination (60 μSv; NCRP 1987, p. 45). Much of the surrounding area, of course, received essentially no dose from the accident. Estimates of excess cancer mortality given by BEIR V range from 600 to 1200 (mean 800) excess deaths per million person-rem (0.06 to 0.12 per person- Sievert).[10] Applying these risk coefficients to our aggregate 80 km (50 mile) population dose estimates implies 1 to 5 (mean 3) excess cancer deaths in the population of 2 million persons.

6 CONCLUSION

Radiation dosimetry data for the Three Mile Island accident of the March 1979 were analyzed in order to obtain revised estimates of the noble gas releases and attendant population doses during the first day and a half of the accident, when the bulk of the releases occurred. This re-analysis was performed for the Three Mile Island Public Health Fund as a public charge in an attempt to close gaps and remove inconsistencies which appeared in previous analyses of the accident.

---

[10] Estimates of lifetime risk due to a single exposure, from Table 4.2, p. 172, of NRC (1990), using an average of male and female estimates and 90% confidence intervals.

The meteorological dispersion and dosimetry model applied for this analysis included refinements--for changing wind direction, full terrain effects, plant-site building and cooling tower effects, finite cloud dose integration, and ground correction--which had not been collectively incorporated in previous analyses of the accident. A new method was developed that enabled the estimation of time-dependent rates of radioactivity release by utilizing dose measurements accumulated through time by thermoluminescent dosimeters distributed in the area surrounding the plant. A distinctive aspect of the present analysis is statistical treatment of the all of the dosimeter data and their uncertainties. By including all dosimeter data and carrying out an extensive error analysis, the need for engineering judgements about which data to include was minimized. The meteorological model was then used to project the possible doses to locations in the vicinity of the plant. A constrained, weighted, multivariate regression procedure was used to estimate the time pattern of releases that best fits the data from all of the dosimeters. Finally, the meteorological model was applied again in order to predict doses to the surrounding population on the basis of the estimated release rates.

Sensitivity analyses were performed to determine to effects of assumptions regarding plume rise, wind direction, and, energy dependence of the dosimeters. A probabilistic analysis was used to quantify the uncertainty due to inability to fully resolve to timing of the releases. Estimates of the noble gas radioactivity released were found to be most sensitive to plume rise, with uncertainties in the release timing also being important. The net uncertainty in estimated releases is about 30% (corresponding to one standard deviation) and for the population dose is about 25%. Our best estimate of the noble gas activity release is 820 (-310 +220) PBq, or 22 (-8 +6) MCi for the first day and a half of the accident. The corresponding population dose is 37 (-9 +7) person-Sv within 80 km (50 miles) of the plant. This implies an estimated 3 ($\pm$2) excess cancer deaths in the population of 2 million persons.

It was also found that block doses based on the fits to dosimeters correlate well with block doses based on the adjusted area monitor data, which serves to validate the use of the latter in the

exposure model for a concurrent study of cancer epidemiology in the vicinity of Three Mile Island. The geographically detailed dose estimates developed here also provide a TMI dose assessment data base available for further studies if warranted.

Finally, several points should be noted. First, the population dose estimates reported here do not differ significantly from the estimates reported by the official studies of the TMI accident and therefore leave unchanged the expectations of little or no detectable cancers due to the radioactivity releases from the TMI accident. Second, although the essential modeling and statistical tools used for this study existed at the time of the TMI accident in 1979, these tools had not been previously assembled and demonstrated for analyzing a reactor accident (either in actuality or as part of an emergency preparedness exercise). This reassessment of the TMI accident has therefore provided a valuable opportunity to demonstrate the utility of these methods for a real-world incident. It is hoped that this study might be a prototype of the types of analyses that can be applied to other past, present, or future situations which may result in public exposure to excess radiation.

ACKNOWLEDGMENTS

The authors express their gratitude to many individuals whose efforts contributed significantly to the work reported here. Valerie Harms provided invaluable assistance in tracking down and organizing much of the voluminous reference material and data collected for this study. John Arbo assisted in the development of the dose integration algorithm, review of TLD data, and finding technical information regarding the dosimetry analysis. George Colbert handled cartographic tasks needed to accurately specify locations of population blocks, TLDs, and terrain features. Metin Yersel assisted with meteorological analyses. A.H. Wilcox (Pepper, Hamilton, and Scheetz, Philadelphia, PA) assisted by providing access to sources of information regarding TMI. Keith Woodard (Pickard, Lowe, and. Garrick, Inc.) assisted by sharing information used in previous analyses of . the accident. Sid Porter (Porter Consultants, Ardmore, PA) generously provided locations, exposure times, and other important data regarding the TLDs in use at the time of the accident.

Appendix A

Airborne radioactivity transport model

In this appendix, we describe the model used to calculate the radiation doses at receptor locations surrounding the plant due to airborne radioactivity emissions during the Three Mile Island accident. Conceptually, the model involves two problems: (1) determining the concentrations of an airborne substance due to atmospheric dispersion from a point source and (2) determining the absorbed radiation doses received on the ground when the airborne substance is a radioactive gas (in this gas, a gamma-emitting mixture of noble gases, primarily ^{133}Xe). This modeled process for projecting dose estimates on receptors is illustrated in Figure A-1.

A.1 Dispersion model

The atmospheric dispersion part of the model is basically a variable-trajectory, Gaussian-puff model with enhancements to account for complex terrain, effects of plant structures on flow, and thermal plume rise. Releases are represented as puffs of 15-minute duration which are tracked following the time-varying wind direction, rather than following a straight line based on wind direction at time of release. Concentrations around the center of the puff are modeled with a spatial Gaussian distribution. The spatial standard deviations of concentration (in the downwind, crosswind, and vertical directions), termed dispersion parameters, vary with the downwind distance of the puff. Crosswind and vertical dispersion parameters are based on the Pasquill-Gifford set for Gaussian plumes and the downwind dispersion parameter is taken identical to the crosswind parameter to ensure symmetrical puffs.[1]

The use of variable-trajectory puffs is one difference between our dispersion model and the standard models used to analyze hypothetical reactor accidents. Ideally for a variable-trajectory model, one would have wind data for downwind sites, not just for the source. Lacking such data around TMI, it was necessary to assume that data at the reactor site reflects downwind conditions, at least before terrain effects are incorporated.[2] Our sensitivity tests showed that for the particular weather conditions at TMI during the accident, the dose pattern from the variable-trajectory model does not differ significantly from that of a straight-line plume model. This is because for the times of the largest radioactivity release, during the evening of March 28, winds were quite steady.[3]

Primary inputs to the model are 15-minute wind speed, wind direction, and atmospheric stability data recorded at the TMI plant. The data were recorded as 15-minute averages by two sensors on the TMI tower. The data are complete except for a four-hour period (15:45-19:30) on March 28 when one of the sensors reported intermittently. Readings were averaged when they were available for both sensors; when the one sensor was not working, data was extrapolated by adding to the working sensor's reading one-half of the average difference between the two readings when both sensors were working. The[4]

---

[1] See Pasquill (1974) and Randerson (1984), in which Chapter 13 (S. Barr and W.E. Clements) discusses Gaussian formulations and further estimates of and corrections to the Pasquil-Gifford parameters.

[2] For example, the RAC2 model of Ritchie *et al.* (1984). Our model is similar to the proprietary variable wind mode of Pergola *et al.* (1986).

[3] Field tests have verified that this assumption is better as wind speeds increase (Hanna 1982, p. 309); although the TMI accident meteorology does not always meet these conditions, since there are no further data, the on-site measurements remain the best indicators of downwind conditions.

[4] Data were made available by Woodard and Potter and are tabulated in Beyea (1987).

average vertical temperature gradient is used to assign the atmospheric stability class that determines the dispersion parameters during each 15-minute interval. Outdoor temperatures for the first day and a half of the accident (from National Weather Service data for Harrisburg, PA) are plotted here in Figure A-l a.

Also input to the model are terrain contours at 100 foot (30.48 m) intervals above sea level, plus the contour at the 465 foot (142 m) height of the reactor vent stack.[5] An elevation plot of the terrain is shown in Figure A-2 (see Figure 4 in the main text for a contour map). The ground level elevation at the base of the unit-2 reactor is 308 ft (94 m).

The effects on dispersion of the hilly topography around the plant were modeled by tracking a puffs centerline motion with respect to terrain features according to potential flow theory.[6] Modeled puffs passed over elevated areas if momentum were sufficient, otherwise, the puffs went around the elevated area, splitting in two or going to one side depending on the size of the feature and width of the plume. Illustrations of puff paths are shown in Figures A-3 and A-4. Greater complexities arising from flow stagnation were not modeled. In order to carefully specify the plume shape near the plant, which would particularly affect the doses to the nearby dosimeters, the effects of plant buildings on the flow were modeled by extrapolating from the calculations by Halitsky.[7] (These effects are most important for the no plume rise case.) Flow disturbance by the cooling towers was handled by treating them as terrain features. Further details on the model are given by Beyea (1987). It turns out the our results are not very dependent on the terrain modeling. The effect of terrain on the dose pattern around TMI was not, however, known prior to our incorporation of terrain handling features into our model.

As discussed in the main text, plume rise has a greater effect on the resulting doses than terrain representation. The plume rise for the puffs was calculated following the discussion of Briggs (Chapter 8 in Randerson 1984; the following citations are to equations in this reference). Plume rise is modeled using cases that depend on the atmospheric conditions. In particular, for the stable conditions present during the times of important releases, we used Equation (8.70) with buoyancy and momentum fluxes initialized according to Equations (8.35) and (8.36) and a value of 0.7 for the entrainment coefficient. Outdoor temperatures during the release period are shown in Figure A-5. Note that the outdoor

---

[5] Contour d to were generalized from a re iced rac ng of 1:24,000 U.S. Geological Survey quadrangles by eorge Colbert, cartographer (ew York).

[6] The od for handling terrain effects are similar to those of Petersen (1986) and ERT (1980, V1, 951); for specifics, see Beyea (1987).

[7] Woodard and Potter, Appendix F.

temperature had dropped to around 6°C (44°F) during the evening of March 28, indicating that buoyant plume rise is likely during this time when the peak releases occurred--this matter is discussed more fully in the main text.

A.2 **Doses from radioactive plumes**

Doses of gamma radiation absorbed at a receptor from a passing radioactive plume were calculated as the sum of doses from the series of puffs used to represent the plume. This was done separately for each puff, i.e., each 15-minute release of unit activity, and for each position of the puff as it is propagated by the dispersion model. The point of closest passage of a puff to a receptor was used to define the geometry for the calculation (see Figure A-3). The result is a point kernel method of dose summation over space and time, using a finite plume integration based on breaking each puff into spatial bins treated as point sources. Puffs were treated as stationary during each 15-minute time step. The resulting dose factors, representing the dose rate at a receptor from a puff of unit activity release, were checked against the estimates published by Imai and Hjima (1970). The exposure from each point in a puff accounted for radiation attenuation through air, buildup from scattering in air, and scattering from the ground.

Exposures were calculated assuming a single 80 keV energy, the dominant radiation that would be received from ^{133}Xe. It was unnecessary to correct for decay in transit because the 5-day half-life of ^{133}Xe is much longer than transit times. These assumptions become progressively better after the early hours of the accident. We did incorporate an energy correction, based on the analysis in Appendix G of Woodard and Potter, into one of our sensitivity runs (case F, Table 6). This reduced the release and dose estimates by about 30%; however, we have reason to believe that the algorithm we used results in an overcorrection. Because the effect is not severe and moreover since our analysis indicates that the significant releases occurred after 10 hours from the start of the accident, further accounting of the energy mix is not likely to change the results significantly.

Conventional finite plume calculations neglect the impact of the ground (other than as a barrier to the plume) on gamma doses. The ground correction algorithm of Jacob and Paretzke (1985) was incorporated into our dose calculations for receptor points; although we include this correction in our calculations, sensitivity checks indicate that the effect is small. Further details on the integration algorithm and other features of the dosimetry model are given in Beyea (1987).

---

[8] A point kernal integration method Published by, homas *et al.*, originally designed for us ances within 1000 meters of the release point, was modified to extend the integration out to 10,000 meters. A tape copy of the program was made available to us by J.E. Cline.

Appendix **B**

Analysis of TLD data

Thermoluminescent dosimeters (TLDs) were the primary field instruments located in the area surrounding the Three Mile Island plant for the purpose of monitoring gamma-emitting radioactivity released from the plant.[9] At the time of the accident, two types of TLDs were in use at TMI. The primary set were $CaSO_4$:Dy (calcium sulfate doped with dysprosium) dosimeters, supplied by Teledyne Isotopes, Incorporated, at 20 locations. At ten of these locations, there was a supplemental set of $CaSO_4$:Tm (calcium sulfate doped with thulium) dosimeters, known as the "quality control dosimeters," supplied by Radiation Management Corporation (RMC).

The dosimeters around TMI were generally read quarterly until the accident, after which they were read every several days. Data prior to the accident are found in the Radiological Environmental Monitoring Program (REMP) reports[10] prepared for Metropolitan Edison by Radiation Management Corporation. Sources reporting TLD data for the TMI accident are Battist *et al.* (1979); Pickard, Lowe, and Garrick (1979); Auxier *et al.* (1979); and Rogovin (1979). The most comprehensive source of TLD data is the Pickard, Lowe, and Garrick report. Auxier *et al.* cite "Metropolitan Edison Company material supplied to the commission at their request."[11] Battist *et al.* do not cite references for the data and Rogovin cites the Auxier *et al.* report. (A comparison of reported TLD data for TMI is included here as a supplement to this appendix.) Within a few days of the accident, more TLDs were placed by various parties; however, since our present concern is with the noble gas releases which occurred early in the accident, only the dosimeters in place on March 28, 1979 are discussed here.

B.1 The TLD data record for TMI

Dosimeter data in the vicinity of the Three Mile Island plant are available since 1973 from the radiation monitoring program for the plant. Data prior to the accident were obtained from in the annual

---

[9] Thermoluminescence is a property of certain materials by which the material, when heated, emits light in reation to the dose of radiation which it has received. A TLD is a device containing material which has thermoluminsecent properties and having a design suitable for reproducibly measuring radiation doses. See Horowitz (1984) for a general discussion of TLDs.

[10] A Radiological Environmental Monitoring Program is required around all nuclear power stations; the annual reports on this program for the TMI station are listed as references under the acronym REMP by year of data reported.

[11] It is our understanding that Porter and Goertz, Consultants, Inc., of Philadelphia, PA, were contracted by Metropolitan Edison Company to handle the environmental dosimetry and that they are the original source of data analyzed in the reports cited here.

REMP reports (1973 to 1978) and are compiled in Table D-2 at the end of this report. Our primary concern here is with the earliest dose measurements recorded following the start of the accident. These data were obtained from TLDs collected on March 29, 1988. Table B-1 lists TLD data from this first period. The dosimeters had not been read since the last routine quarterly period (a six-month period for the three locations 14S2, 16A 1, and 10131). The tabulation includes the number of days elapsed since the TLDs were last read and the number of hours from the beginning of the accident to the time the dosimeters were collected. Listed for each location are the total dose (including background, uncorrected for energy response) in mrad accumulated through March 29, 1979 and the standard error of dose based on variations when reading each dosimeter.

The data in Table B-1 are taken from Pickard, Lowe, and Garrick, Table D-4. This tabulation matches Table 3-3 of Battist *et* al. and, except for an insignificant difference in the reading for dosimeter 1S2, it also matches Table A-17 of Auxier *et al.* and Table 11-20 of Rogovin. Information regarding the dosimeter locations required correction, since it was found that the coordinates given in earlier reports were not accurate (one dosimeter would have been located in the Susquehana River). At our request, TLD locations were rechecked by the consultant handling dosimetry at the time of the accident.[12] Plotting on survey maps resulted in an revised set of TLD coordinates.[13] We use the revised coordinates for our analysis and believe them to be the most accurate information available on the locations of TLD dose measurements for,the TMI accident.

[12] Corrected TLD locations were supplied by S.W. Porter, who also supplied collection times for the TLDs, based on information provided by the contractor who handled distribution and collection of the dosimeters before and during the March 1979 accident (R.L. Laughlin, memorandum of November 20, 1979, included with S.W. Porter, personal communication, April 18, 1988).

[13] Cartographic assistance was provided by George Colbert.

TABLE B-1. TLD readings for first collection period following TMI accident

	TLD	LABEL	KEY	DAYS	HOURS	DOSE1	STD1	BKGI	BMED	BSIG
1	1	1S1	0	92	36.67	97.9	1.9	4.67	5.4	1.2
2	1	ISI	3	92	36.67	95.7	5.0	5.71	5.4	1.2
3	2	2S2	0	92	37.25	43.7	4.4	4.07	4.7	0.5
4	3	4S2	0	92	37.12	35.5	4.3	4.80	5.6	1.3
5	3	4S2	3	92	37.12	31.4	1.6	4.91	5.6	1.3
6	4	5S2	0	92	37.08	30.5	1.3	4.30	5.0	1.3
7	4	5S2	3	92	37.08	27.7	4.0	4.32	5.0	1.3
8	5	9S1	0	92	36.92	25.0	3.0	4.67	5.5	0.4
9	6	11S1	0	92	36.83	216.0	24.1	5.07	5.8	1.1
10	6	1151	3	92	36.83	168.5	15.6	5.35	5.8	1.1
11	7	14S1	1	183	32.25	131.2	20.6	2.17	5.0	0.9
12	7	1451	2	183	32.25	148.3	9.7	2.17	5.0	0.9
13	8	16S1	0	92	36.75	1044.2	128.2	6.40	6.1	1.3
14	8	1651	3	92	36.75	929.4	90.5	3.93	6.1	1.3
15	9	4A I	0	92	29.33	20.2	1.3	4.60	5.2	0.5
16	10	5A I	0	92	29.17	18.6	1.0	4.60	5.2	0.6
17	10	5A1	3	92	29.17	16.1	1.3	4.57	5.2	0.6
18	11	16A1	1	183	32.17	907.7	49.4	2.03	4.7	0.5
19	11	16A1	2	183	32.17	453.4	12.2	2.03	4.7	0.5
20	12	IOBI	1	183	32.42	40.6	3.5	1.97	5.9	0.5
21	12	10B1	2	183	32.42	36.6	1.3	1.97	5.9	0.5
22	13	12B1	0	92	31.83	16.3	0.9	3.57	4.5	0.6
23	14	I CI	0	92	34.75	20.1	1.2	4.10	4.6	0.5
24	15	8C1	0	92	29.50	13.0	0.3	3.50	4.1	1.6
25	15	8C1	3a	92	29.50	12.6	0.6	4.07	4.1	1.6
26	16	7F1	0	92	30.00	24.1	1.8	6.57	7.7	0.8
27	16	7F1	3	92	30.00	23.3	0.5	6.15	7.7	0.8
28	17	4G1	0	92	38.17	17.2	2.1	5.30	5.9	1.0
29	17	4G1	3	92	38.17	17.7	0.1	4.94	5.9	1.0
30	18	7G1	Ob	92	30.33	25.8	0.6	7.20	8.5	3.2
31	19	9G1	0	92	30.83	21.3	1.4	5.60	6.2	0.7
32	20	15G1	0 ,	92	33.42	18.4	2.0	5.13	5.8	1.1
33	20	15G1	3	92	33.42	17.6	0.6	4.70	5.8	1.1

Column	Description
KEY	0 = Teledyne; 1,2 = Teledyne duplicates; 3 = RMC a = BKGI is 2nd quarter 1978; b = BKG1 is 4th quarter 1978
DAYS	Days of exposure since since previous dosimeter reading
HOURS	Hours of accident exposure, starting 4:00 am 3/28/79 (see Table B-5)
DOSE1	Doses read on 3/29/79 (mrad)
STD1	Standard error of dose readings (mrad)
BKG1	Average first quarter 1978 dose, except as noted for a,b (mrad/month)
BMED	Median dose 1973-78 (mrad/month)
BSIG	Standard error of BMED (mrad/month)

B.1.1 Background subtraction

For the purpose of assessing the radiation doses attributable to the TMI accident, we define the "background" dose at a location as the dose that would be received had the accident not occurred (including

doses attributable to normal operation of the plant). Doses from natural background gamma radiation in the United States average 4 (±2) mrad/month, with approximately equal contributions from cosmic and terrestrial sources (NCRP 94). It is necessary to subtract estimated background doses from the measured doses to obtain an estimate of the radiation dose due to the accident. A summary of the historical data from TLDs surrounding the TMI plant is given in Table D-2. Listed for each location are the day of reading and the number of days elapsed since the previous reading, the dose in mrad per standard month,[14] and two standard deviations of the dose based on the four sections of dosimeter material scanned when reading the TLD. See the notes following the table for an explanation of the codes in the headings and for missing data. The average of pre-accident median exposures over all of the TMI monitoring locations is 5.5 (±0.8) mrad per month.

One way to correct for background is to use the corresponding quarterly reading for the previous year. Such a method for background correction was used by Battist *et al.* and Auxier *et al.,* whose results were used by Rogovin. The BKG1 column in Table B-1 lists the first quarter 1978 values as mrad/standard month (a standard month is defined as 365/12 = 30.4 days). A background subtraction according to

NET! = DOSEI - (DAYS/30.4)*BKG1

yields the net (accident-only) dose estimate listed under the NET1 column of Table B-2.

The reason given by Battist *et al. (p.* 33) for using only first quarter 1978 data to estimate background exposures is so that "any seasonal effect on background should be minimized." In general, there may be seasonal variations in background, for example, due to solar cycles and to the attenuation of terrestrial radiation by snow cover. Reliance on a single quarter out of five years of available data seems somewhat questionable in terms of reliability, however, and so we felt it worthwhile to analyze the historical data to see if seasonal trends were apparent.

We examined 5 years of TLD readings prior to the accident and used the median values of the 1973-78 data for each TLD site as our estimates for background doses[15]. These estimates are shown in

---

[14] Measured doses are reported. herein the conventional units of absorbed dose, mrad, for consistency with previous work on the accident (1 mrad = 0.01 mGy). Average dose rates per month are calculated for a standard month length of 30.4 days.

[15] For consistency with Battist *et al.*, the 7 1 background value is taken from last quarter 1978 because "the first quarter exposure for 197 (15.8 mrad/std.mo.) was substantially greater than that for subsequent quarters."

[16] The median is more robust than the mean in the sense of, being insensitive to outliers (which might be due to unusual circumstances, such as fallout from atomic bomb tests); see, e.g., Mosteller and Rourke.

TABLE B-2. Net and energy corrected TLD doses

	LABEL	KEY	NETI	CNETI	NETM	NSIG	CNETM
1	1S1	0	83.8	70.3	81.5	4.1	68.4
2	1S1	3	78.4	78.4	79.3	6.1	79.3
3	2S2	0	31.4	26.3	29.4	4.6	24.7
4	4S2	0	21.0	17.6	18.5	5.8	15.5
5	4S2	3	16.5	16.5	14.4	4.2	14.4
6	5S2	0	17.5	14.6	15.3	4.1	12.8
7	5S2	3	14.6	14.6	12.5	5.6	12.5
8	9S1	0	10.9	9.1	8.3	3.2	6.9
9	11S1	0	200.7	168.6	198.4	24.3	166.7
10	11S1	3	152.3	152.3	150.9	15.9	150.9
11	1451	1	118.1	99.2	101.1	21.3	84.9
12	1451	2	135.2	113.6	118.2	11.1	99.3
13	1651	0	1024.8	861.2	1025.7	128.2	861.9
14	1651	3	917.5	917.5	910.9	90.5	910.9
15	4A1	0	6.3	5.2	4.4	1.9	3.7
16	5A1	0	4.7	3.9	2.8	2.0	2.3
17	5A1	3	2.3	2.2	0.3	2.2	0.3
18	16A1	1	895.5	752.5	879.4	49.4	738.9
19	16A1	2	441.2	370.7	425.1	12.5	357.2
20	10B1	1	28.7	24.1	5.0	4.6	4.2
21	10B1	2	24.7	20.7	1.0	3.2	0.8
22	12B1	0	5.5	4.6	2.6	2.0	2.1
23	1C1	0	7.7	6.4	6.1	1.9	5.1
24	8C1	0	2.4	2.0	0.5	4.8	0.4
25	8C1	3	0.3	0.2	0.1	4.8	0.1
26	7F1	0	4.2	3.5	0.8	3.0	0.6
27	7F1	3	4.7	4.6	0.0	2.4	0.0
28	4G1	0	1.2	0.9	0.0	3.6	0.0
29	4G1	3	2.8	2.7	0.0	3.0	0.0
30	7G1	0	4.0	3.3	0.0	9.7	0.0
31	9G1	0	4.4	3.6	2.5	2.5	2.1
32	15G1	0	2.9	2.4	0.8	3.8	0.6
33	15G1	3	3.4	3.3	0.0	3.3	0.0

Column	Description
KEY	0 = Teledyne; 1,2 = Teledyne duplicates; 3 = RMC
NET1	Dose net of 1st quarter 1978 background subtraction (mrad)
CNET1	NET1 with Teledyne response corrected by 1/1.19 (mrad)
NETM	Dose net of 1973-78 median background subtraction (mrad)
NSIG	Standard error of NETM, computed as $NSIG = STD1 + (DAYS/30.4)\ BSIG$
CNETM	NETM with Teledyne repsonse corrected by 1/1.19 (mrad)

Table B-2. Previous analysts used either first quarter 1978 doses (e.g., Battist *et al.)* or average 1978 doses (Pickard, Lowe, and Garrick). The first quarter 1978 doses are all slightly lower than the 1973-78 medians, falling two standard errors below the 1973-78 median at three locations (14S2, 16A1, IOBI), which happen to be the sites where the first quarter reading is from a 6-month exposure period because river conditions preclude a last-quarter reading. The average 1978 doses (which are higher than the first

quarter doses) are significantly higher than the 1973-78 medians at only two locations (11 S1 and 16S 1). We found no consistent seasonal trends in the 1973-78 data from the TMI dosimeters. While the 1973-78 medians generally differ little from the background estimates based on 1978 data alone, using a larger data base yields more reliable estimates of the average background and provides, moreover, estimates of the variance of background radiation which are helpful for error analysis of the dose measurements.

Our background correction procedure for the first period of the TMI accident used the gross dose readings ending March 29, 1978 and the 1973-78 medians, with net doses computed as

NETM = DOSEI - (DAYS/30.4)*BMED

The results are also shown in Table B-2. The NSIG column gives a standard error estimate reflecting the combined reading uncertainty and the background uncertainty (STD1 and BSIG in Table B-1, respectively).

B.1.2 Transit exposure

Another source of TLD exposure not due to accident releases is radiation exposure during transportation and storage of the dosimeters between their monitoring sites and the laboratory where they are read. Such transit doses depend on the thickness of shielding used when the dosimeters were not deployed, the handling, and the radiation environment in areas through which they pass during transportation. Exact pickup times for the TLDs were supplied for this study along with the following information regarding the treatment of TLDs during the TMI accident:[17]

> Teledyne TLDs were normally annealed at the sample collector's home the day before placement in the field. The controls were annealed prior to shipment of the set of TLDs back to the lab for analysis. RMC TLDs were annealed at RMC a day or two prior to placement in the field. They were picked up by a sample runner and brought back to the sample collector's home prior to placement in the field. Their controls were not annealed prior to shipment back to lab. Beginning 4-6-79, the TLDs after annealing were kept in a lead-lined card file box until placed in the field. The removed TLDs were also kept in the lead container until shipment to lab.

No further details on the handling of the TLDs were available in time for the preparation of this report. In particular, we were lacking information on whether the dosimeters were shielded during transit prior to April 6, 1979. Therefore, corrections for possible transit doses have not been made. Although it is not expected that such information would have an impact on first period results, it makes a reliable

[17] R.L. Laughlin, memorandum of November 20, 1979, included with S.W. Porter, personal communication, April 18, 1988.

analysis of the second and subsequent periods (following March 29, 1979) difficult. Further information related to TLD handling and the paths taken during transit recently provided by the defendants' counsel of the TMI Public Health Fund may be of help in resolving these issues.

B.1.3 Energy response correction

Auxier *et al.* discuss the likely over-response of the Dy-doped (Teledyne) dosimeters to the relatively low energy (30 keV and 80 keV) radiation from ^{133}Xe released at TMI as compared to the higher energy (660 keV from ^{137}Cs) used for calibrating these TLDs. Since the RMC dosimeters have shields designed to correct for this over-response, Auxier *et al.* estimated a response correction factors for the Teledyne dosimeters based on an average of their ratios with the RMC dosimeters. Auxier *et al.* used only five of the ten locations, arguing that the readings at the other locations were not sufficiently different from. background to be reliable. Battist *et al.* (pp. 15-16) and Pickard, Lowe, and Garrick (p. 4-16 and Appendix G) both discuss the energy dependence of TLD response but do not apply a correction for it, the later reporting that the over-response is probably not greater than a factor of 1.5.

A further complication in interpreting such field data is the possible contamination by beta radiation of the readings, which are intended to represent only gamma doses. Such "beta feed-through" would occur only when the TLDs were immersed in the plume. To examine this and other issues, several analysts performed post-hoc calibrations of TLDs of the type used at TMI. Plato *et al.* (1980) and Oately *et al.* (1981) tested the response of the RMC dosimeters (Panasonic type 804, $CaSO_4$:Tm) to ^{133}Xe in both submersion and distant source geometries. The dosimeters were found to over-respond to submersion and to under-respond to a distant source, with a 5-fold difference (0.4 to 2) in the mean deep-dose response. Riley *et al.* (1982) tested both the Teledyne and RMC dosimeters for their response to a distant source of ^{133}Xe at various angles. Both type of dosimeters were found to over-respond on average, and the over-response was greater when only the 80 keV radiation (having a longer path in air) was present, the lower energy (30 keV) ^{133}Xe radiation being filtered out. The mean over-response was 1.6 times the calibration dose for the Teledyne dosimeters and 1.3 for the RMC dosimeters, confirming the relative response characteristics of the two types of TLDs that had been inferred by Auxier *et al.*

We conclude that it is appropriate to do a correction of the Teledyne dosimeters against the RMC dosimeters, in order to place the readings from both types of dosimeters on the same scale. That scale remains, however, very uncertain in terms of the actual level of absorbed dose to be inferred from the

TLD data. Therefore, error weighting of the TLD data should be large enough span the response uncertainty. Note that such factor-of-two magnitude uncertainties do not preclude using the TLD data for dose assessment because the range of recorded doses spans three orders of magnitude.

A plot of the Teledyne versus RMC dosimeter readings is shown in Figure B-1, in which a log-log scale is used because of the large range of doses measured for the first period. The correspondence is appears quite linear, with most points being slightly above the 45-degree line. Regressing the Teledyne against the RMC readings for the five locations having doses significantly elevated above background (1S1, 4S2, 5S2, 11S1, and 16S1) using a multiplicative model (equivalent to a log-log regression) yields an estimate of 1.19 (±0.01) for the correction factor, with a RMS residual error of 10% of dose. A multiplicative model is appropriate in this case because the range of doses is so large that the error is better treated as proportional to dose rather than as a constant additive error. The resulting estimate of 1.19 is the same for both the NETI and NETM columns, that is to say, it is not sensitive to the method of background subtraction. This estimate matches the result obtained by Auxier *et al. (p.* 83 and Table A-15).

Dividing the NET! column by the factor 1.19 yields the corrected dose estimates which are listed in the CNETI column of Table B-2. The resulting Teledyne doses match those reported by Auxier *et al.* (Table A-18) and Rogovin (Table II-21) `with the exception of locations 14S 1, 16A 1, and I0BI. A serious error, probably typographical, occurs in the value reported by Auxier *et al.* (and Rogovin, which is based on Auxier *et al.)* for location 14S1. The reported value of 11.6 mrad is an order of magnitude lower than the value of 108.7 mrad obtained as the weighted average of the two dosimeters. As discussed here in Section B.5.4, Auxier *et al.* seem to have used three months instead of six when calculating the background correction for locations 1451, 16A1, and 10B1, resulting in a slight overestimate of net dose for the latter two sites, but then must have dropped the leading "1" for location 14S1 to obtain the erroneous value reported in their table.

The CNETM column of Table B-2 gives the energy-corrected net dose after background subtraction based on the median historical doses. The NSIG column represents the standard error based on reading error for the dose measured for the period ending 3/29/79 and on the variability of background dose; it does not include an uncertainty factor for the energy response. Based on the NSIG error alone and assuming normal error distribution, doses at eight (5A 1, I0BI, 12B1, 8C 1, 7F1, 4G1, 7G 1, and 15G 1) of the twenty locations are not significantly different from zero.

B.2 Data for input to dose assessment

The base case analysis reported in section 3 of the main text uses the Teledyne values from the NETM column of Table B-2. These are also tabulated in Table 1 of the main text, which also lists the TLD monitoring site coordinates. For locations having duplicate dosimeters, a single dose value was calculated as the weighted average of the energy-corrected net doses (CNETM column of Table B-2, with inverse standard errors used for weighting). This calculation yields the values shown in Table B-3. In all instances except location 16A1, doses from duplicate dosimeters values match well, whether they be from the same type dosimeter or from a different type, e.g., mixed Teledyne and RMC. An overall estimate of the error in the net dose values was obtained by combining the standard errors from Table B-2 with the error represented by the difference between duplicate readings; this overall error is shown under the S.E. column of Table B-3.

The duplicate readings for location 16A1 differ by a factor of two; their weighted average, computed as described above, is the value given for this site in Table B-3. Regarding site 16A 1, Auxier *et al.* state (p. 89)

> After carefully examining the situation, the task group determined that the larger of the two values was more likely to be correct, so the smaller value was discarded. The shielding of one dosimeter by the other and inadequate heating of the dosimeter were given as reasons for an incorrect, reduced value; no plausible reasons were given for an incorrect high reading.

Rejection of the lower reading for site 16A1 would therefore based on an educated guess; unfortunately, this site having a big discrepancy is also the site showing the second highest dose. To see how sensitive the source term and population dose estimates would be to this reading, the key analyses were performed twice, using the single high reading and using the average reading as the dose for location 16A1. As noted in section 4 of the main text, this had little effect on the release estimation and dose assessment results.

TABLE B-3. Estimated net TLD doses averaged by location

	LABEL		DOSE	S.E.	%ERR
I	1S1		72.8	8.5	12
2	2S2		24.7	4.6	19
3	4S2		14.9	3.5	23
4	5S2		12.7	3.4	27
5	9S1		6.9	3.2	46
6	11S1		157.1	17.6	11
7	14S1		94.4	14.5	15
8	1651		890.6	82.6	9
9	4A1		3.7	1.9	51
10	5A1		1.3	2.1	100+
11	16A1	**	516.8	321.5	62
12	10B1		2.2	3.6	100+
13	12B1		2.1	2.0	95
14	1C1		5.1	1.9	37
15	8C1		0.3	3.4	100+
16	7F1		0.3	1.9	100+
17	4G1		0.0	2.3	100+
18	7G1		0.0	9.7	100+
19	9G1		2.1	2.5	100+
20	15G1		0.3	2.5	100+
11	16A1	**	879.4	49.4	6

Column	Description
DOSE	Net absorbed dose (mrad) through TLD collection time on 3/29/79.
S.E.	Estimated standard error of dose, based on: (1) variability among the four different areas of each dosimeter; (2) variability of background radiation; (3) variability of duplicate dosimeters at same location.
%ERR	Error as a percentage of dose (S.E./DOSE).

** The higher value for site 16A1 is obtained when the low duplicate reading is discarded and the lower value is the weighted average (see Table B-2).

B.3 Error analysis

At this point it is useful to summarize the various sources of uncertainty in the dose measurements obtained from the TLDs. These are:

1. Reading error. The Teledyne and RMC dosimeters utilize different measurement systems but both result in multiple readouts of dose for each dosimeter location. The reported dose is the average and the reported standard error is the standard deviation of these readouts[18]. We refer to this measure of dose uncertainty as the reading error.

[18] See Auxier *et al.*, pp. 65ff. To the REMP reports the error is often reported as two standard deviations of the readouts; we divided by two to obtain the standard errors tabulated here.

2. Background error. The variability in doses measured in years prior to the accident results in an uncertainty in the background dose which is subtracted from the measured doses in order to determine the dose attributable to the accident. As discussed above, we estimate this uncertainty from the interquartile range of the historical doses (which was generally close to their sample standard deviation), using the median and IQR rather than the mean and standard deviation because they are less sensitive to outliers.
3. Calibration error. The response of TLDs to radiation exposure is not known except by calibrating the instruments against some standard. Even after such calibration, some variability remains, a large part of which is due to the dependence of response on the energy of the incident radiation as well as on the geometry of exposure. As noted in our discussion of the data in Table B-2, the energy response calibration was addressed by using the RMC dosimeters as a reference. Because the response of the RMC dosimeters is itself uncertain, an overall calibration uncertainty on the order of a factor of two is likely to remain.
4. Redundancy error. By redundancy error we mean the uncertainty reflected in the fact that TLDs at the same location do not give the same doses within the confidence interval suggested by the reading error. The worst example of this is for location 16A1, where the readings of two Teledyne dosimeters differ by a factor of two. Note that what we are terming redundancy error includes unknown calibration errors as well as other unspecified sources of error.

The three sites having redundant Teledyne TLDs are 14S1, 16A1, and 10B1, for which the dose measurements differ by 12%, 67%, and 10%, respectively (percent variations around the average of the two values). The differences for 1451 and 10B1 are easily within a 95% normal confidence interval based on their reading errors, giving no reason to suggest an additional source of uncertainty. Assuming we do not reject the lower value at site 16A1, however, we should consider the possibility of a larger uncertainty. We therefore averaged the percent errors for the three sites, giving 30% as an estimate of redundancy error. To check the effect of the data weighting implied by this error estimate, the source term estimation was performed using redundancy errors of 10%, 30%, and 50%. As discussed in section 4 of the main text, this was found to have little effect on the results for release estimation and dose projection. The choice of error weighting applied to the TLD data is certainly much less critical than choices made for parameters such as plume rise and wind direction bias.

BA Information from TMI dosimetry contractor

This section contains information related to the TLDs based on the records of the contractor[19] who handled environmental dosimetry around the TMI plant before and during the 1979 accident at TMI unit 2. This information was obtained for the Three Mile Island Public Health Fund Dosimetry Project with the assistance of General Public Utilities' counsel[20] and consultant.[21] Much of this information has not been previously published in the literature regarding the TMI accident and is collected here as a matter of public record as well as for reference by the analyses presented in this report.

Table B-4 lists descriptions of the TLD sites and gives elevation information for the ground at the site and for TLD as mounted at the site.[22] Also given are the solid angles of exposure for the mounted TLDs as estimated by R.L. Laughlin. Table B-5 is a copy of the list of start and stop times for TLD exposure periods and a transcription of the notes regarding the times and the annealing procedures.[23]

[19] R.L. Laughlin of Elizabethtown State College, Elizabethtown, PA.

[20] Represented by A.H. Wilcox of Pepper, Hamilton, and Scheetz, Attorneys at Law, Philadelphia, PA.

[21] S.W. Porter, Porter Consultants, Inc., Ardmore, PA.

[22] Sources are "TLD mounting procedure at TMI, Marc 1 79" notes, initialed 5/17 88 by R.L. Laughlin, and "Ron Laughlin TMI TLD/sample route of /29/89" (received with A. . Wilcox letter to J. Beyea, May 16, 1989); "TMI TLD locations - March 1979" table of Porter Consultants, March 1988 (received with S.W. Porter letter of J. Arbo, April 18, 1988).

[23] Source is writeup dated 11/20/79 by R.L. Laughlin (received with S.W. Porter letter of J. Arbo, April 18, 1988).

TABLE B-4. TLD monitoring sites and exposure geometry

Site	Location description	Elevations (ft) Ground	TLD	Exposure geometry
1S1	TMI N meteorology station	300	303	4p
2S2	TMI entrance, N bridge	300	304	3p
4S2	top of E dike even with cooling tower	310	313	4p
5S2	top of E dike near cross fence	310	313	4p
9S1	S beach along Island Rd. across from E dam	290	294	3p
11S1	W fence at mech. draft cooling tower	300	303	4p
14S1	picnic area E side of Shelley Island	280	283	4p
1651	gate in fence, N boat dock	300	303	4p
4A1	Laurel Rd. E of route 441	330	336	3p
5A I	front of TMI observation center, route 441	340	343	4p
16A1	S end of Kohr Island	280	283	4p
10131	S beach of Shelley Island near corn field	285	288	4p
12B1	Goldsboro air station, fishing creek	290	293	4p
1C1	Mill St. substation, Middletown	302	305	4p
8C1	Collins substation, Falmouth	318	321	4p
7F1	Dragers farm, off Engles Tollgate Rd.	340	343	4p
4G1	route 241, pole J-1813	455	461	4p
7G1	Columbia water treatment plant, along river	250	255	2p
9G1	York substation, S of route 30, edge of Prospect Hill cemetery	385	388	4p
15G1	W Fairview substation, by railroad	344	347	4p

TABLE B-5. Start and stop times for TLD exposure periods
(continued--transcription of R.L. Laughlin notes dated 11/20/79)

Except for the times given for 12/27/78 (start time only), the times indicated represent the stop time of one period of exposure and the start time of the next period of exposure.

Teledyne TLDs were normally annealed at the sample collector's home the day before placement in the field. The controls were reannealed prior to shipment of the set of TLDs back to the lab for analysis.

RMC TLDs were annealed at RMC a day or two prior to placement in the field. They were picked up by a sample runner and brought to the sample collector's home prior to placement in the field. Their controls were not reannealed prior to shipment back to the lab.

Beginning 4/6/79, the TLDs after annealing were kept in a lead-lined card file box until placed in the field. The removed TLDs were also kept in the lead container until shipment to the lab.

Times and dates when Teledyne TLDs were annealed:

For set removed on	set annealed	controls annealed
3/29/79	pm 12/26/78 **	pm 3/29/79
3/31/79	pm 3/27/79	15:00 3/31/79
4/3/79	pm 3/30/79	18:30 4/3/79
4/6/79	22:00 4/2/79	22:00 4/6/79
4/9/79	22:00 4/5/79	19:00 4/9/79
4/12/79	20:00 4/8/79	22:00 4/12/79
4/15/79	20:00 4/11/79	18:00 4/15/79

** the island set (14S1, 16A1, 10B1) were annealed 9/26/78.

B.5 Supplement

A comparison of TMI reports discussing TLD data.
Prepared by John Arbo, New York, NY, May 1988.

B.5.1 Introduction

This section contains a comparison of dose and error calculations and reportage, for individual Met-Ed Teledyne TLDs, by Battist, Auxier, and Rogovin[24].

Battist does not provide specific references for data sources. Auxier does provide such references, but many are just "[paraphrased] material supplied by Met-Ed" and, so, are not directly accessible for checking. Rogovin--at least as regards the final result of net exposure which is of interest here--simply cites Auxier.

B.5.2 Total exposures reported

I compared total exposure values reported for Met-Ed Teledyne TLDs by

Battist, Table 3-3, page 24

Auxier, Table A-17, page 87

Rogovin, Table II-20, page 391

Identical total exposures are reported for all TLD sites and exposure periods by all three sources excepting for

(1) site I S2, exposure period 12/27/78 - 3/29/79
Battist reports 97.9 ±1.9 mR
Auxier, Rogovin report 97.2 mR

(2) site 9S2, exposure period 3/29/79 - 3/31/79
Battist reports 25.3 ±2.6 mR
Auxier, Rogovin report 25.1 mR

(3) site 5A1, exposure period 3/29/79 - 3/31/79
Battist, Auxier, and Rogovin all report 8.3 mR in the main tables but Battist also reports two "additional values" of 7.8 ±1.5 mR and 7.4 ±1.2 mR in footnote (3) of Table 3-3.
[ed. note: also found in Auxier, Table A-11]

Neither Auxier nor Rogovin mentions the exceptions with respect to Battist noted above. Battist does not report exposures terminating later than 4/6/79 (the Battist report was early and preliminary).

For each total exposure reported, Battist lists a statistical error as "... ±standard deviation per exposure period" calculated as the "... standard deviation of the multiple readings" (Battist, p. 15, §1). Presumably, the phrase "multiple readings" refers to "... measurements of exposure ... made on each of

[24] Battist *et al.* (1979), Auxier *et al.* (1979), and Rogovin (1979), respectively.

four separate areas of the dosimeters" (Battist, p. 13, §2). Where more than a single TLD was in place, Battist reports the total exposure and associated error separately for each TLD (e.g., 5A1, 16A1, 14S1, and 10B1). Auxier and Rogovin do not report such errors, although such errors are discussed and assessed in Auxier (p. 65, 70, and Table A-11). [I discuss estimation of error more generally later in this report.]

B.5.3 Background data reported

Background is reported as exposure rate in mR/mo (for a standard month = 30.4 days) rather than as exposure per measuring period. Identical first quarter 1978 exposure rates were reported by all three sources (Battist, Table 3.5, p. 78; Auxier, Table A-17, p. 87; Rogovin, Table II-20, p. 391), excepting for site 7G1, for which Battist reports 15.8 ±0.7 mR/mo versus 7.2 mR/mo reported by Auxier and Rogovin. However, Battist (p. 33, §2) notes that site 7G1 is "inside a brick building" and that the 15.8 mR/mo first quarter 1978 rate is anomalously high. Battist elects to use the last quarter 1978 value of 7.2 mR/mo as the background rate for site 7G1. Thus, all three sources effectively report identical background rates for the purpose of calculating net doses. Neither Auxier nor Rogovin mentions this exception. Battist does not offer any possible reason for the high first quarter 1978 exposure rate at site 7G1. Neither does the 1978 REMP report, stating that "TLDs indicate only natural environmental radiation was observed in 1978" (p. 4, §2). Table 3-5 of Battist, which gives data for all quarters of 1978, was found to be identical with Table B-23 of the Met-Ed 1978 REMP, excepting for (1) the error associated with the first quarter for site 10B1: Battist gives ±0.20 while the REMP gives ±0.10 and (2) as noted by Battist in footnote "**" of Table 3-5, identification of sites 11S1 and 14S1, which were "originally reported [in the REMPI, erroneously, as stations 11S2 and 14S2."

B.5.4 Calculation of net exposures

Battist does not report the net exposures for each TLD (only collective dose estimates are given). Like Auxier and Rogovin, Battist subtracts background based on measured first quarter 1978 exposure rates (except for site 7G1, as previously noted). Unlike Auxier and Rogovin, Battist does not apply energy-dependence correction factors to adjust net exposures, although the matter is discussed (Battist, pp. 15-16). Rogovin (Table 11-21) and Auxier (Table A-18) report identical net exposures for Met-Ed TLDs. Rogovin cites Auxier, Table A-18, as the source for net exposures (Rogovin, reference number 149, p. 442). Auxier lists estimated errors for each net exposure. Rogovin, without comment, does not. Therefore, only the Auxier results will be discussed further here.

To calculate net exposures and associated errors, Auxier uses the following assumptions and methods:

For total exposures (Auxier, p.89, §2):

(1) Auxier states that the total exposures (given in Table A-17) were "adjusted for transit and instrumental background, but not historical background." Neither transit nor instrumental background adjustments are specified.

(2) For the earliest post-accident exposure period,

a) At sites 16A1, 14S1, and 10B1, two Teledyne TLDs (instead of only one) were left at each site for 6 months (instead of only 3) because of river icing. Presumably, the starting date for these TLDs was 9/27/78 (i.e., start of fourth quarter according to the 1978 REMP) (also confirmed by 4/18/88 private communication from Sid Porter[25]). So the exposure period was 9/27/78 to 3/29/79 or 182 days, assuming identical start/stop times.

At site 16A1, the measured exposures from the two TLDs were discordant by nearly a factor of 2. The higher exposure is used; the lower exposure is rejected because of possible "shielding of one dosimeter by the other, and inadequate heating of the dosimeter" (I found no other discussion of this).

For sites 14S1 and 10B1, the total exposure at each site was taken as the average of the two measured exposures at each site.

b) At all other locations, a single Teledyne TLD was in place from 12/27/78 to 3/29/79, or 92 days, assuming identical start/stop times.

Background is estimated using first quarter 1978 exposure rates recorded at each dosimeter site (except for site 7G1, for which the fourth quarter 1978 rate was used, as previously noted). Specifically, the background data used by Auxier were taken from the 1978 REMP, Table B-23. These data are given in terms of dose rate with units of mR per standard month, where a standard month equals 30.4 days. The total quarterly exposures for 1978 are not reported in the 1978 REMP, so I cannot confirm the accuracy of the exposure rate calculations. For the post-accident exposure periods given in Table A-17, the number of days in each period [listed in table below], while not specified exactly by Auxier, can be deduced either from the start/stop dates (assuming identical start/stop times) or from requirements for calculation of the net exposures reported in Table A-18 [Auxier]. The number of days per period

[25] Porter Consultants, Inc., 125 Argyle Road, Ardmore, PA.

was checked against the pick-up time table in Sid Porter's communication dated 4/18/88. They are correct within about ±6 hours--more detailed calculations can be done using the actual start/stop times to improve the accuracy of the background correction.

Locations	Exposure period	No. of days
Sites 16A1, 1451, 10B1	9/29/78 - 3/29/79	182
All other sites	12/27/78 - 3/29/79	92
For all sites	3/29/79 - 3/31/79	2
For all sites	3/31/79 - 4/ 3/79	3
For all sites	4/ 3/79 - 4/ 6/79	3
For all sites	4/ 6/79 - 4/ 9/79	3
For all sites	4/ 9/79 - 4/12/79	3
For all sites	4/12/79 - 4/15/79	3

Because the Teledyne TLDs over-respond to low energy radiation, Auxier estimates energy-dependence corrections factors which are to be divided into the net exposure after background subtraction, to yield the adjusted, final net exposure. Auxier uses 1.19 as the correction factor for the early post-accident period of 3/28 - 3/29/79 (corresponding to the TLD exposure period from 9/27/79 or 12/27/78 to 3/29/79) and 1.5 for later exposure periods. Auxier argues (pp. 77-85) that the factor of 1.19 is appropriate for the early post-accident period because of the presumed higher average energy of the early post-accident gamma exposure from radio-krypton while the later periods are dominated by lower energy radio-xenons which require a larger correction for over-response. Auxier cites the observed ratios of doses from Teledyne TLDs relative to corresponding doses from RMC TLDs as support for the values chosen for the energy dependence correction factors. Thus, the algorithm used by Auxier to calculate net exposure is

$$N = (T - (D/30.4)xB) / F$$

where
- N = net exposure (mR)
- T = total exposure (mR) for the period
- B = background exposure rate (mR/mo)
- D = number of days in the exposure period
- F = energy-dependence correction factor,
  - 1.19 for exposures up to 3/29/79
  - 1.5 for exposures after 3/29/79

[Editorial note: Arbo provided sample calculations for sites ICI and I1S1 which are not included here.]

Serious error was found in the calculation by Auxier of net dose for sites 16A1, 1451, and 10B1 for the period ending 3/29/79:

16A1: T = 907.7 mR (high value only)
- = 2.03 mR/mo, D = 182 days, F = 1.19
- = (907.7 - (182/30.4)x2.03) / 1.19 = 752.6 mR

versus 758.0 mR reported in Auxier.
Auxier appears to have used D = 92 days instead of 182 days, which yields a result of 757.6 -- 758.0

14S 1: T = average of 2 TLDs
= (131.2 + 148.3)/2 = 139.75
- = 2.17 mR/mo, D = 182 days, F 1.19
- = (139.75 - (182/30.4)x2.17) / 1.19 = 106.52 mR

versus 11.9 mR in Auxier!
Auxier may have used D=92 days, giving 111.9 mR, and then dropped the leading "1" (i.e., a typo) ??

10131: T = average of 2 TLDs
(40.6 + 36.6)/2 = 38.6 mR
- = 1.97 mR/mo, D = 182 days, F = 1.19
- = (38.6 - (182/30.4)x1.97) / 1.19 = 22.5 mR

versus 27.4 mR reported in Auxier.
Auxier appears again to have used D = 92 days.

Appendix C

Comparisons of dose patterns

One of the objectives of the work reported here was to provide a validation and sensitivity analysis of the doses to population blocks that were used for a concurrent epidemiological investigation of cancer in the vicinity of Three Mile Island.[26] The model used to calculate the doses for that study was an earlier version of the base case model described in this paper. The source term used was a set of relative release rates based on the adjusted area radiation monitor data given by Pickard, Lowe, and Garrick. The TMI epidemiology study therefore did not utilize release rates estimated by back calculation from TLDs and it did not include the refinements for ground correction and cooling tower wake effects. We recalculated the doses to population blocks under varying modeling assumptions in order to examine how the model assumptions affect the geographic pattern of doses around TMI. These results were compared to two reference cases: (a) the model used for the epidemiology study and (b) our base case model as described in Section 3 of this paper. For each model variation, we (1) computed doses over the study area blocks, (2) computed the correlation[27] of the these doses with those of the two reference models, and (3) plotted the relative differences between these block doses and the reference case doses.

Table C-1 lists the resulting correlation coefficients. Dose patterns that correlate well with the epidemiology study can be expected to have little effect on the outcome of the study. Examining Table C-1, it can be seen that the correlations are quite good except for the wind direction shifts. This suggests that possible errors in the wind direction data used in the dispersion model, particularly if the wind were more westerly than assumed (the -5° case), would be the dominant uncertainty (among those due to dispersion modeling) in interpreting epidemiological results. Note, however, that the nominal wind direction gives the best fit to the TLD data.

---

[26] Hatch *et al.* (forthcoming), of which J. Beyea is a co-author, referenced here as the "epidemiology study."

[27] Pearson correlation coefficient, see, e.g., Mosteller and Rourke, p. 291.

TABLE C-1. Correlations of block doses generated under varying model assumptions to block doses of base case models.

Case	Modeling assumptions[a]	Correlations with: Epi study	Case A
A.	Base case as given in this paper(b)	0.971	1
B.	No plume rise, meandering plume	0.983	0.986
C.	100°C thermal plume rise	0.956	0.968
D.	+5° wind shift	0.924	0.942
E.	-5° wind shift	0.705	0.734
F.	Energy-corrected TLD data[c]	0.956	0.996
I.	Straight line plume	0.954	0.970
J.	Straight line plume, no plume rise	0.963	0.957
K.	Straight, adj. source term(d)	0.963	0.967
L.	Straight/no rise, adj. source term[d]	0.962	0.955

NOTES

(a) Only the assumption in which each case differs from the base case is listed here. For further details, see the discussion of sensitivity analyses in Section 4.1 of the main text.

(b) The base case model involves puffs changing direction with the wind and with effects of terrain and cooling towers, ground correction (but no building shielding) for gamma doses, and nominal Teledyne TLD, data.

(c) Other TLC-related assumptions (data weighting, treatment of 16A 1) had so little effect that they are not considered here.

(d) Source term based on adjusted area monitor trend from Pickard, Lowe, and Garrick multiplied by a constant scale factor estimated by a weighted least-squares fit to our set of data for the 20 TLDs.

The dose pattern projected by the base case model (Case A) was shown in Figure 6 of the main text. The dose pattern within the 10-mile radius study area projected by the dose model used for the epidemiology study is shown here in Figure C-1(a). Part (b) of the figure shows the differences in the block dose patterns projected by the Case A and the epidemiology study models. Plotted for each plot is the percent difference, calculated as a relative difference by scaling the doses from each model so that the maximum block dose is given a value of 100 and then subtracting the resulting scaled epidemiology study dose from that of Case A. For example, the greatest difference in relative dose occurs in block 8, where the Case A model prediction is lower than the epidemiology study model prediction by 22% of the maximum predicted block dose. (Refer to Figure 1 of the main text and Table D-1 for block locations and identifying numbers.) Figures C-2 and C-3 show the relative dose differences similarly calculated for other modeling cases.

Figure C-2 illustrates the effect of changing the plume rise assumption on the dose distribution patterns by showing the relative dose differences of the Case A model, which assumes 10° thermal plume buoyancy, with (a) the Case B model, which has no plume rise, and (b) the Case C model, which assumes 100° thermal plume buoyancy. The block receiving the highest dose is block 74 for all cases A, B, and C, and so the relative dose difference for this block (about 4Z miles out in the NNW sector) is zero in the figures. Figure C-2(a) shows that assuming no plume rise generally lowers the relative doses; Figure C-2(b) shows that increasing the plume rise lowers the doses in the northern sector but tends to raise them in the NW and somewhat in the NE relative to Case A, as might be expected on the basis of terrain in those areas. In either case, most changes are insignificant in terms of the overall pattern, as indicated by the correlation coefficients of well over 0.9 listed in Table C-1.

Figure C-3 illustrates the effect of changing the assumption regarding a possible bias in the wind direction. The base case model (Case A) assumes zero bias, i.e., that the average wind directions over the puff propagation path are the same as those recorded at the TMI tower. The effects on the projected block dose pattern of +5° (modeling Case D) and -5° (modeling Case E) shifts in wind direction are shown in Figures C-3 (a) and (b), respectively. A +5° (clockwise) shift does not change the position of the block projected to receive the highest dose but displaces the relative levels of dose to a few blocks in the NNW area by 20-30%; the number of blocks significantly affected is small enough that the correlation of the overall pattern to the base case pattern remains high (0.92). A -5° (counterclockwise) shift in average wind direction results in more pronounced changes in the dose pattern. The location of

the highest doses shifts to block 73 (4 miles out in the NNW sector) but it is only 12% higher than its Case A level (block 73 was a close second to block 74 in Case A). However, block 74 shows the largest drop, by 60%, and other blocks along that direction show significant decreases, with increases in the blocks to the NW as would be expected by the wind shifting towards that direction. As noted above, these changes in the relative dose pattern result in a pattern that does not correlate as well ($r^2 = 0.7$) with either Case A or the epidemiology study dose patterns.

Appendix D

Data Tables

TABLE D-1. Population and location of study blocks around Three Mile Island

Block	Population	X	Y	Z	Distance	Azimuth	sector	
3	615	1804	262	93	1.133	81.7	5	E
4	0	3615	-1186	125	2.364	108.2	6	ESE
5	584	1928	-3114	116	2.276	148.2	8	SSE
6	744	751	-4643	110	2.922	170.8	9	S
7	1807	-2448	-3003	138	2.408	219.2	11	SW
8	480	-2147	278	91	1.345	277.4	13	W
11	853	2281	6418	155	4.232	19.6	2	NNE
12	1955	5215	3389	147	3.865	57.0	4	ENE
13	1352	6489	-280	143	4.036	92.5	5	E
14	0	4549	-3921	129	3.732	130.8	7	SE
15	1433	1227	-6342	115	4.014	169.0	9	S
16	1553	-4388	-2257	164	3.066	242.8	12	WSW
17	2493	-5094	526	138	3.182	275.9	13	W
22	2403	2576	10026	174	6.432	14.4	2	NNE
23	1380	5741	7655	216	5.945	36.9	3	NE
24	916	8796	5474	146	6.438	58.1	4	ENE
25	1056	9727	1872	151	6.155	79.1	5	E
26	3865	10270	512	134	6.389	87.1	5	E
27	4399	10715	-720	138	6.673	93.8	5	E
28	1569	9908	-1874	143	6.265	100.7	5	E
29	659	9128	-4497	134	6.323	116.2	6	ESE
30	905	6874	-5694	116	5.546	129.6	7	SE
31	856	2542	-10829	147	6.912	166.8	8	SSE
32	5683	-119	-9771	132	6.072	180.7	9	S
33	2366	-3616	-8753	137	5.885	202.4	10	SSW
34	1122	-7755	-8357	215	7.084	222.9	11	SW
35	999	-7716	-4515	160	5.555	239.7	12	WSW
36	2097	-9842	-2446	164	6.302	256.0	12	WSW
37	1078	-12952	-322	197	8.050	268.6	13	W
41	2878	161	14339	91	8.911	0.6	1	N
42	4391	1379	12484	106	7.804	6.3	1	N
43	8804	5014	13610	132	9.012	20.2	2	NNE
44	3890	7456	11438	154	8.484	33.1	2	NNE
45	1031	10438	8615	166	8.410	50.5	3	NE
46	1382	13914	2689	134	8.806	79.1	5	E
47	1443	13600	-1104	134	8.479	94.6	5	E
48	1953	12564	-4940	107	8.389	111.5	6	ESE
49	1988	11095	-8788	91	8.795	128.4	7	SE
50	562	3292	-13181	191	8.442	166.0	8	SSE
51	809	-813	-14142	135	8.802	183.3	9	S
52	1109	-3225	-13911	129	8.873	193.1	10	SSW
53	895	-7114	-12520	151	8.948	209.6	10	SSW
58	1324	2507	17152	91	10.771	8.3	1	N
59	2982	6905	16375	96	11.043	22.9	2	NNE
60	0	17677	5094	159	11.431	73.9	4	ENE
61	0	17835	-1469	117	11.120	94.7	5	E
62	1438	15466	-8780	91	11.051	119.6	6	ESE
63	6341	-1522	-17582	133	10.966	184.9	9	S
64	1718	-5792	-15383	131	10.214	200.6	10	SSW

See the notes on the last page of this table for column definitions.

TABLE D-1. (continued)

Block	Population	X	Y	Z	Distance	Azimuth	Sector	
71	1571	-1134	4251	91	2.734	345.1	16	NNW
72	2232	250	4605	91	2.866	3.1	1	N
73	2664	-3556	5459	91	4.048	326.9	16	NNW
74	1714	-3132	6675	91	4.582	334.9	16	NNW
75	3081	-1525	6137	91	3.929	346.0	16	NNW
76	4816	-174	6518	91	4.052	358.5	1	N
77	4308	-7401	7756	91	6.661	316.3	15	NW
78	1986	-5785	8045	91	6.157	324.3	15	NW
79	2896	-4483	9847	91	6.723	335.5	16	NNW
80	0	-2241	9657	91	6.160	346.9	16	NNW
81	0	-706	10276	91	6.400	356.1	1	N
82	8418	-9526	9968	91	8.567	316.3	15	NW
83	6387	-7234	11202	92	8.286	327.1	16	NNW
84	1925	-4994	11277	98	7.664	336.1	16	NNW
85	3794	-2811	12473	91	7.945	347.3	16	NNW
86	0	-6066	3748	195	4.431	301.7	14	WNW
87	0	-6602	2363	175	4.357	289.7	14	WNW
88	728	-9271	5495	114	6.697	300.7	14	WNW
89	2287	-9945	3406	201	6.532	288.9	14	WNW
90	2647	-15191	4506	154	9.846	286.5	14	WNW
91	3176	-12874	6160	135	8.868	295.6	14	WNW
92	1119	192	2764	91	1.721	4.0	1	N
93	9387	-10806	7409	91	8.142	304.4	15	NW
94	513	986	3502	117	2.261	15.7	2	NNE
99	0	14495	-11435	115	11.472	128.3	7	SE
101	12663	0	24140	0	15.000	0.0	1	N
102	18240	9238	22303	0	15.000	22.5	2	NNE
103	39726	17070	17070	0	15.000	45.0	3	NE
104	10205	22303	9238	0	15.000	67.5	4	ENE
105	18853	24140	0	0	15.000	90.0	5	E
106	34339	22303	-9238	0	15.000	112.5	6	ESE
107	20152	17070	-17070	0	15.000	135.0	7	SE
108	44204	9238	-22303	0	15.000	157.5	8	SSE
109	111002	0	-24140	0	15.000	180.0	9	S
110	31917	-9238	-22303	0	15.000	202.5	10	SSW
111	11801	-17070	-17070	0	15.000	225.0	11	SW
112	5882	-22303	-9238	0	15.000	247.5	12	WSW
113	21769	-24140	-0	0	15.000	270.0	13	W
114	70460	-22303	9238	0	15.000	292.5	14	WNW
115	99593	-17070	17070	0	15.000	315.0	15	NW
116	26482	-9238	22303	0	15.000	337.5	16	NNW
117	9005	0	40234	0	25.000	0.0	1	N
118	6826	15397	37171	0	25.000	22.5	2	NNE
119	38979	28449	28449	0	25.000	45.0	3	NE
120	14757	37171	15397	0	25.000	67.5	4	ENE
121	62028	40234	0	0	25.000	90.0	5	E
122	124988	37171	-15397	0	25.000	112.5	6	ESE
123	10000	28449	-28449	0	25.000	135.0	7	SE
124	10774	15397	-37171	0	25.000	157.5	8	SSE

TABLE D- 1. (continued)

Block	Population	X	Y	Z	Distance	Azimuth	Sector	
125	14648	0	-40234	0	25.000	180.0	9	S
126	44031	-15397	-37171	0	25.000	202.5	10	SSW
127	19931	-28449	-28449	0	25.000	225.0	11	SW
128	7996	-37171	-15397	0	25.000	247.5	12	WSW
129	35025	-40234	-0	0	25.000	270.0	13	W
130	14188	-37171	15397	0	25.000	292.5	14	WNW
131	9308	-28449	28449	0	25.000	315.0	15	NW
132	10517	-15397	37171	0	25.000	337.5	16	NNW
133	8941	0	56327	0	35.000	0.0	1	N
134	14478	21555	52039	0	35.000	22.5	2	NNE
135	9546	39829	39829	0	35.000	45.0	3	NE
136	45445	52039	21555	0	35.000	67.5	4	ENE
137	42445	56327	0	0	35.000	90.0	5	E
138	27822	52039	-21555	0	35.000	112.5	6	ESE
139	10600	39829	-39829	0	35.000	135.0	7	SE
140	15097	21555	-52039	0	35.000	157.5	8	SSE
141	13477	0	-56327	0	35.000	180.0	9	S
142	18596	-21555	-52039	0	35.000	202.5	10	SSW
143	25536	-39829	-39829	0	35.000	225.0	11	SW
144	8948	-52039	-21555	0	35.000	247.5	12	WSW
145	10370	-56327	-0	0	35.000	270.0	13	W
146	5333	-52039	21555	0	35.000	292.5	14	WNW
147	9970	-39829	39829	0	35.000	315.0	15	NW
148	7256	-21555	52039	0	35.000	337.5	16	NNW
149	47588	0	72420	0	45.000	0.0	1	N
150	45115	27714	66908	0	45.000	22.5	2	NNE
151	62345	51209	51209	0	45.000	45.0	3	NE
152	177672	66908	27714	0	45.000	67.5	4	ENE
153	38754	72420	0	0	45.000	90.0	5	E
154	42737	66908	-27714	0	45.000	112.5	6	ESE
155	26958	51209	-51209	0	45.000	135.0	7	SE
156	66763	27714	-66908	0	45.000	157.5	8	SSE
157	75781	0	-72420	0	45.000	180.0	9	S
158	37729	-27714	-66908	0	45.000	202.5	10	SSW
159	18979	-51209	-51209	0	45.000	225.0	11	SW
160	23010	-66908	-27714	0	45.000	247.5	12	WSW
161	20602	-72420	-0	0	45.000	270.0	13	W
162	3681	-66908	27714	0	45.000	292.5	14	WNW
163	12630	-51209	51209	0	45.000	315.0	15	NW
164	12866	-27714	66908	0	45.000	337.5	16	NNW

NOTES:

Blocks numbered 3-99 are in the 10-mile radius area defined for the TMI epidemiology study (Hatch *et al.);* of these 74 blocks, 65 are populated, averaging 2500 persons per block. Blocks numbered 101-164 are located between 10 and 50 miles and were defined for this study.

X, Y, and Z coordinates are in meters, referenced from the TMI unit 2 stack (Pennsylvania UTM coordinates 530.6, 459.8). Distance is in miles from TMI unit 2 stack and azimuth is in degrees.

TABLE D-2. TLD *data in vicinity of Three Mile island* *D-2.1*
Quarterly data 1973 - 1978

DATE mm dd yy	day	LOCATIONS 1S2	s.e.	2S2	s.e.	4S2	s.e.	5S2	s.e.	9S2	s.e.
03 31 73	90	6.1	0.4	6.1	0.4	6.9	1.3	6.1	0.4	5.6	0.4
06 30 73	91	10.0	2.2	5.6	0.4	5.6	0.9	4.3	0.9	4.8	0.9
09 30 73	92	8.7	0.4	7.4	0.4	6.5	0.9	6.1	0.9	6.1	0.4
12 31 73	92	6.5	0.4	5.6	0.9	6.5	0.4	5.2	0.9	3.9	0.4
02 28 74	59	-9.0	0.0	-9.0	0.0	-9.0	0.0	-9.0	0.0	-9.0	0.0
03 31 74	31	6.10	0.53	4.94	0.53	5.61	0.37	4.53	0.33	5.90	0.51
04 28 7428		5.09	0.14	4.31	0.38	4.70	0.36	4.16	0.31	5.17	0.71-
05 25 74	27	5.26	0.76	4.36	0.44	5.16	0.29	4.05	0.37	5.33	0.62
06 29 74	35	5.35	0.83	4.68	0.38	9.60	1.01	11.2	0.38	5.43	0:56
09 28 74	91	5.73	0.39	4.83	0.81	5.23	0.39	4.19	0.37	5.39	0.29
12 28 74	91	5.42	0.65	4.81	0.76	5.47	0.77	4.64	0.88	6.01	1.03
01 27 75	30	5.35	0.19	4.74	0.09"	5.35	0.45	4.52	0.06	5.61	0.34
02 25 75	29	4.84	0.11	4.32	0.43	4.78	0.32	4.35	0.65	5.08	0.47
04 01 75	35	5.06	0.48	4.48	0.36	4.93	0.47	4.00	0.15	5.31	0.78
04 29 75	28	5.34	0.54	4.62	0.41	5.65	0.2G	5.26	0.32	5.52	0.39
05 31 75	32	5.43	0.24	4.20	0.50	5.05	0.41	4.67	0.35	4.97	0.31
06 28 75	28	5.06	0.40	4_76	0.15	5.59	0.3G	5.01	0.15	5.61	0.22
07 2675	28	4.9	0.4	4.7	0.4	5.0	0.5	4.6	0.1	5.0	0.4
08 30 75	35	5.2	0.6	4.4	0.2	5.2	0.4	4.8	0.2	5.6	0.4
10 04 75	35	5.4	0.3	4.7	0.4	5.4	0.2	4.9	0.3	5.5	0.5
12 24 75	81	5.5	0.5	4.6	0.5	5.3	0.3	5.1	0.3	5.4	0.3
01 01 76	88	10.2	0.0	-4.0	0.0	10.6	0.0	9.5	0.0	-4.0	0.0
03 31 76	90	9	0.0	-4 0	0.0	7	0	6,55	0	-4.0	0.0
06 30 76	1	.21	0.0	-4.0	0.0	6.38	.0	5.78	0.0	-4.0	0.0
09 30 76	92	6.28	0.0	0	00	6.05	0.0	5.78	0.0	-4.0	0.0
12 3176,	92.	9.35	0.	-4.	0.0	7.90	0.0	7.01	0.0	-4.0	0.0
03 30 77	91	6.71	0.19	4.85	0.53	6.65	0.60	5.84	0.22	6.11	0.59
06 29 77	91	5.57	0.15	4.71	0.34	5.71	0.88	5.16	0.22	5.67	0.30
09 2077,	91	5.26	05	1	0,14)	5.27	0.28	4.79	0.40	5.33	0.20
12 3077	93	7.0	0.8	S.4	.1.2	7.4	1.2	6.5	1.4	6.8	0.6
03 29.78	oo	4.67	0.13		0.13	4.80	0.20	4.30	0.13	4.67	0.10
06 28 78	91	7.37	0.47	6.03	0.1V	8.07	0.27	8.00	0.27	8.53	0.33
0936 78	94		0.13	4.73	n.33	5.17	0.13	5.03	0.40	5.57	0.20
12 27 78	88	5.37	0.20	4.20	0.20	4.33	0.27	4.23	0.10	5.67	0.37
03 29 79	92	32.3	1.3	14.4	2.9	11.7	2.8	10.1	0.9	8.3	2.0

TABLE D-2 continued

DATE mm	dd	AA	day		s.e.	1S91		4A1	s.e.	WE		12B1	s.e.
10	31	73	90	6vS	0v9	7.4	0.5	W0 G∨9		6.5	W0	6.1	0v6
06	30	73	91	9vE	1.3	W0 9A		5.2	1.3	5.6	1.3	8',	1.3
10	31	73	92	6v9	0v5	6.1	0.9	6.9	W0	6v9	0vQ	5.6	0v6
12	31	73	92	5.6	0.9	9vT	0.9	5.2	0v6	WE	0v6	5.2	1.7
02	28	M	59	-9.0	0v0	-9v0	0v0	-9v0	0.0	-9.0	0.0	-9v0	0v0
10	31	74	31	5.19	W0	6.18	1.19	W0 00'S		5.70	W0	69',	0.25
01	28	74	28	96W	0.46	5.36	0.33	8Ev0 TOP		5.00	0.57	4.07	0.29
06	25	M	27	5.24	0.26	5.35	0.44	5.17	0.49	WE	O=	4.39	T9v0
06	29	M	35	5.30	0.05	-5.0	0.0	5.74	0.35	WE	0.33	4.29	02.0
09	28	74	91	5.16	0.24	WE	0.47	5.17	0.28	5.26	0.21	890	0.31
12	28	IL	16	5.77	89vT	6.47	0.78	5.67	58 o	023	1.02	4.77	S8v0
01	27	75	0C	6.20	0~8C	6.01	ENO	WE	silO	WE	0.34	W0 E94	
02	25		29	5.36	0v09	5.52	0.32	W ?	0.37	5.02	0.64	6Cv0 TWO	
10	TO		2C	5.51	0.72	5.99	0.53	MO go s		4.92	0.53	4.89	f9v0
10	29		28	9 LO	WO	6v09	0v99	5.26	0.67	GOO WE		4.26	0Cv0
C0	TC	75	32	1 O2	0.10	8I7	0.33	4.84	0.20	ETA	0.45	4.05	0.34
09	28	A	28	5.36	0.27	5.38	0.43	5.00	99v0	5.04	8Cv0	4.46	0.53
02	26	SL	28	W9	0.4	5.2	0.2	4.9	M0	5.0	W0	4.2	0.2
08	30	OS	QC	5.7	0v6	SIG	0.1	5.2	0v6	5.2	0.2	W0 SIP	
01	PO	SL	35	5.6	0.6	5.4	C∨0	0'E	0vS	5.2	W0	4.4	3v0
12	24	SL	81	67	0.2	8vS	0.3	's!	0.2	TIE	E∨0	1 O	0.1
01	01	96	88	11.0	0.0	10.8	0.0	-6.0	0v0	7.3	0.0	-4.0	0 0
03	31	76	90	06Z	0.0	7.97	0.0	-Av0	0.0	-4.0	0 0	ON	0 0
06	30	76	91	6v9T	0v0	6.71	0v0	-6v0	0.0	0 W	0v0	0vI-	0v0
60	OE		92	6.08	0v0v	6.as	0 0	-4 0	0 0	-4.0	0.0	OC	0v0
12	31	A	92	9.19	0 0	10 38	0.0	-4.0	0v0	-6v0	0v0	-4.0	0v0
00	00				1.10	7.12	0.38	5.47	0v60	5.74	0v99	4.78	0.73
06	29	77	1	6.16	0 49	6 54	1.24	5.53	8C'0	5.65	0.33	99v?	0.43
09	28	77	91	9 10	0 68	6.23	0.60	5.31	0.32	5.07	0.19	4.33	0.17
12	00	A	E6	8.7	1.4	8v6	1.6	W0 9v9		6.1	0vd	5.5	0.2
00	29	78	89	5.07	0.20	6vA	0.27	Av60	0.20	1.09	0vW	ME	0.07
06	28	78	91	17.00	0 dp	?'6T	0.7	7.57	13 o	7.47	0.17	6v60	0.30
09	00	78	94	6.50	0.27	6v9	0.0w	0.20	CO s	4.57	0.27	4.03	0.23
O	A	78	88	5.60	0.10	5.60	0.27	13 s	0v0C	4.63	0.23	4 10	01,0
03	29	79	92	71.4	15.9			6.7	0.9	6.1	0.7	pIG	0v6

TABLE D-2 continued

DATE mm	dd			1C1	s.e.	7F1		4G1	s.e.	9G1		15G1	s.e.
	--	--	---										
03	31	73	90	-4.0	0.0	9.6	0.0	7.4	0.0	7.8	1.7	-4.0	0.0
06	30	73	91	-4.0	0.0	6.1	2.2	8.0	0.4	5.6	1.3	-4.0	0.0
09	30	73	92	-4.0	0.0	7.8	0.9	6.9	0.9	6.5	0.9	-4.0	0.0
12	31	73	92	-4.0	0.0	7.4	0.9	5.2	1.3	6.9	2.6	-4.0	0.0
02	28	74	59	-4.0	0.0	-7.0		-9.0	0.0	-9.0	0.0	-9.0	0.0
03	31	74	31	5.02	0.25	7.89	1.29	6.43	0.37	6.31	0.19	-2.0	0.0
04	28	74	28	6.09	0.60	7.66	0.58	9.66	0.83	6.03	0.46	5.28	0.28
05	25	74	27	4.20	0.37	7.33	0.60	5.24	0.50	5.70	0.49	5.08	0.23
06	29	74	36	4.79	0.27	7.23	0.34	5.92	0.17	6.54	0.28	6.03	0.14
09	28	74	91	5.19	0.25	7.95	0.67	5.67	0.66	6.27	0.29	6.02	
12	28	74	91	5.08	0.79	8.20		6.07	0.18	6.00	0.38	6.19	0.67
01	27	75	30	4.81	0.28	7.81	0.30	5.85	0.09	6.17	0.10	5.73	0.23
02	25	75	29	4.23	0.30	7.02	0.69	5.49	0.43	5.80	0.26	5.21	0.13
03	10	76	96	4.29	0.48	7.84	0.19	5.82	0.47	6.21	0.30	5.92	0.59
04	29	76	28	4.68	0.25	7.96	0.27	5.85	0.47	6.09	0.42	5.65	0.24
05	10	76	96	4.32	0.08	7.50	0.09	5.30	0.57	5.75	0.56	5.47	0.44
06	09	76	28	4.30	0.09	7.42	0.25	5.41	0.59	5.92	0.17	5.48	0.19
07	29	76	28	4.3	0.3	7.2	0.2	5.7	0.2	5.4	0.1		0.2
08	30	76	96	4.7	0.2	7.7	0.2	5.8	0.0	6.2	0.7	5.8	0.3
10	04	75	56	4.10	0.3	7.4	0.4	5.7	0.8	6.2	0.0		0.0
12	24	75	81	4.7	0.0	7.4	0.2	3.8	0.0	6.0	0.7	5.7	0.2
01	01	76	88	-6.0	0.0	-4.0	0.0	-4.0	0.0	-0.0	0.0	-0.0	0.0
03	31	76	90	-1.0	0.0	6.0	0.0	8.0	0.0	8.0	0.0	8.01	0.0
06	30	76	91	-4.0	0.0	8.72	0.0	6.75	0.0	6.9	0.0	7.12	0.0
09	30	76	92		0.0	8.69	0.0	6.97	0.0	6.91	0.0	8.0	0.0
12	31	76			0.0	10.71		9.29	0.0	9.8	0.0	7.1	0.0
03	30	77	91	5.37	0.47	7.76	0.79	6.21	0.34	6.9	0.34	6.77	0.0
06	29	77	91	4.77	0.43	8.18	0.36	6.01	0.44	6.61	0.31	6.55	0.22
09	28	77	91	4.57	0.21	7.10	0.30	5.87	0.38	5.9	0.20	5.9	0.1
12	30	77	90	5.4	0.6	9.5	1.0	7.9	0.0	7.8	0.8	7.7	0.8
03	29	78	89	4.10	0.20	6.57	0.17	5.30	0.30	5.60	0.10	5.13	0.10
06	28	78	91	6.43	0.23	11.9	0.0	8.53	0.40	9.47	0.50	8.1	0.4
09	30	78	94	4.13	0.00	7.40	0.43	5.77	0.13	5.09	0.20	5.23	0.4
12	27	78	88	4.33	0.27	7.50	0.20	5.90	0.33	5.4	0.50	5.63	0.0
01	29	79	92	6.6	0.9	8.0	1.2	5.7	1.4	7.0	0.6	6.1	1.3

DATE				LOCATIONS					
mm	dd	yy	day	14S2	s.e.	16A1	s.e.	100	s.e.
03	31	73	90	-9.0	0.0	-9.0	0.0	-9.0	0.0
06	30	73	91	4.3	0.4	5.2	0.4	5.6	0.9
09	30	73	92	-9.0	0.0	6.1	0.4	6.5	0.9
12	31	73	92	-9.0	0.0	-9.0	0.0	-9.0	0.0
02	28	74	59	-9.0	0.0	-9.0	0.0	-9.0	0.0
03	31	74	31	5.44	0.19	-2.0	0.0	.2.0	0.0
04	28	74	28	5.69	0.53	4.65	0.09	5.71	0.85
05	25	74	27	5.61	0.51	4.42	0.54	5.98	0.21
06	29	74	35	5.13	0.32	4.69	0.17	5.81	0.66
09	28	74	91	4.92	0.53	4.62	0.68	6.17	0.46
12	28	74	91	-3.0	0.0	-3.0	0.0	-3.0	0.0
01	27	75	30	4.94	0.24	5.04	0.56	5.75	0.44
02	25	75	29	-2.0	0.0	-2.0	0.0	-2.0	0.0
04	01	75	35	4.67	0.11	4.61	0.32	5.36	0.39
04	29	75	28	-5.0	0.0	4.75	0.45	6.13	0.23
05	31	75	32	4.78	0.61	4.44	0.42	5.70	0.29
06	28	75	28	4.95	0.68	4.61	0.20	5.71	0.30
07	2G	75	28	.1.0	0.0	4.4	0.3	5.7	0.1
08	30	75	35	4.3	0.4	4.7	0.1	5.9	0.4
10	04	75	35	5.1	0.5	4.5	0.7	5.7	0.5
12	24	75	81	A 0	0.0 '"	-3.0	0.0	-3.0	0.0
01	01	76	88	-4.0	0.0	-4.0	0.0	-4.0	0.0
03	31	76	90.	-4.0	0.0	-4.0	0.0	-4.0	0.0
06	30	7G	91	-4.0	0.0.	-4.0	0.0 '	_4.0	0.0
09	30	76	92	-4.0	0.w	-4.0	^.0	-4.0	0.0
12	31	76	92	-4.0	0.0	-3.0	0.0	3.0	0.0
03	30	77		-1.0	0.0 .	4.98	0.30	6.15	0.89
06	29	77	91,	^"1.0	0.0	4.70	0.14	6.41	0.58
09	28	77	91	-1.0	0.0	4.64	0.20	6.16	0.79
12	30	77	93	-3.0	0.0	-3.0	0.0	-3.0	0.0
03	29	78	89	2.17	0.13:	2.03	0.07	1.97	0.10
06	28	78	91	12.2	0.4	7.83	0.37	9.43	0.37
09	30	78	94	5.77	0~73	5.13	0.23	6.57	0.10
12	2778		88	^ ^	0.0.	-3.0	0.0	-3.0 .	0.0
03	29	79	92	23.6	7.9	89.8	16.8	6.2	1.2

TABLE D-2 continued

DATE mm	dd	yy	day	LOCATIONS 8C1	s.e.	8S1	s.e.	1F1	s.e.	7G1	s.e.
03	31	73	90			6.9	0.4	3.7	0.4		
06	30	73	91			5.6	0.4	6.5	0.9		
09	30	73	92			5.6	0.4	8.7	0.3		
12	31	73	92			5.6	0.9	6.5	0.9		
02	28	74	59								
03	31	74	31								
04	28	74	28								
05	25	74	27								
06	29	74	35								
09	28	74	91								
12	28	74	91								
01	27	75	30			5.40	0.24	6.65	0.41		
02	25	75	29			4.90	0.13	5.93	0.w!		
04	01	75	35			5.34	0.43	6.69	0.72		
04	29	75	28			5.13	0.36	6.48	0.64		
05	31	75	32			4.83	0.35	5.93	0.58		
06	A	75	28			5.36	0.27	6.15	0.46		
07	26	75	28			5.3	0.2	6.0	0.6		
08	30	75	35			5.6	04	6.2	0.2		
10	04	75	35			5.1	0.2	6.4	0.3		
12	24	75	81			5.3	0.4	6.2	0.3		
01	01	76	88								
03	31	76	90			6.08	0.0				
06	30	76	91			5.95	0.0				
09	30	7p	92			G.15	0.0.				
12	31	76	92			9.58	0.0				
03	30	77	91	5.29	0.46			4.80	0.32		
06	29	77	91	4.14	0.22			4.47	0.33		
09	28	77	91	3.74	0.40			4.48	0.23		
12	30	77	93	5.7	1.4			-2.0	0.0		
03	29	78	89	3.50	0.23					15.8	0.7
06	28	78	91	5.57	0.30					10.4	0.5
09	30	78	94	4.10	0.17					7.13	0.63
12	27	78	88	3.50	0.13					7.20	0.10
03	29	79	92	4.3	0.2					8.5	0.4

NOTES:

Dosimeters are labeled by their location code as established for the TMI environmental monitoring program.
The first number (1 to 16) designates the compass sector (1=N, 2=NNE, 3=NE, etc.);
The letter (S,A-G) is a code for radial distance from the plant (S=on site, A,B,C etc. for increasing distance).
The last number designates a particular dosimeter for locations where more than one may have been in place.

First column for each location gives the dose in mrad/month on basis of a 30.4 day standard month.

Missing value codes:
-1.0 "TLDs were stolen.''
-2.0 "No sample received" or collected due to severe weather."
-3.0 "Not collected Nov-Feb" (6-month sampling period in winter).
-4.0 Location not reported in records for the time period.
-5.0 " "TLDs lost or "lost due to vandalism."
-9.0 Data missing, no explanation given.

The "s.e." column qives corresponding 2 standard error based on readings from the four elements in each dosimeter.
An entry of 0.0 indicates that the error estimate is missing.

Dates are ending dates for a dosage periods, where "mm dd yy" is month, day, year. (End of month is assumed for data from earlier year when exact dates are not specified in the REMP reports.)
The "day" column is the number of days in the period.

Data through 78-12-27 are from the Metropolitan Edison Company Radiological Environmental Monitoring Reports for 1'75 to 1978, prepared by Teledyne Isotopes, 50 Van Buren Avenue, Westwood, NJ 07675, as provided by S.W. Porter with letter to John Arbo dated Dec. 23, 1987.

Data for 79-03- 9 (during accident) are from Table D-4 in TDR-TMI-116, Assessment of Offsite Radiation Doses from the Three Mile Island Unit Accident, revision 0, July 31, 1979 (Pickard, Lowe, and Garrick).

The 5S3 column shows data for sensor designated 5S2 starting 78-03-29.
The 118 column shows data for sensor designated 1151 starting 78-03 29.
For 14S2 and 16A1, the 79-03-29 value is the average of two readings spanning the 6-month period starting 78-09-30 (78-09-27 in TDR-TMI-116).

\DATA\TLDOSE 5/8/89

Appendix E

Sensitivity analysis for plume rise

This appendix provides some details of the sensitivity analysis for plume rise that were not covered in the discussion given in Section 4 of the main text. As noted in Section 4, the effect of plume rise on estimates of released activity and population dose was examined by running the dispersion model for three cases of buoyancy temperature difference. These results are given in the table below (the temperature differences of 0°C, 10°C, and 100°C are cases B, A, and C, respectively, as listed earlier in Table 6).

Table E-1. Release and dose estimates for three plume rise cases

Case	Temperature difference	Final rise above vent stack (m)	Release (MCi)	Population dose (person-Sv)
B	0°C	0	9	20
A	10°C	51	22	37
C	100°C	90	45	45

The activity release and population dose estimates from the three cases were fit to the buoyancy temperature difference that specifies the plume rise, using a logarithmic curve to allow interpolation to intermediate values. The curve fit uses the three-parameter logarithmic function

$$y = a + b \ln (1 + x/c)$$

where x is temperature difference and y is release or population dose, as the case may be. The fitted parameter values are given in the Table E-2. The resulting curves were shown in Figure 10 of the main text.

Table E-2. Parameters for log curve fits against temperature difference

Parameter:	a	b	c
Activity release (MCi)	9	11.82	4.987
Population dose (person-Sv)	20	3.485	0.07669

Since the actual temperature difference driving plume buoyancy is not known, the problem is treated by assuming a probability distribution for what the actual temperature difference might have been. Three cases of temperature distributions are shown here in Figure E-1. All of the distributions

are log-normal, which is a convenient function for strictly-positive values (the exhaust gases were no cooler than outdoor temperature). The means and standard deviations are given on the figure captions. A judgement that 10°C is the most likely value implies distributions having a mean of 10, as in parts (a) and (b) of the figure. Considering values up to 100°C implies a long right tail, which occurs with standard deviations of about 10 or larger. The skewness of the resulting distributions implies that even for means of 10, the medians will be less than 10. Cumulative probabilities at four levels are noted below each figure; for example, on Figure E-1(a), Pr(x < 7.1) is 0.50.

Given that some buoyant rise was very likely, these sensitivity curves and temperature difference distributions suggest that the release and dose estimates for around 10°C plume rise should be quite robust. By choosing a a particular distribution for the temperature difference, one can obtain confidence intervals for the release and dose by evaluating the fitted sensitivity curves at the temperature values corresponding to the desired probabilities. Table E-3 shows such results using a log-normal distribution for the temperature difference, with (a) mean 10°C and standard deviation 10°C; (b) mean 10°C and standard deviation 20°C.

Table E-3. Confidence intervals for release and population dose

Based on log-normally distributed buoyancy temperature difference (DT) for determining plume rise, during first day and a half of TMI accident.

(a) mean DT 10°C, standard deviation 10°C (t 1.956, r 0.833)

	DT (°C)	Release (MCi)	Population dose (person-Sv)
Lower95%	1.3	12	30
Lower68%	3.1	15	33
Mean	10.0	22	37
Upper68%	16.3	26	39
Upper95%	37.4	34	42

(a) mean DT 10°C, standard deviation 20°C (t 1.498, r 1.269)

	DT	Release (M 10)	Population dose (person-Sv)
Lower95%	0.4		24
Lower68%	1.3	12	30
Mean	10.0	22	37
Upper68%	15.9	26	39
Upper95%	56.5	39	43

Temperature intervals were found by inverse transformation from the standard normal distribution corresponding to the respective log-normal distribution. The release and dose values were then computed based on the curve fits given above. The 68% interval corresponds to one standard error;

the 95% interval corresponds to two standard errors. Using the distribution having a standard deviation of 10°C, as in case (a) of the Table E-3 for example, implies that the estimated total release is 22 (-7,+4) MCi and that the estimated 80 km (50-mile) population dose is 37 (-4,+2) person-Sv, i.e., 3700 (-400,+200) person-rem. The intervals are skewed to the left rather than symmetric because of the assumed log normal shape of the temperature difference distribution and the levelling off of the release and dose sensitivity curves at higher temperature differences.

For the results stated in the main text, the values from the distribution having a 10°C standard deviation are chosen, since they reflect a greater certainty that the plume temperature difference was closer to the assumed mean of 10°C than it was to either of the extremes (0 °C or 100 °C).

REFERENCES

Aamodt, M.M., and N.O. Aamodt, petitioners versus U.S. Nuclear Regulatory Commission, Docket No. 50-289. Aamodt motions for investigation of licensee's reports of radioactive releases during the initial days of the TMI-2 accident and postponement of restart decision pending resolution of this investigation, June 21, 1984.

Akers *et al.* Three Mile Island unit 2 fission product inventory estimates. Nuclear Technology 87(1):205-213, August 1989.

Auxier, J.A., *et al.,* Report of the task group on health physics and dosimetry to the President's Commmission on the Accident at Three Mile Island (Report of the Kemeny commission staff). Washington, DC, October 1979.

Battist, L., *et al. (Ad hoc* population dose assessment group), Population dose and health impact of the accident at the Three Mile Island nuclear station (a preliminary assessment for the period March 28 through April 7, 1979). Nuclear Regulatory Commission, Washington, DC, May 10, 1979.

Beyea, J., A study of some of the consequences of hypothetical reactor accidents at Barseback. PU/CEES Report No. 61, Center for Energy and Environmental Studies, Princeton University, Princeton, NJ, January 1978.

Beyea, J., Some long-term consequences of hypothetical major releases of radioactivity to the atmosphere from Three Mile Island. PU/CEES Report No. 109, Center for Energy and Environmental Studies, Princeton University, Princeton, NJ, December 1980.

Beyea, J., A review of dose assessments at Three Mile Island and recommendations for future research. Three Mile Island Public Health Fund, Philadelphia, PA, August 1984.

Beyea, J., Description of dose models used in the epidemiology study. Draft report, National Audubon Society, New York, NY, November 1987.

Beyea, J., and J.M. DeCicco. Re-estimating the noble gas releases from the Three Mile Island accident (report-length version of this paper). National Audubon Society, New York, July 1990.

Draper, N.R., and H. Smith, Applied regression analysis (second edition). John Wiley & Sons, New York, 1981.

ERT, User's Guide to the Rough Terrain Diffusion Model (RTDM), Rev. 3.10. Report PD535-585, Environmental Research and Technology, Inc., Concord, MA, 1985.

ERT, User's Guide for RTDM.WC, a Worst Case version of RTDM. Report M-0186-ODOR, Environmental Research and Technology, Inc., Concord, MA, 1980.

Gerusky, T., Three Mile Island: assessment of radiation exposures and environmental contamination. Annals of the New York Academy of Sciences, 54:365, 1981.

Goldberg, J.F. (ed.), Proceedings of the Workshop on Three Mile Island Dosimetry, November 12-13, 1984. Three Mile Island Public Health Fund, Philadelphia, PA, December 1985.

Gur, *D., et al.,* Radiation dose assignment to individuals residing near the Three Mile Island nuclear station. Proc. Penna. Academy of Science 57:99-102, 1983.

Hanna, S.R., Atmospheric turbulence and air pollution modelling, D. Reidel Publishing Co, 1982.

Hatch, M.C., *et al..* Cancer near the Three Mile Island nuclear plant: radiation emissions. American Journal of Epidemiology, forthcoming 1990.

Hildebrand, J.E., and J.W. Schmidt, TMI experience with beta dosimetry problems. Health Physics 43(1), 1982.

Horowitz, Y.S., Thermoluminescence and thermoluminescent dosimetry. CRC Press, Boca Raton, FL, 1984.

Imai, K., and T. Iijima, Assessment of gamma exposure due to a radioactive cloud released from a point source. Health Physics 18:207-216, 1970.

Jacob, P. and H.G. Paretzke, Air-ground interface correction factors for gamma emitters in air. Health Physics 48:183-191, 1985.

Judge, G.G., and T. Takayama, Inequality restrictions in regression analysis. J. American Statistical Association 61:166-181, 1966.

Kemeny, J.G. (Chairman), Report of the President's Commission on the Accident at Three Mile Island. Washington, DC, October 1979.

Knight, P.K., J.T. Robinson, F.J. Slagle, P.M. Garrett. A review of population radiation exposure at TMI-2. Technology for Energy Corporation, Report NSAC-26, for Nuclear Safety Analysis Center, Electric Power Research Institute, Palo Alto, CA, 1981.

Lawson, C.L., and R.J. Hanson, Solving least squares problems. Prentice Hall, Englewood Cliffs, NJ, 1974.

Miller, C.W., S.J. Cotter, R.E. Moore, and C.A. Little, Estimates of dose to the population within fifty miles due to noble gas releases from the Three Mile Island incident. Proc. Am. Nuc. Soc. and European Nuc. Soc. Thermal Reactor Safety Conference, 2:1336-1343, Knoxville, TN, April 1981.

Mosteller, F., and R.E.K. Rourke, Sturdy statistics: Nonparametrics and order statistics. Addison-Wesley, Reading, MA, 1973.

NCRP 93. Ionizing radiation exposure of the population of the United States. NCRP Report No. 93, National Council on Radiation Protection and Measurements, Bethesda, MD, 1987.

NCRP 94. Exposure of the population in the United States and Canada from natural background radiation, NCRP Report No. 94. National Council on Radiation Protection and Measurements, Bethesda, MD, December 1987.

NEA (Nuclear Energy Agency), International comparison study of reactor accident consequence models. Summary report of the NEA Committee on the Safety of Nuclear Installations. Organization for Economic Cooperation and Development (OECD), Paris, June 1983.

NRC (National Research Council). Health effects of exposure to low levels of ionizing radiation. Committee on the Biological Effects of Ionizing Radiations (BEIR V). National Academy Press, Washington, DC, 1990.

Oately, D., G. Hudson, and P. Plato, Projected response of Panasonic dosimeters to submersion in and distant exposure by ^{133}Xe. Health Physics 41(3):513-525, 1981.

Pasciak, W., E.F. Branagan, F.J. Congel, and J.E. Fairobent, A method for calculating doses to the population from ^{133}Xe releases during the Three Mile Island accident. Health Physics 40:457-465, April 1981.

Pergola, D.V., **R.B.** Harvey, and J.G. Parillo, SB METPAC, a computer software package which evaluates the consequences of an offsite radioactive release, written for the Seabrook Station Site at Seabrook, New Hampshire. Yankee Atomic Electric Company, Framingham, MA, 1986.

Petersen, W.B., INPUFF, A multiple source puff model. Proceedings of the Fifth Joint Conference on Applications of Air Pollution Meteorology, Chapel Hill, NC, November 1986. American Meteorological Society, Boston, MA, 1986.

Pickard, Lowe, and Garrick (1979)--see Woodard and Potter (1979a).

Plato, P., C.G. Hudson, D. Katzman, and R. Sha, Calibration of environmental and personal dosimeters by submersion in and distant exposure to Xe. Health Physics 38(April):523-528, 1980.

Randerson, D. (ed.), Atmospheric Science and Power Production. U.S. Department of Energy, Technical Information Center, 1984.

REMP 1973, Three Mile Island nuclear station, preoperational Radiological Environmental Monitoring Report, 1973 annual report prepared for Metropolitan Edison Company. RMC-TR-75-05, Radiation Management Corporation, Philadelphia, PA, undated.

REMP 1974 - 1975, also by Radiation Management Corporation.

REMP 1975a, Radiological Environmental Quality Assurance Program, 1975 annual report, prepared for Metropolitan Edison Company, Teledyne Isotopes IWL-4000-383, Westwood, NJ, February 1976.

REMP 1976, Radiological Environmental Quality Assurance Program, 1976 annual report, prepared for Metropolitan Edison Company. IWL-4000-404, Teledyne Isotopes, Inc., Westwood, NJ, February 1977.

REMP 1977, Metropolitan Edison Company Radiological Environmental Monitoring Report, 1977 annual report prepared for the Three Mile Island nuclear station, Teledyne Isotopes IWL-5990-427, Westwood, NJ, undated.

REMP 1978, Metropolitan Edison Company Radiological Environmental Monitoring Report, 1978 annual report prepared for the Three Mile Island nuclear station. IWL-5590-443, Teledyne Isotopes, Inc., Westwood, NJ, undated.

Riley, R.J. *et al.*, Evaluation of the response to Xe radiations by thermoluminescent dosimeters used during the accident at Three Mile Island. Health Physics 42:329-334, 1982.

Ritchie, L.T. *et al.* (Sandia National Laboratories), CRAC2 model description. Report NUREG/CR-2552, Nuclear Regulatory Commission, Washington, DC 1984.

Rogovin, M. (director), Three Mile Island: A report to the commissioners and to the public. Nuclear Regulatory Commission Special Inquiry Group, Washington, DC, undated (1979).

Thomas, C.D., J.E. Cline, and P.G. Voilleque, Evaluation of an environs exposure rate monitoring system for post-accident assessment. Report AIF/NESP-023, Science Applications, Inc., Rockville, MD, 1981

Woodard, K., and T.E. Potter (Pickard, Lowe, and Garrick, Inc.). Assessment of offsite radiation doses from the Three Mile Island unit 2 accident, Report TDR-TMI-116, revision 0, prepared for Metropolitan Edison Co., Harrisburg, PA, July 31, 1979 (1979a);

Woodard, K., and T.E. Potter. Assessment of noble gas releases from the Three Mile Island Unit 2 accident. Trans. American Nuclear Society Meeting, San Francisco, CA, November 1979 (1979b).

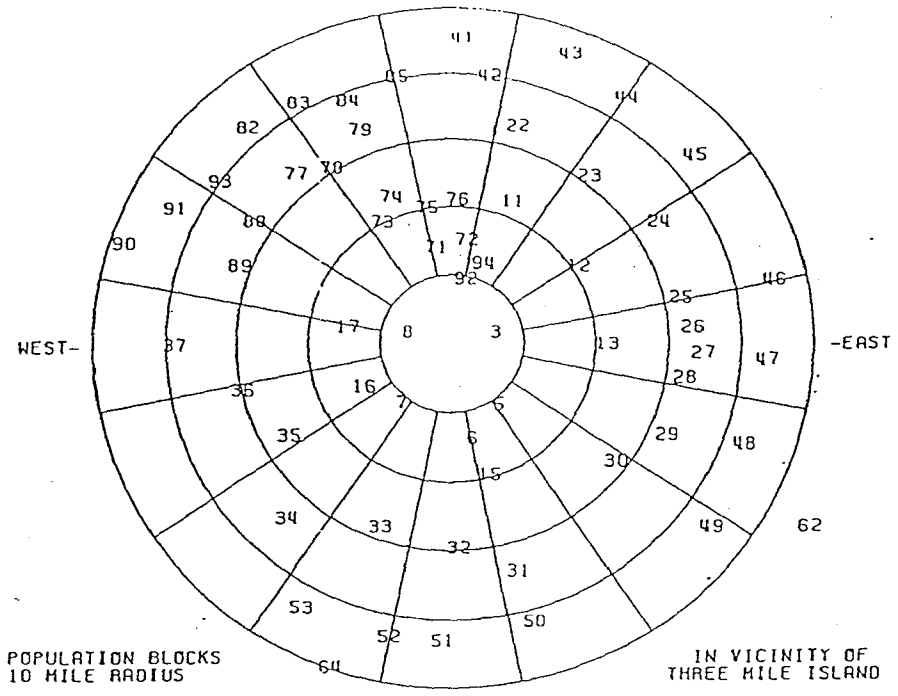

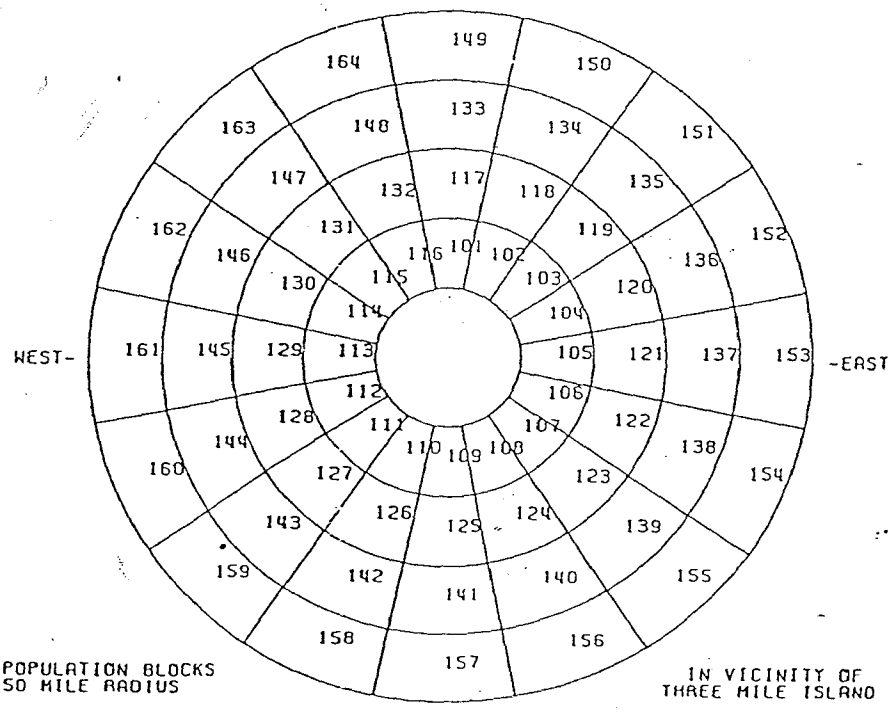

Figure 1. Population block assignments near Three Mile Island
(a) within 10 mile radius, 2 mile grid spacing;
(b) 10 to 50 mile radius, 10 mile grid spacing.
Refer to Table D-1 for precise locations and populations.

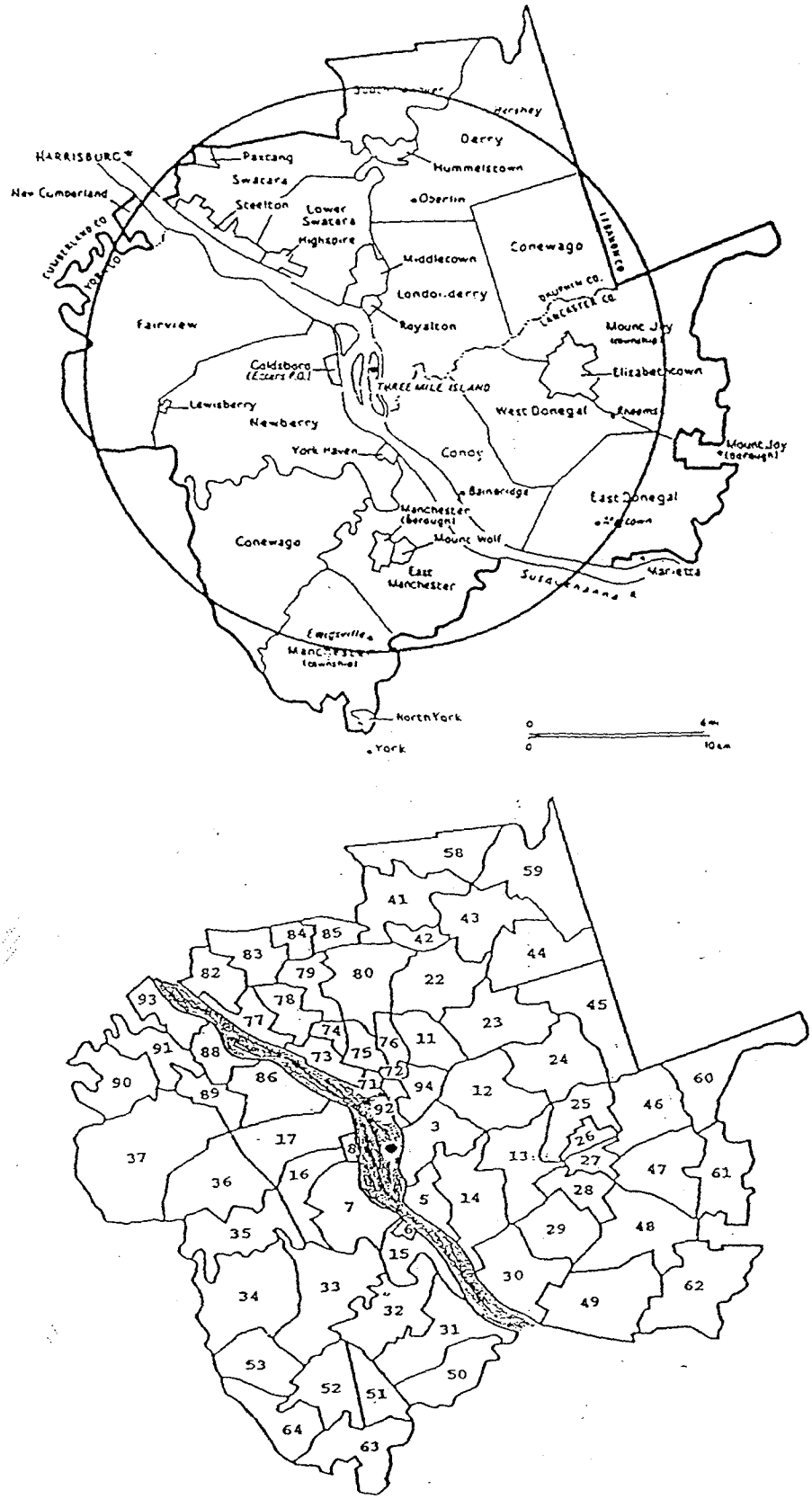

Figure 2. Three Mile Island 10-mile study area (Hatch *et al.*) (a) communities (b) block number assignments.

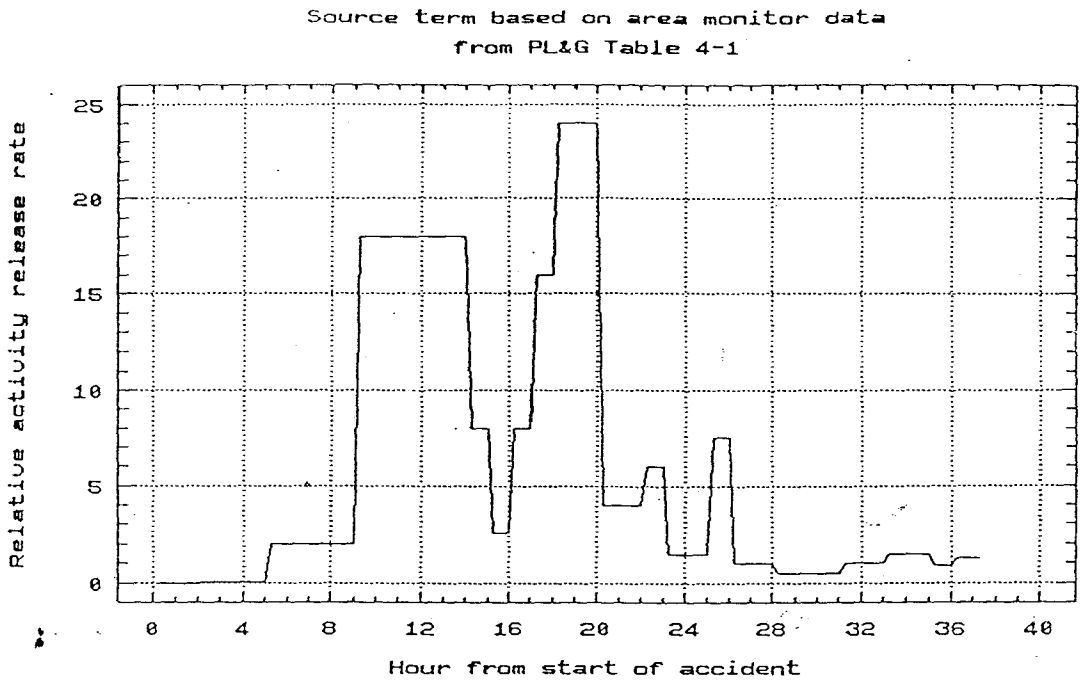

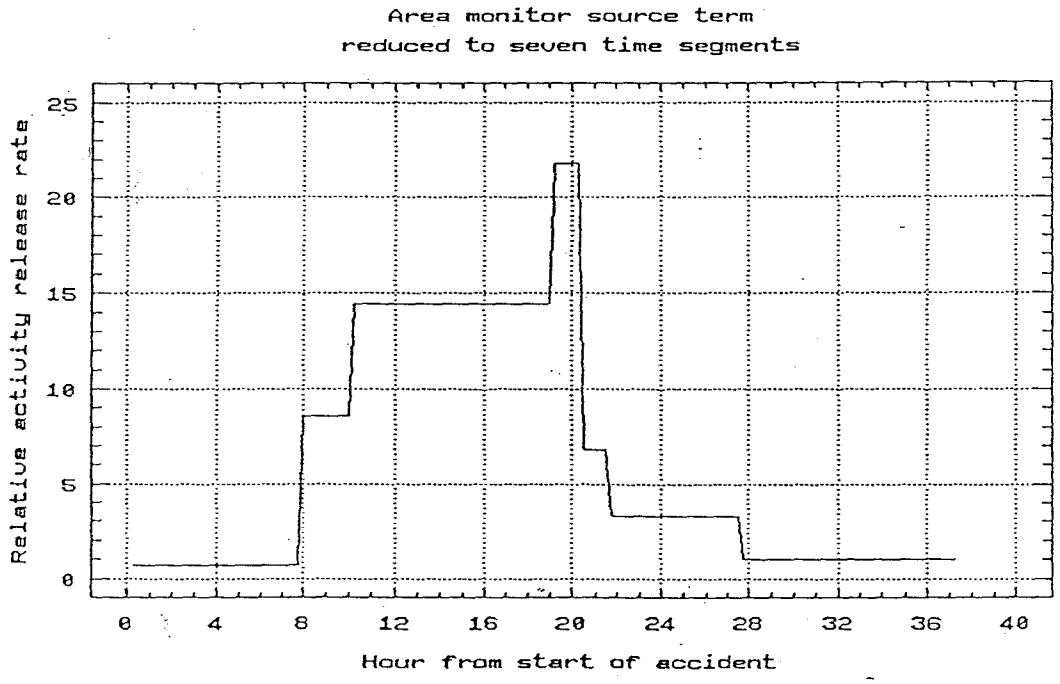

Figure 3. Noble gas source release rates based on area radiation monitor data (source term "P"), from Pickard, Lowe, and Garrick (PL&G)
(a) adjusted exposure rates (PL&G Table 4-1, interpolated to 15-minute intervals, as used by Hatch *et al.*)
(b) rates from (a) averaged over seven time segments.

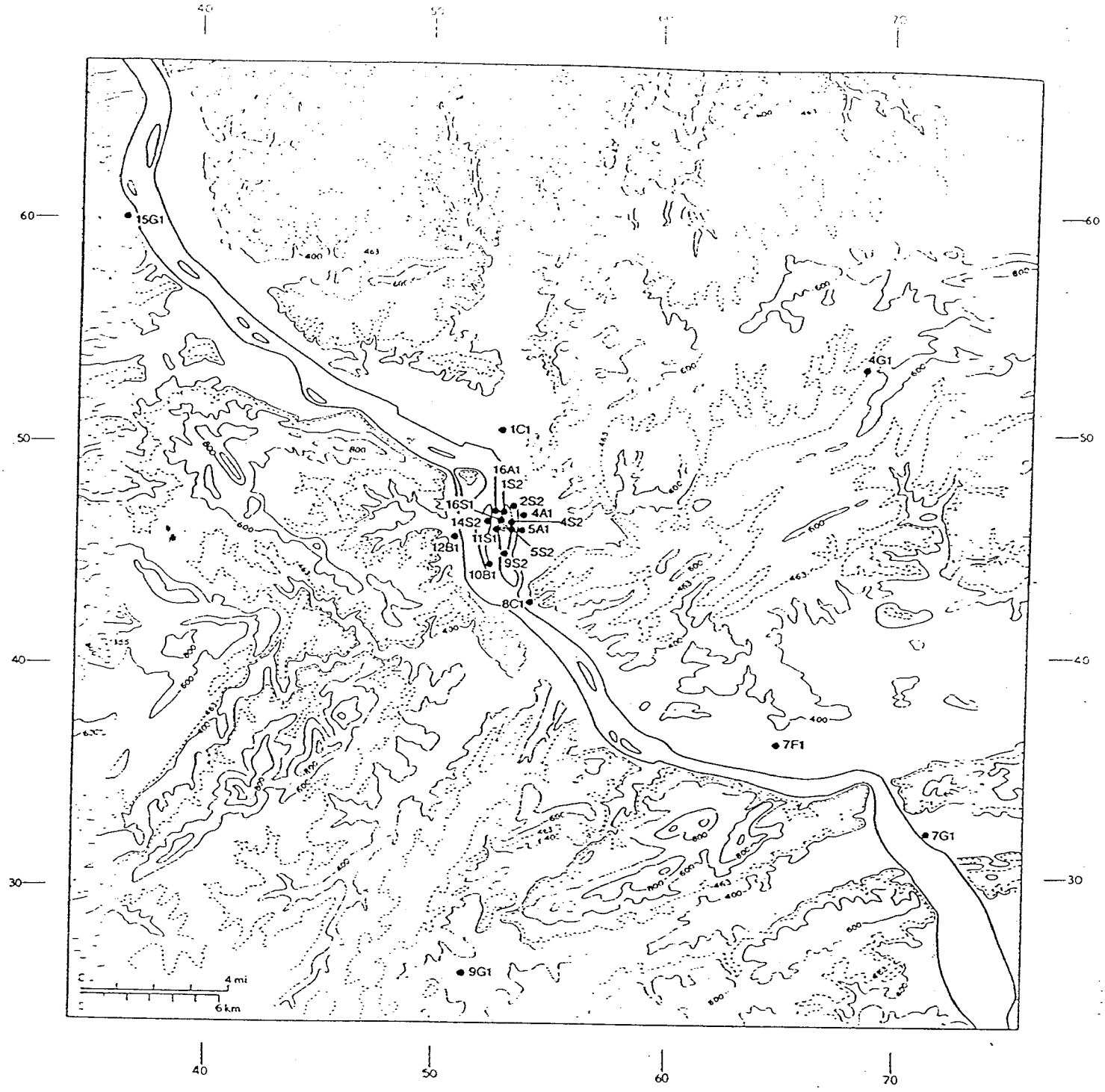

Figure 4. TLD locations and topography in the vicinity of TMI. Contour interval is 200 feet, with an added (dashed) contour at the 423 foot elevation of the TMI unit 2 vent stack.

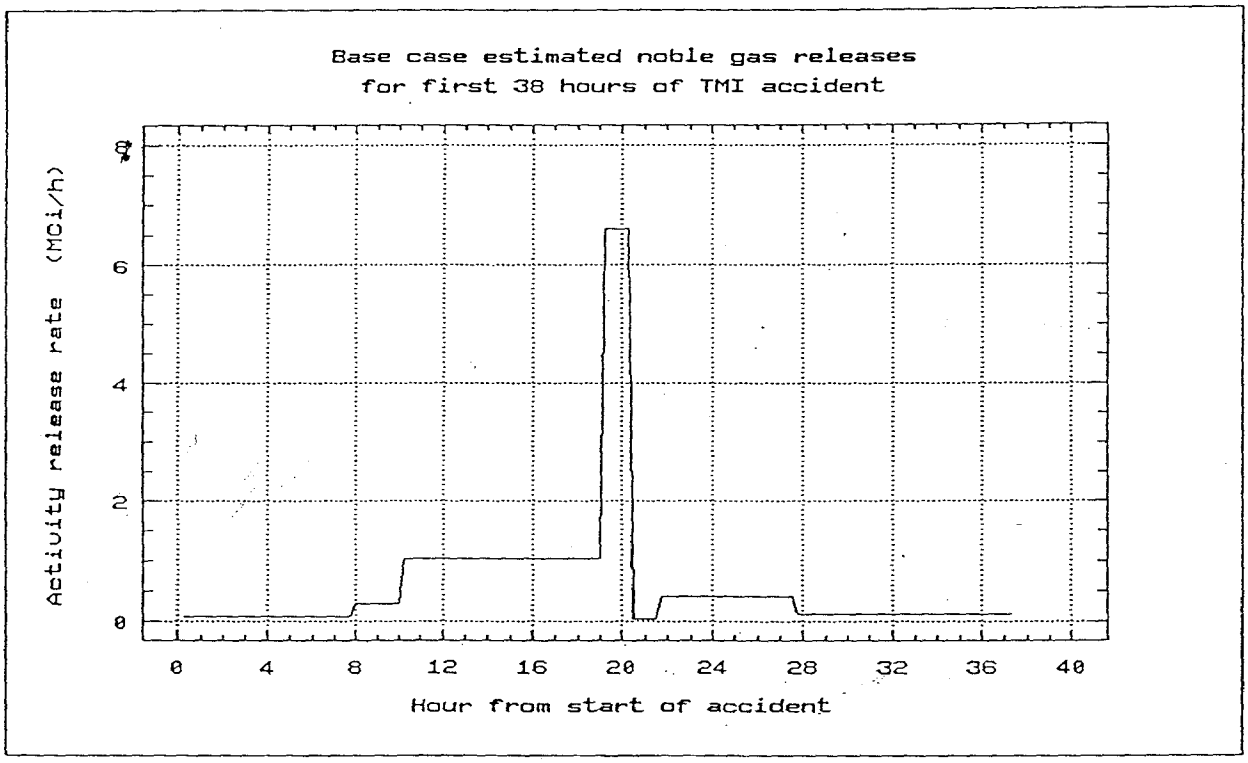

Figure 5. Noble gas release rate estimated by fit to TLD data. First 38 hours of accident, base case model assumptions.

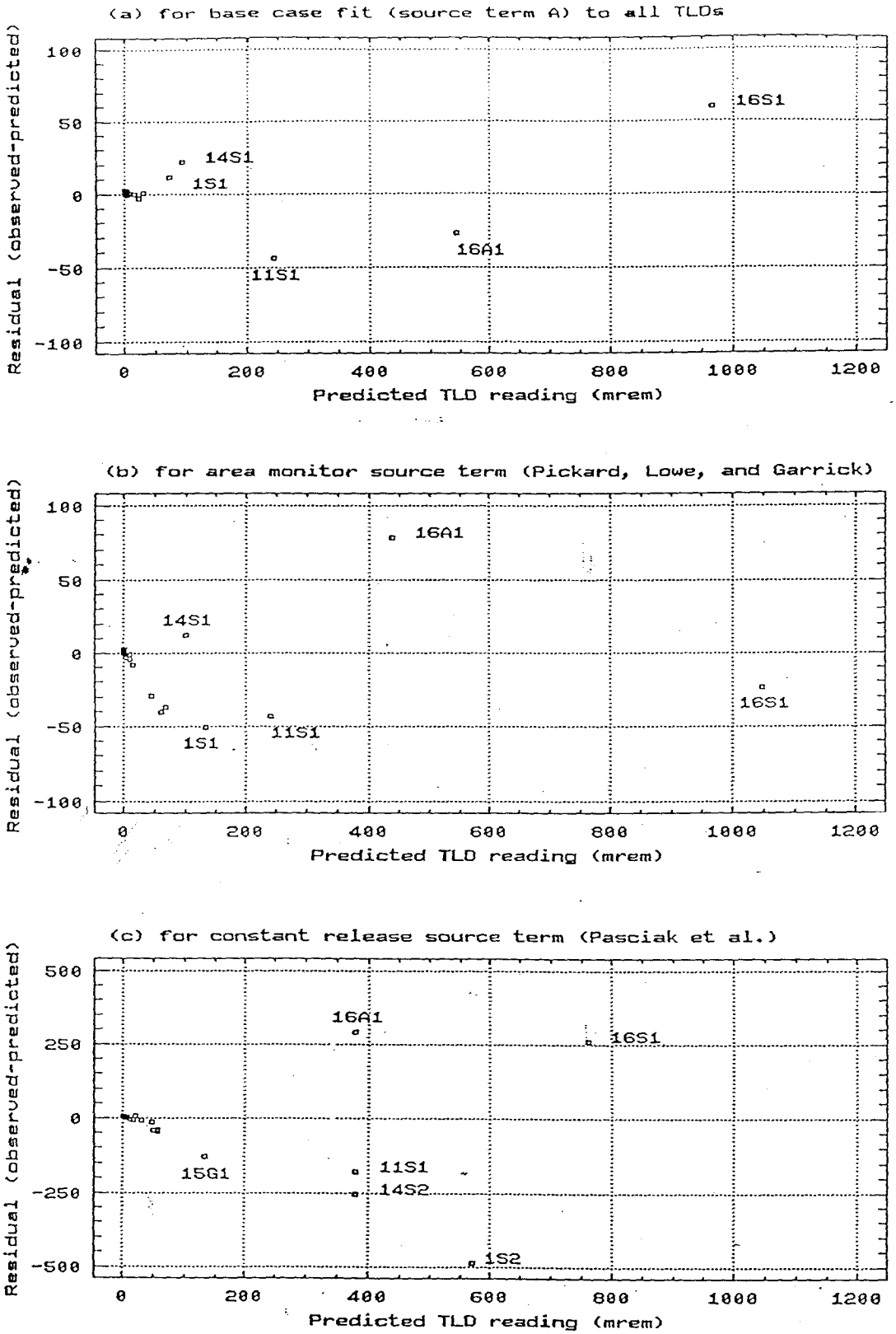

Figure 6. Residual errors in TLD doses predicted by source terms
(a) for base case fit to all TLDs
(b) for area monitor source term of Pickard, Lowe, and Garrick
(c) for constant release rate as used by Pasciak *et al.*

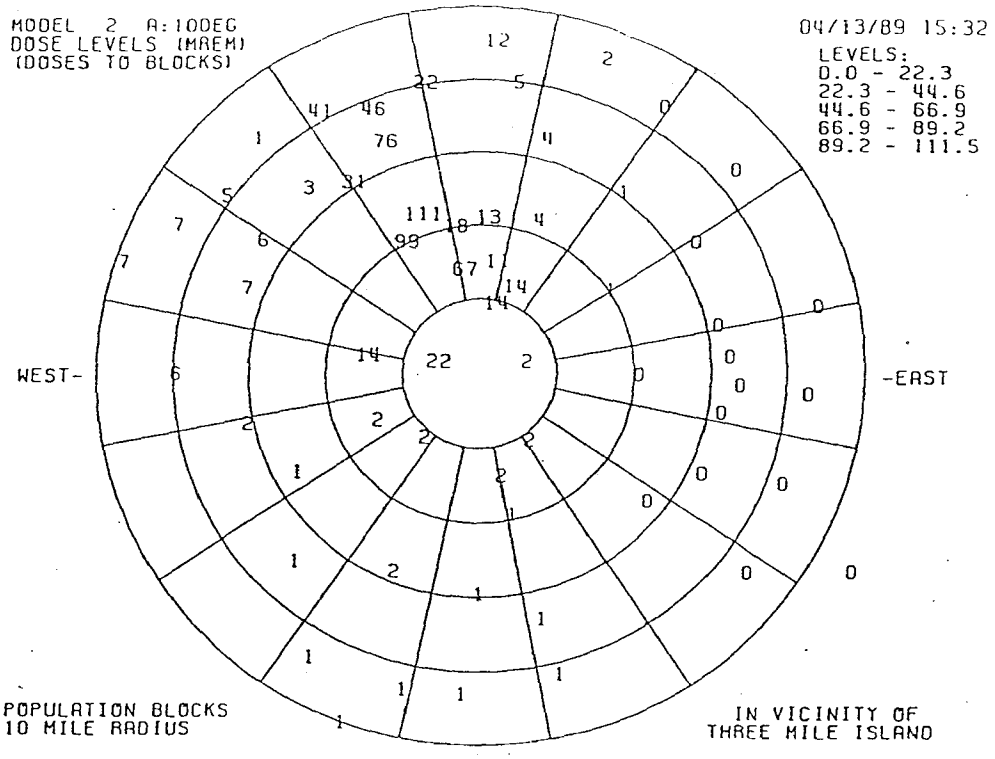

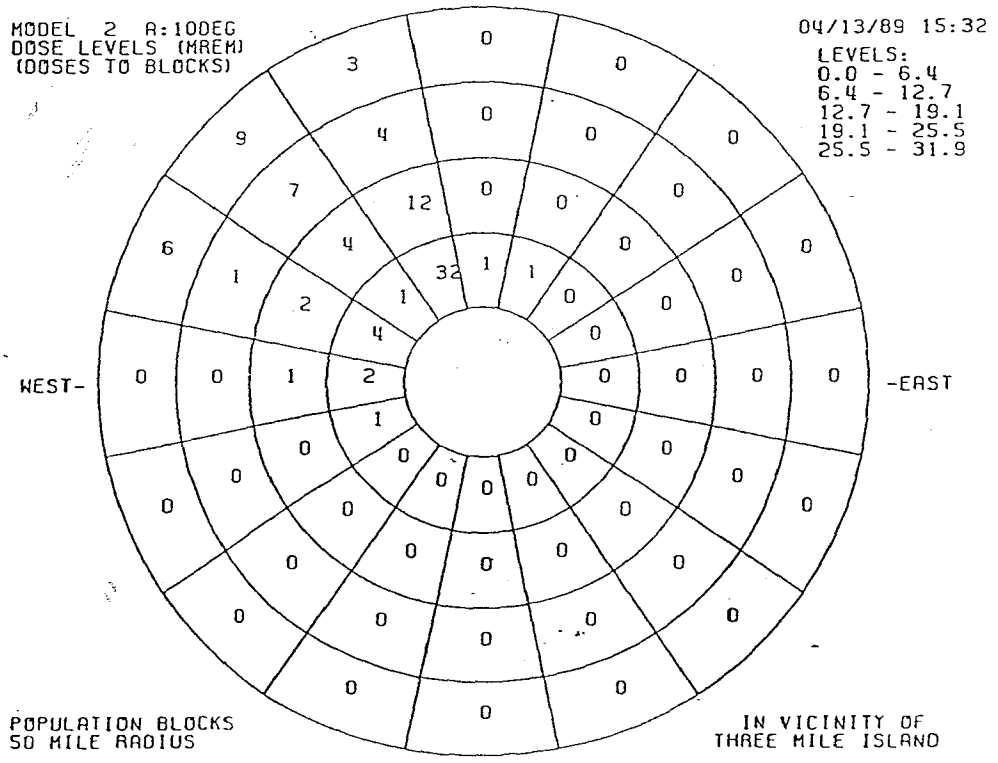

Figure 7. Estimated gamma doses (mrem) to populated blocks
(a) within a 10 mile radius of TMI
(b) from 10 to 50 miles from TMI.

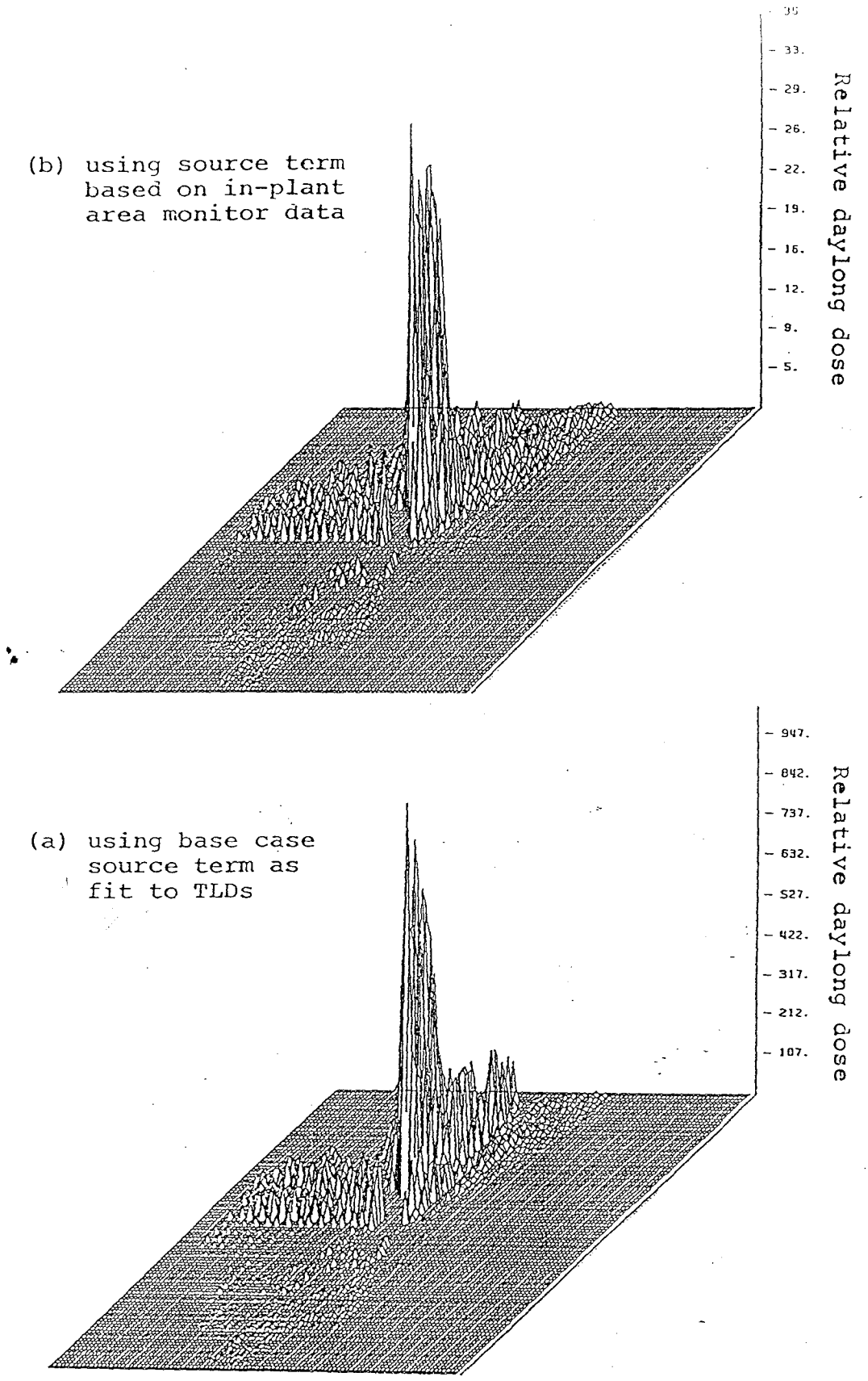

Figure 8. Elevation plots of gamma doses in the vicinity of Three Mile Island. (view from SE to NW)

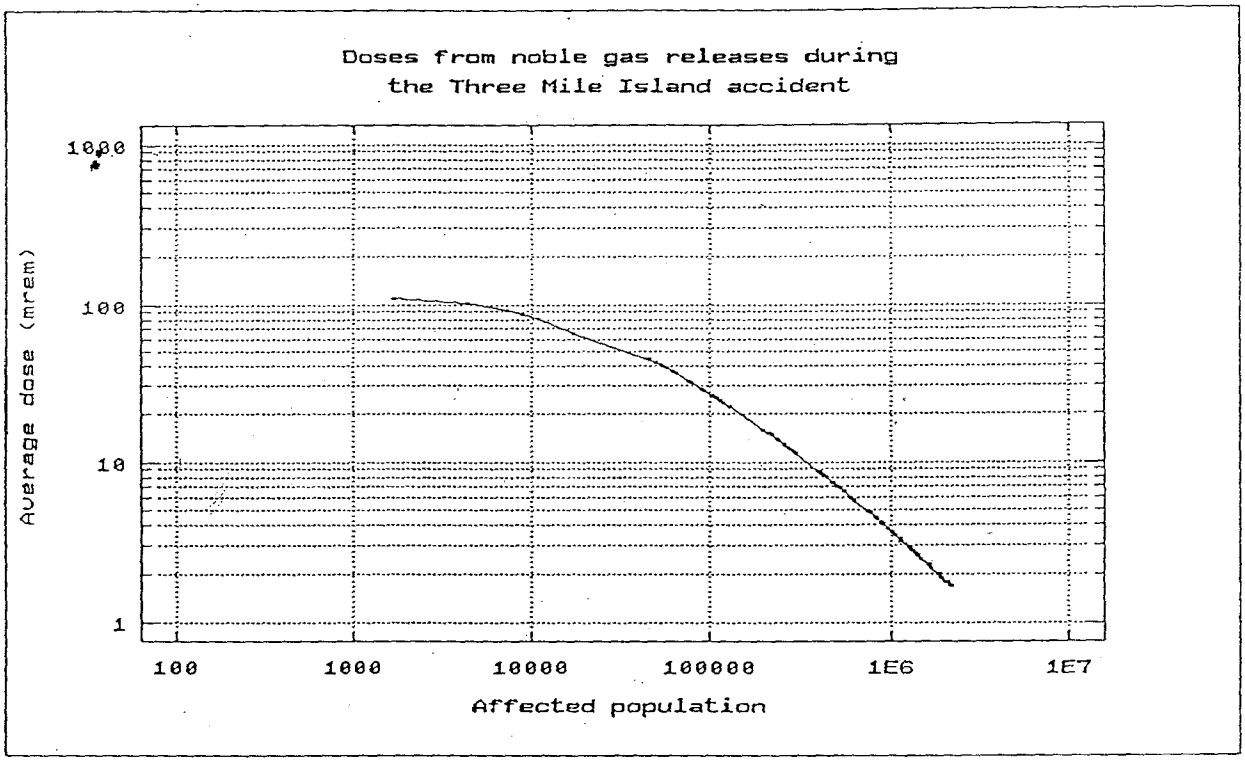

Figure 9. Cumulative distribution of doses by population
Base case assumptions, from releases during first 38 hours.

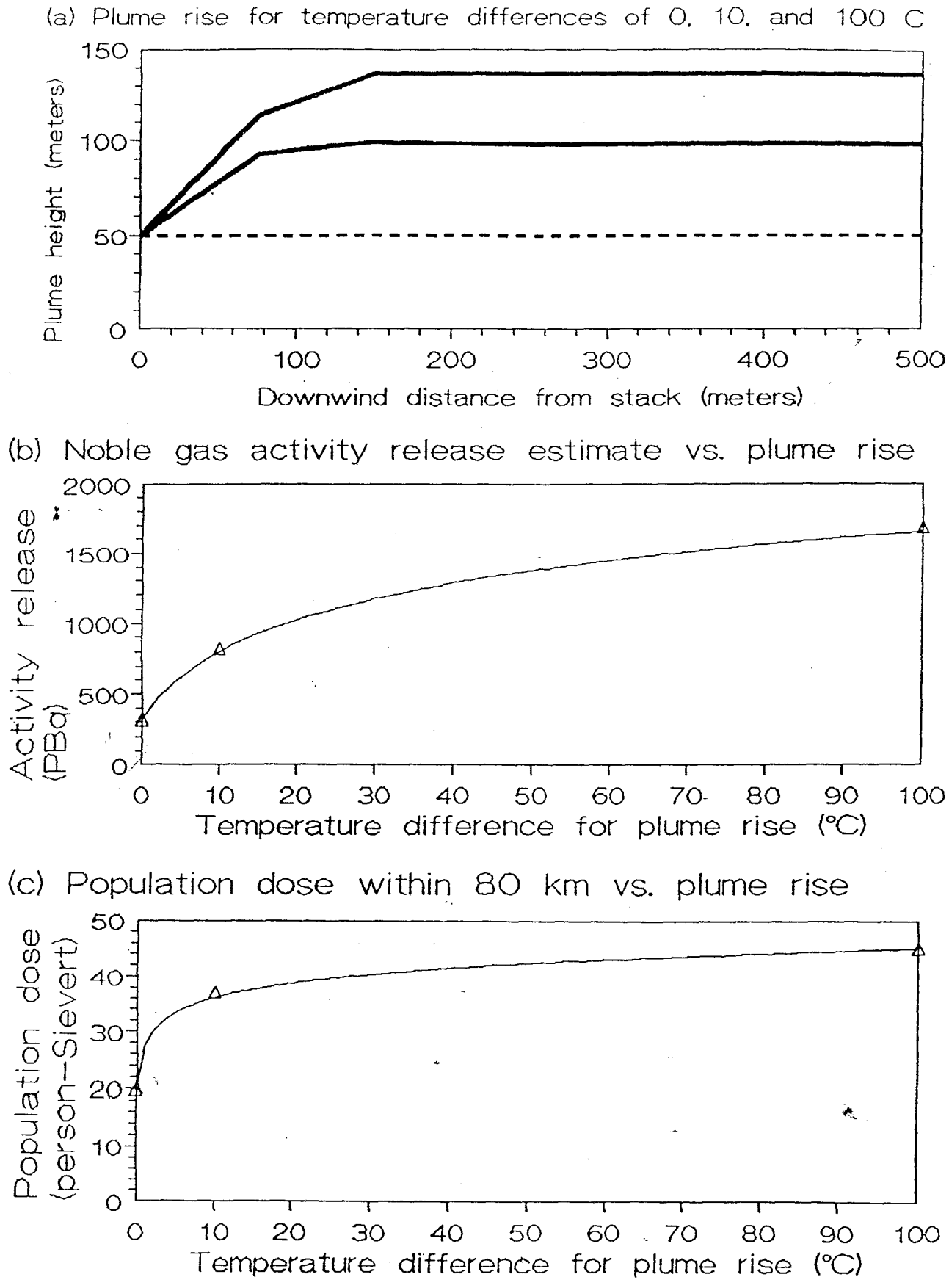

Figure 10. Effect of plume buoyancy temperature difference on plume rise, estimated activity release, and estimated population dose.

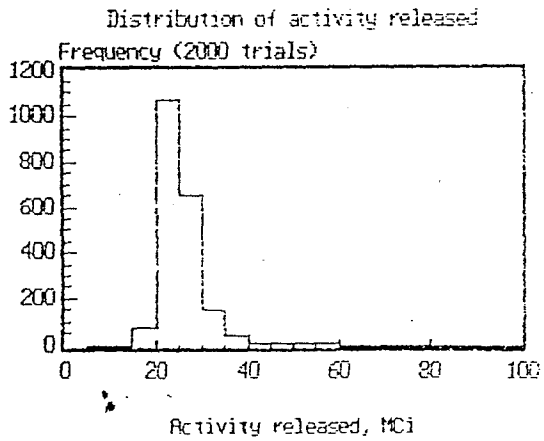

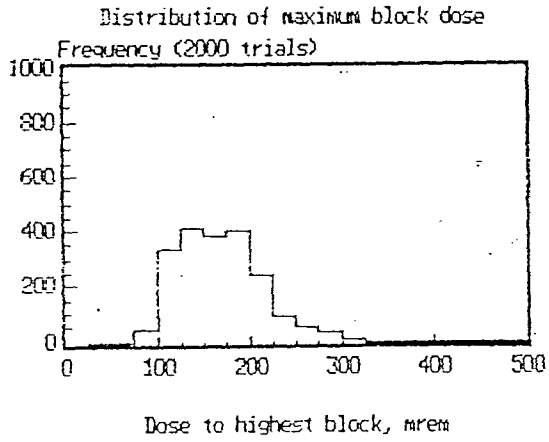

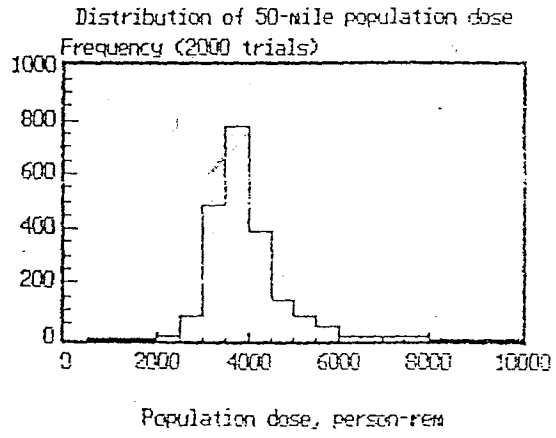

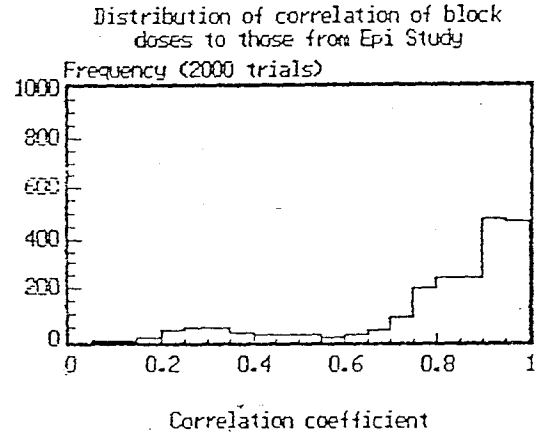

Figure 11. Distributions of parameters estimated by Bayesian analysis
(a) noble gas activity released during first 38 hours
(b) population dose within 50 miles of TMI
(c) dose to block having highest exposure
(d) correlation of dose pattern to dose pattern used in TMI epidemiology study.

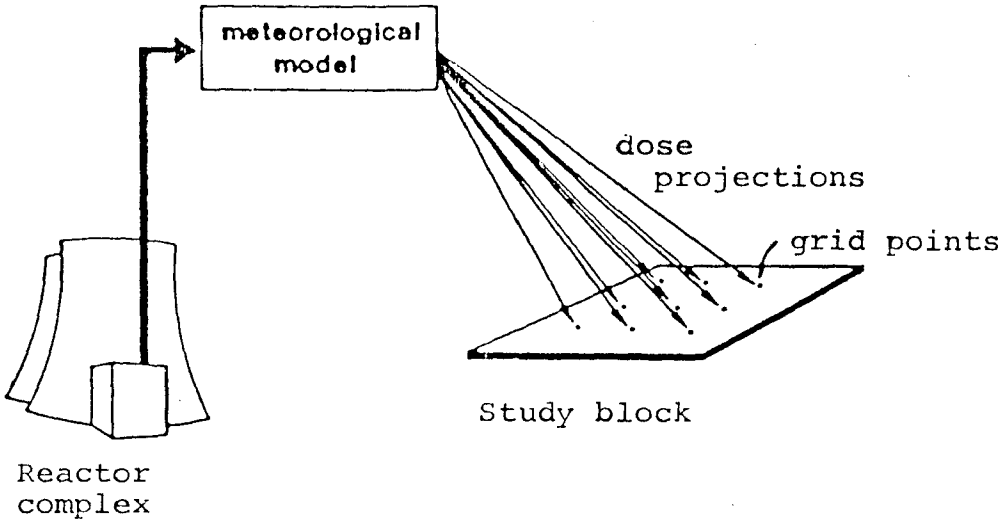

Figure A-1. Schematic of model for projecting doses from airborne radioactive plumes released from a reactor site.

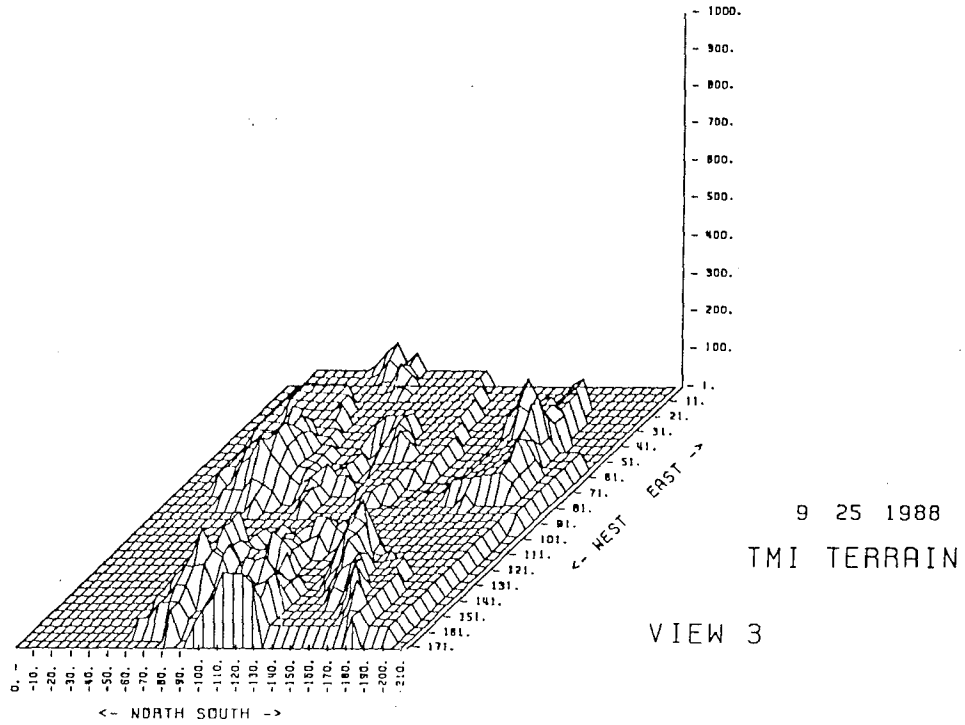

Figure A-2. Terrain elevations in the vicinity of Three Mile Island. Terrain features below stack elevation are omitted.

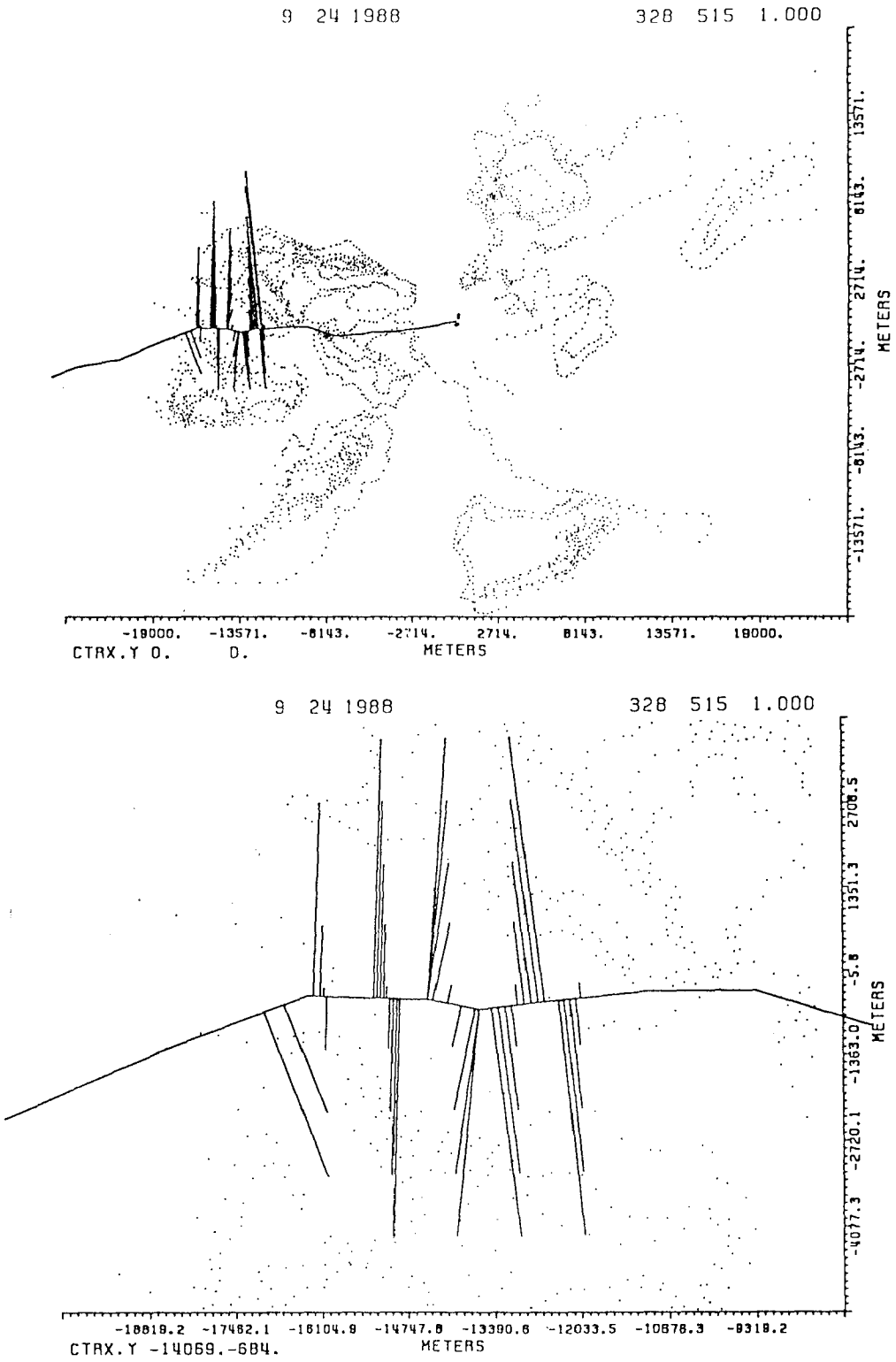

Figure A-3. Calculation of doses to receptors from a passing puff.

Path of plume is represented by the main horizonatally running line. The end points of branches from the line are receptor locations. The dots are points on the terrain contours. Part (b) is a close-up view of (a). Numbers in upper right-hand corner are the date and time the puff was released.

Figure A-4.

Moving puff of radioactivity. The dark concentric circles represent the cooling towers. The lower center line shows an expanding puff of material at different time-intervals. The numbers refer to locations of TLD detectors.

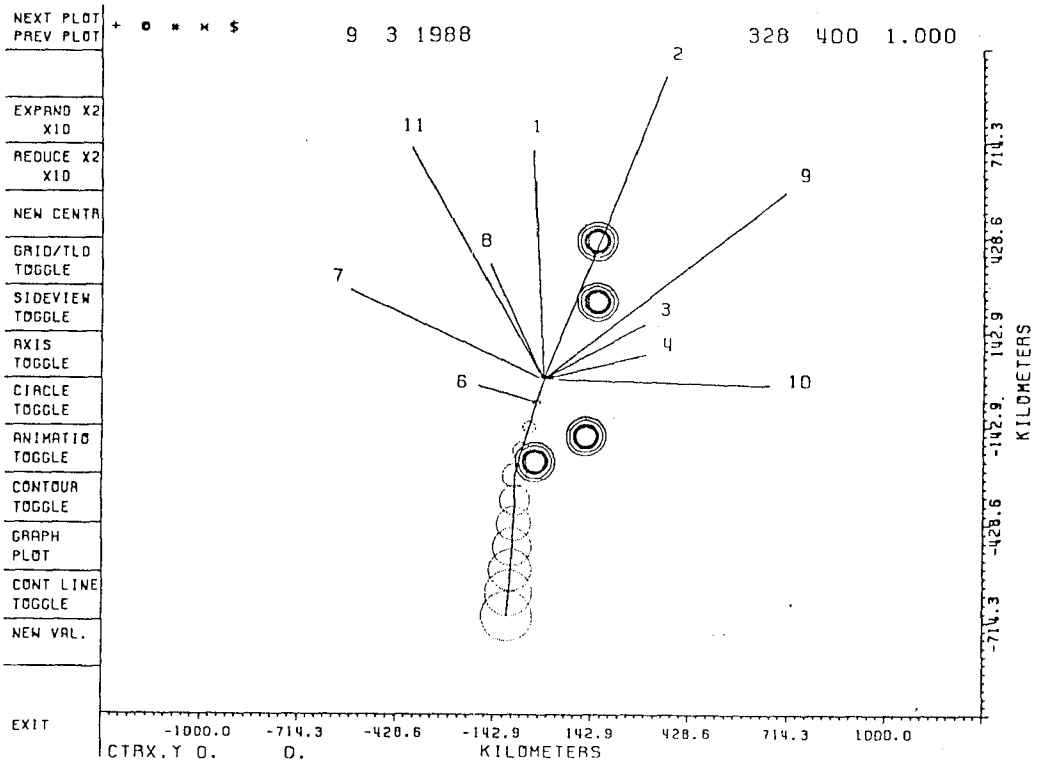

(b) Expanded version of (a) showing terrain contours as well.

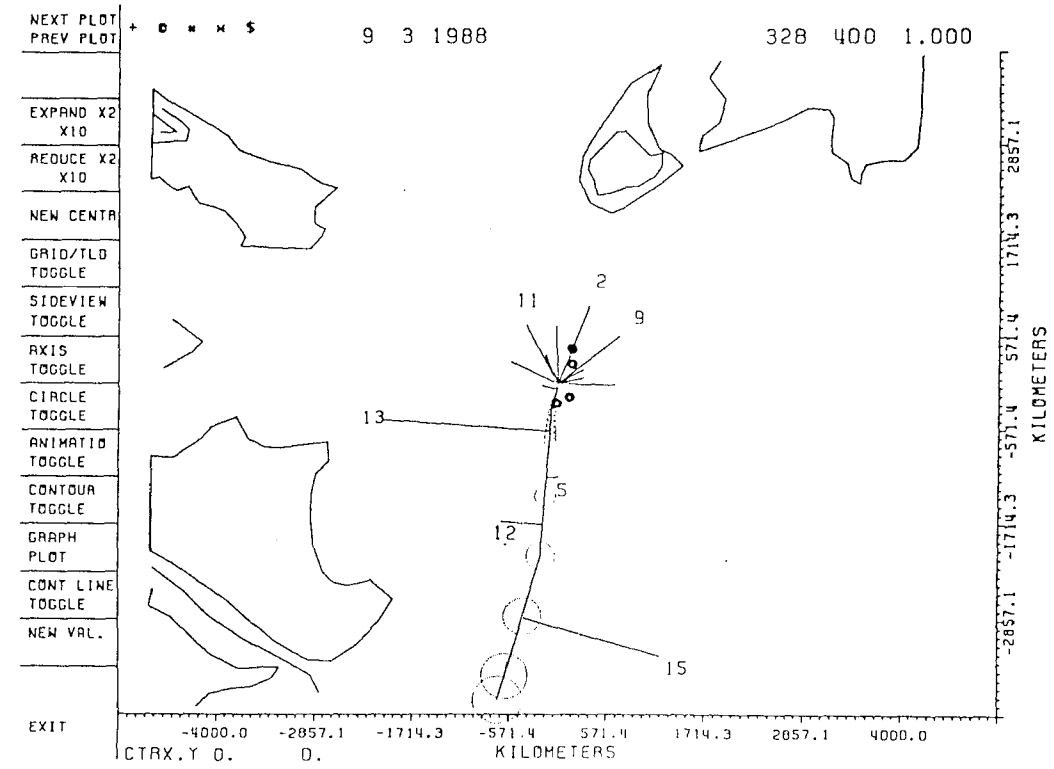

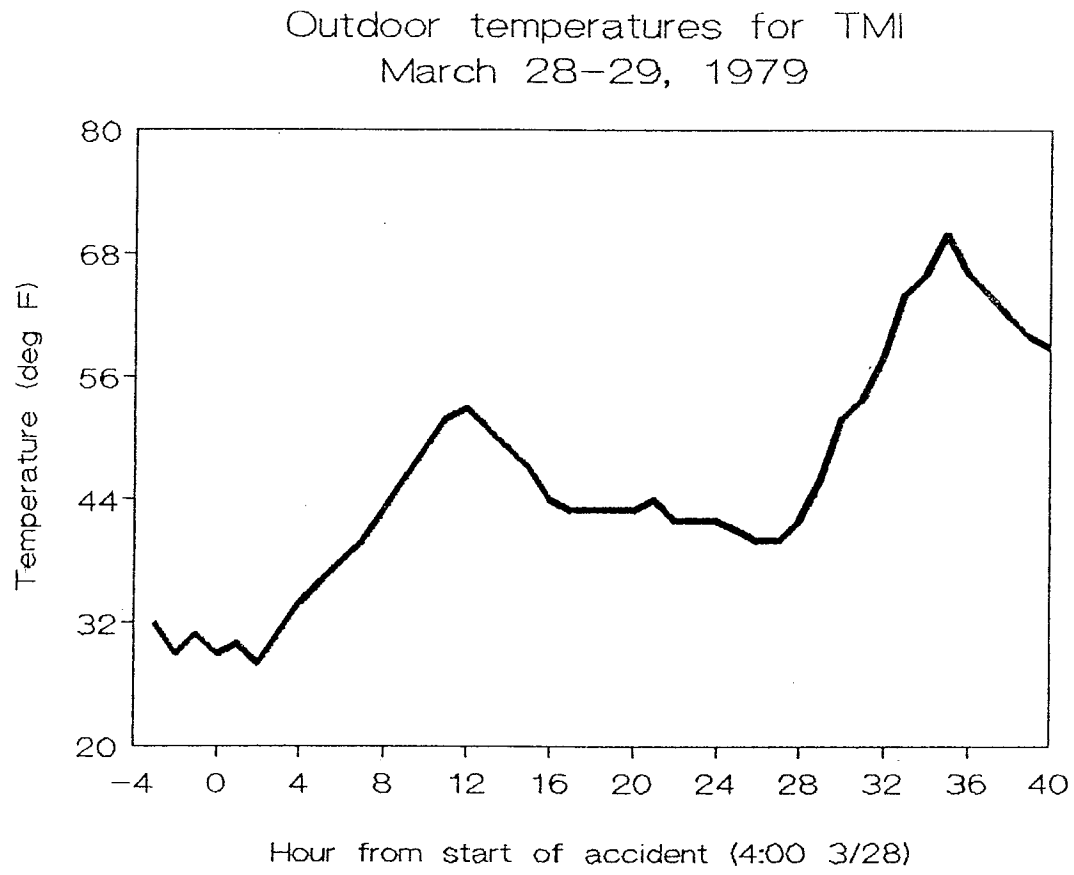

Figure A-5. Outdoor temperatures at Three Mile Island, 28-29 March 1979, based on National Weather Service data for Harrisburg, PA.

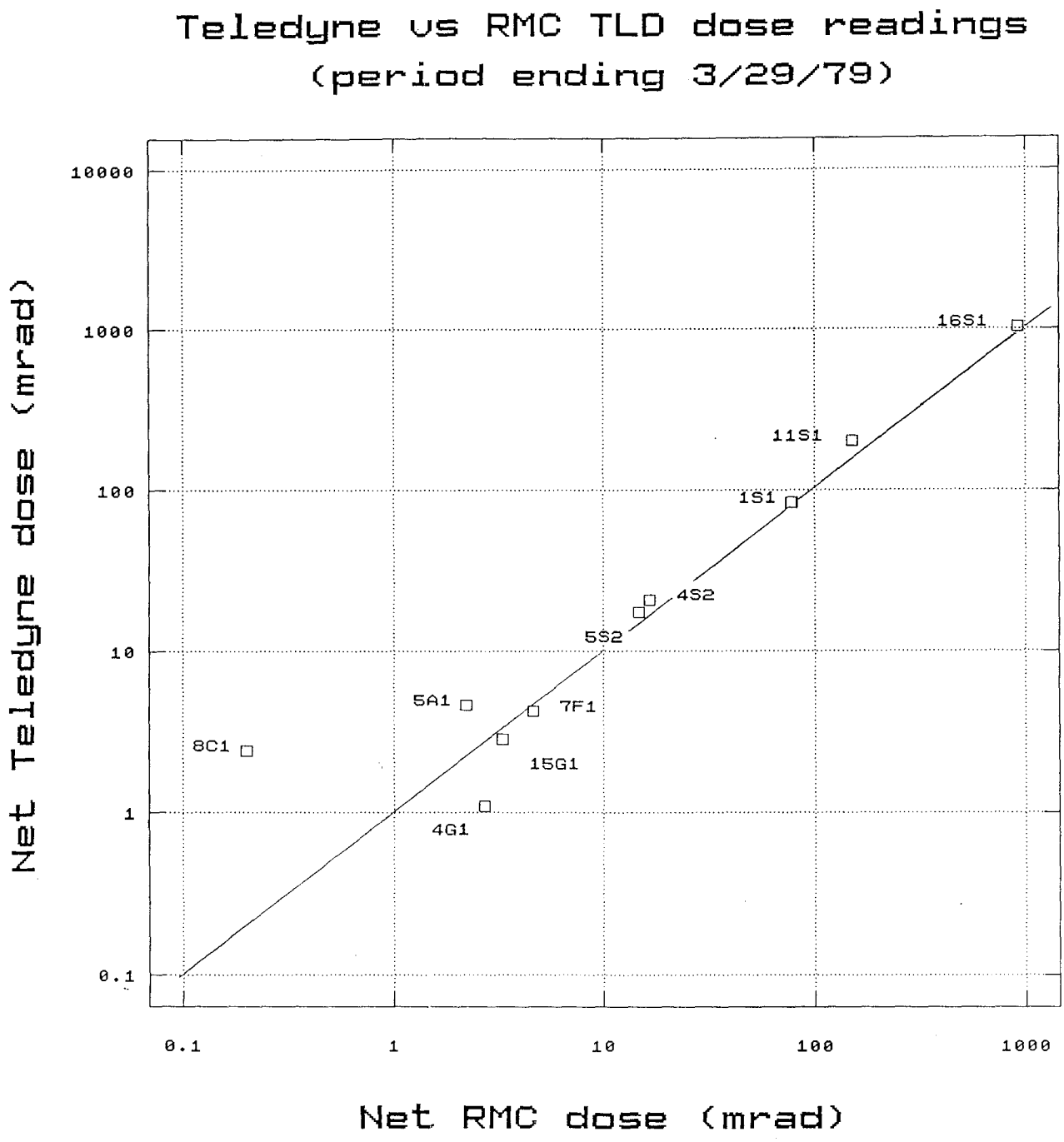

Figure B-1. Teledyne versus RMC dosimeter readings

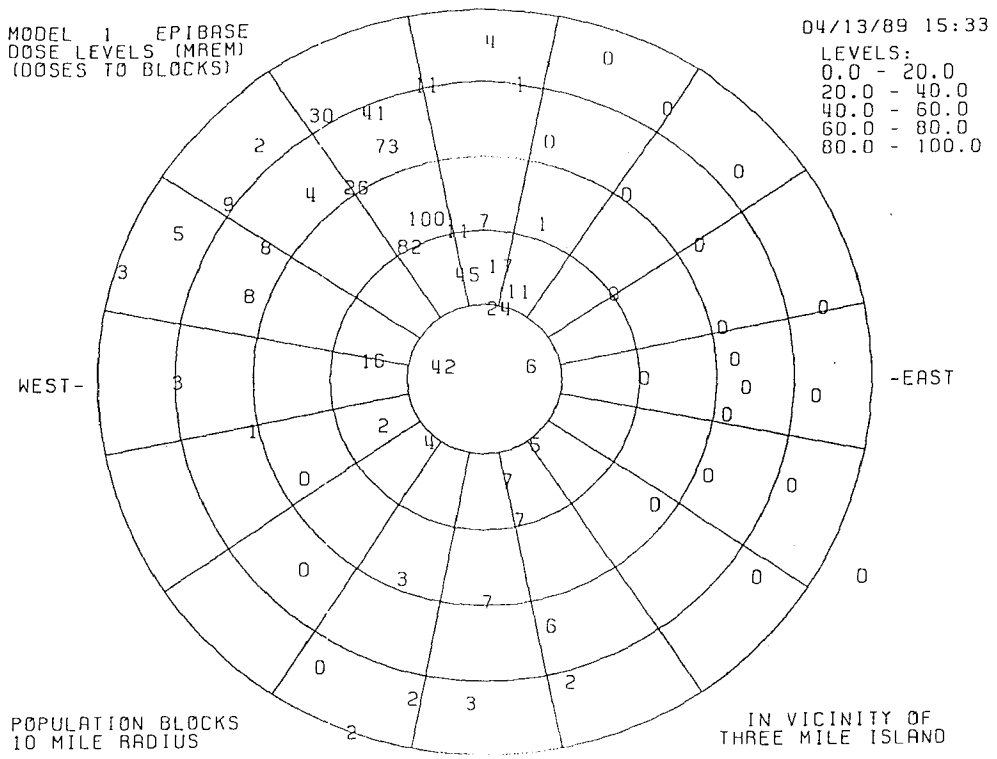

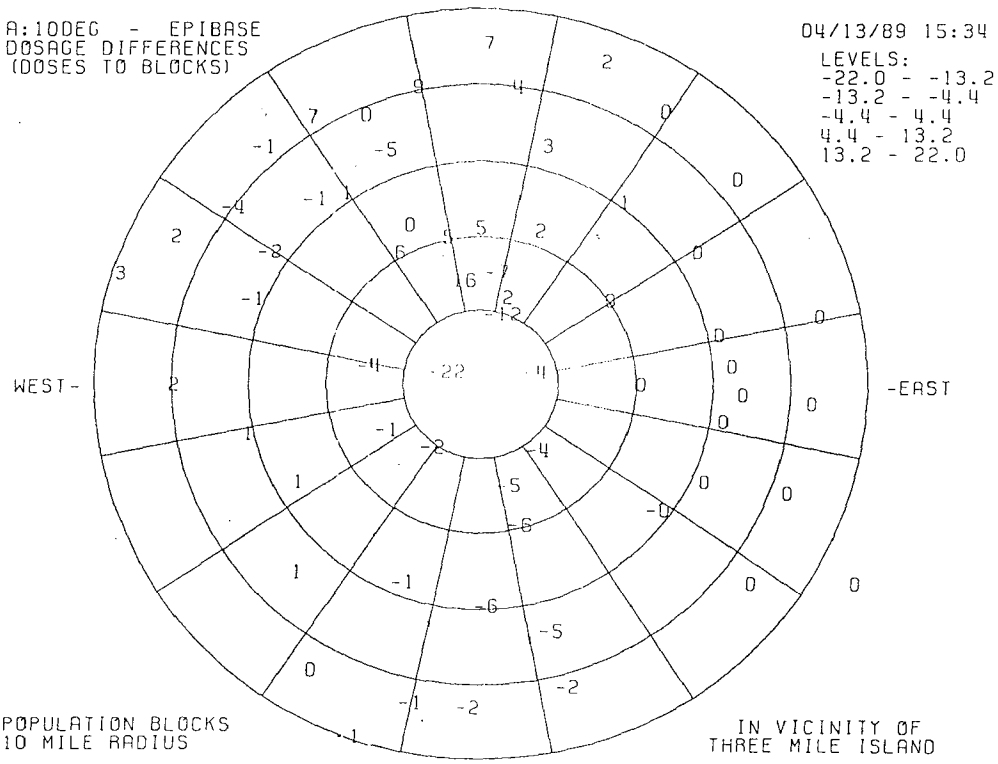

Figure C-1. Dose pattern comparisons with the TMI epidemiology study
(a) block doses using TMI epidemiology study model
(b) relative differences between base case model doses and (a)

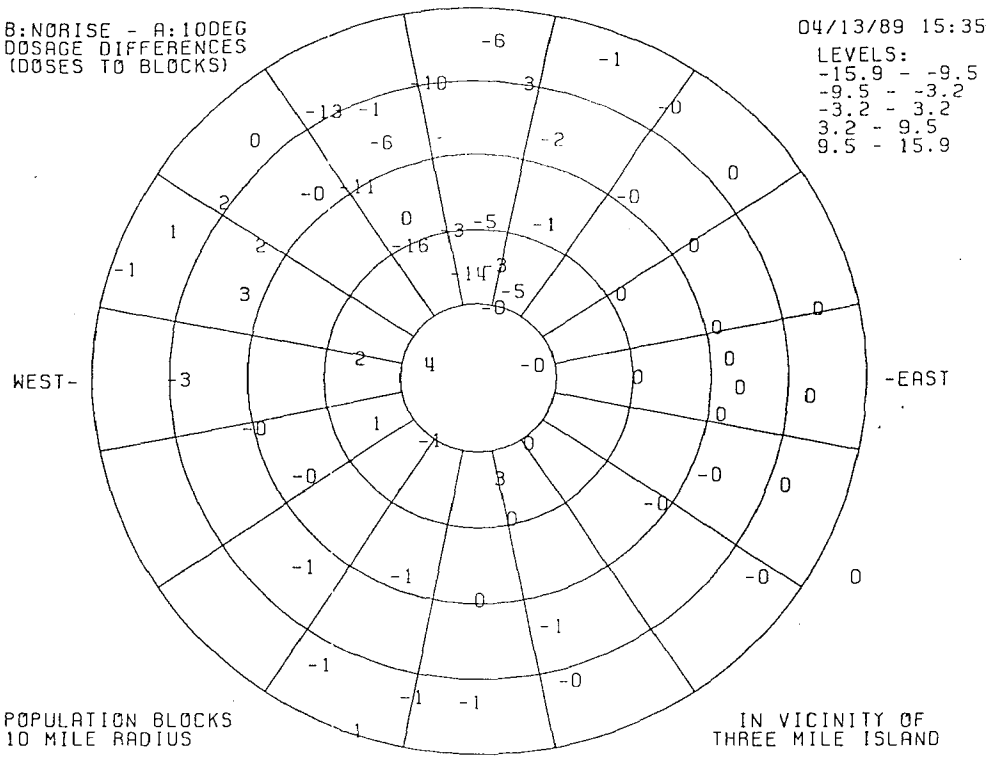

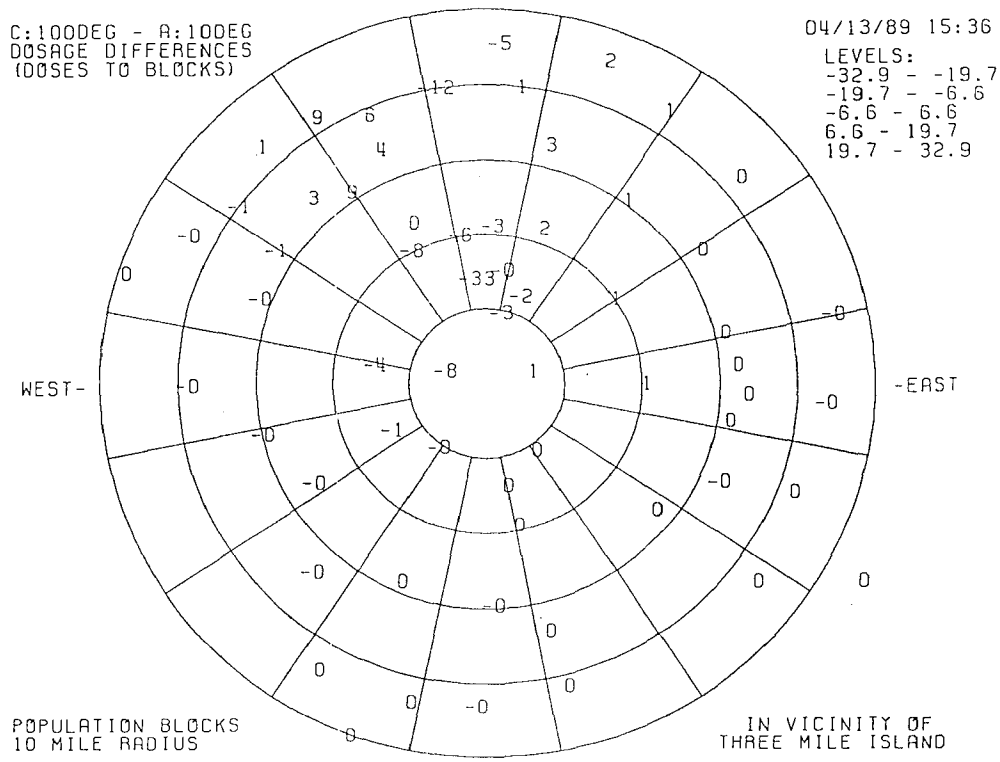

Figure C-2. Dose pattern differences for bounding cases of plume rise relative to base case model (10°C thermal buoyancy)
(a) no plume rise
(b) high plume rise (100°C thermal buoyancy).

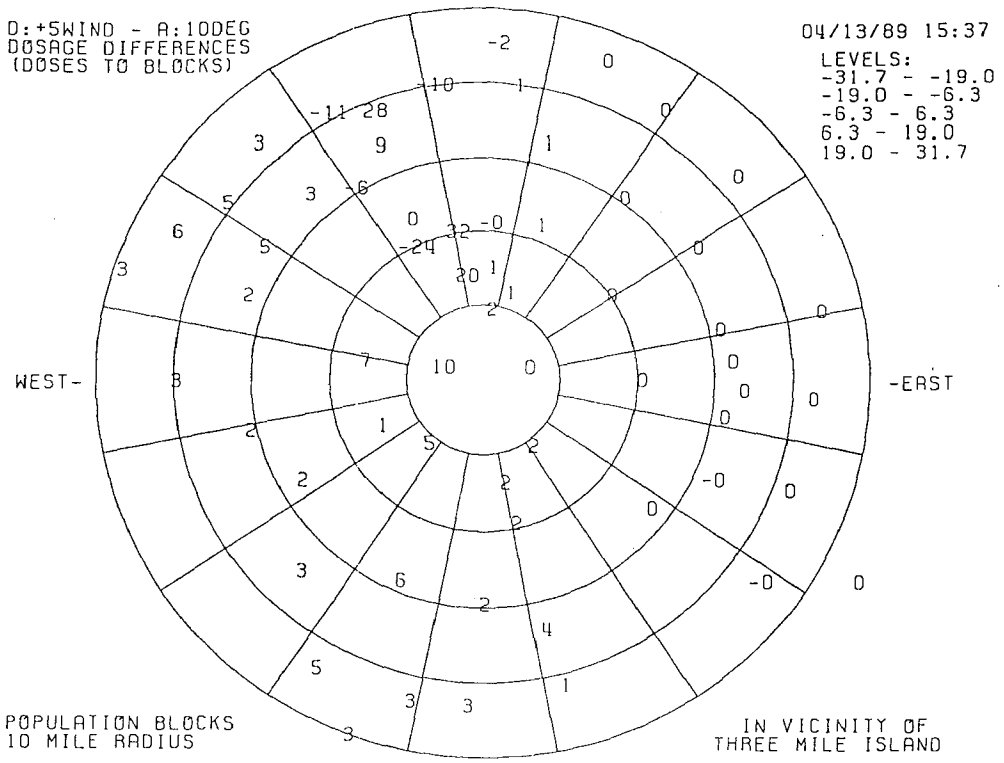

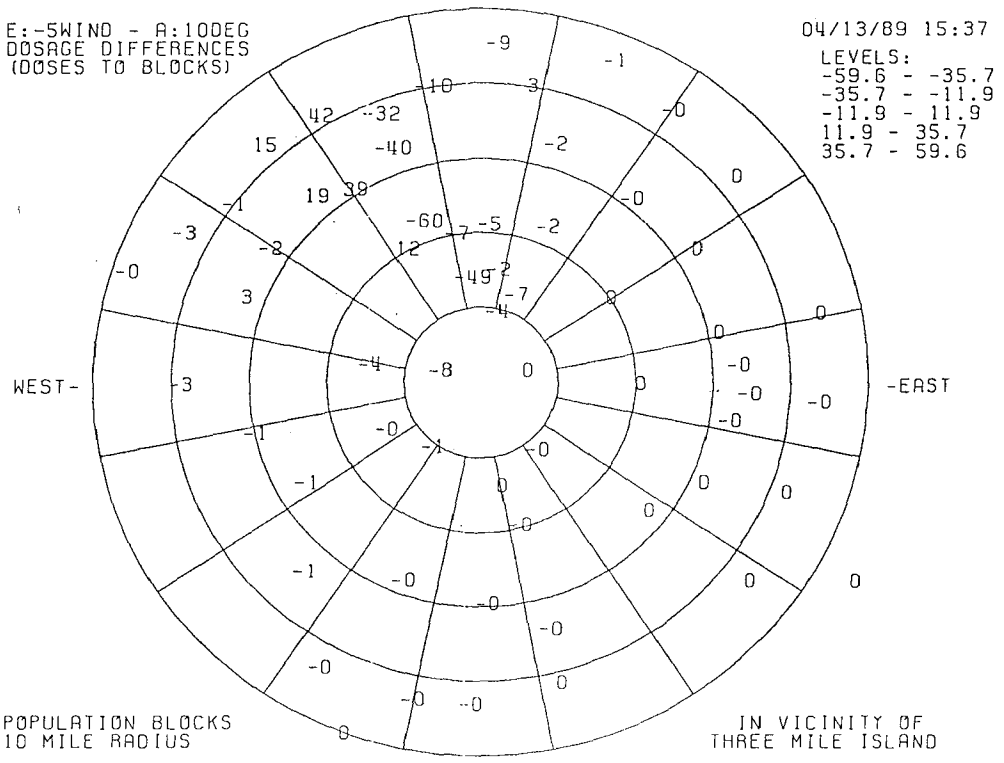

Figure C-3. Dose pattern differences for biases in wind direction
(a) winds shifted +5° from nominal direction
(b) winds shifted -5° from nominal direction.

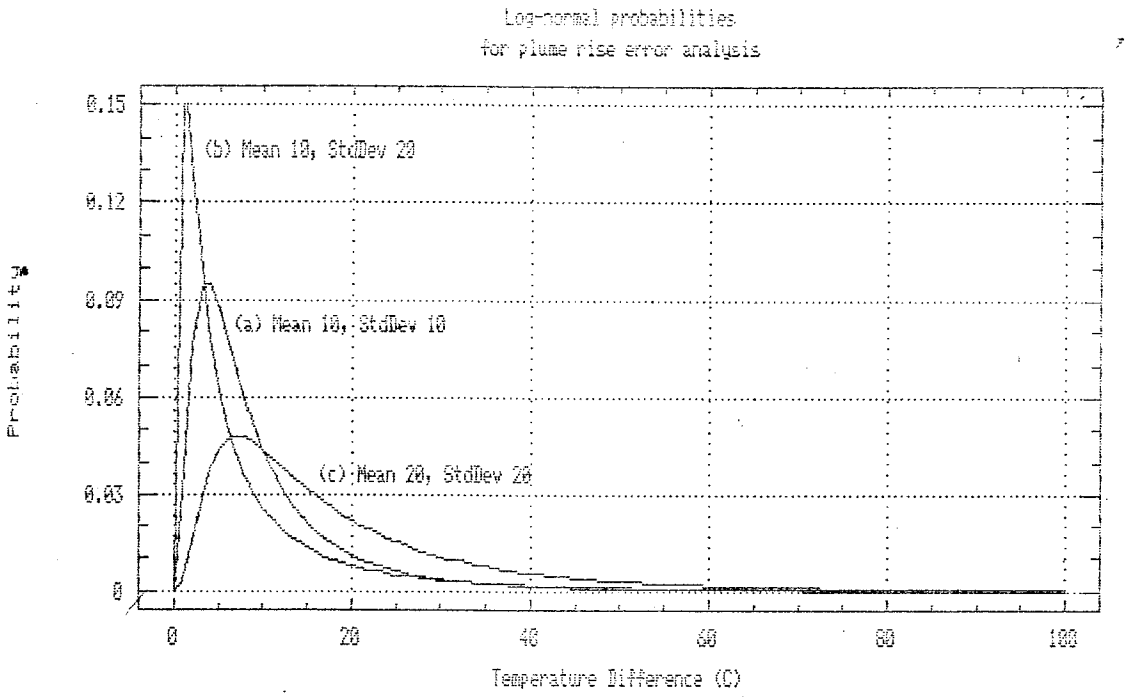

Temperature differences (°C) corresponding to some selected probability levels for the three log-normal distributions

Case	Log-normal distribution parameters: Mean	Std.Dev.	Cumulative probability (P) that the temperature difference is less than or equal to the tabulated value: P=0.05	P=0.16	P=0.50	P=0.68
(a)	10	10	1.8	3.1	7.1	10.4
(b)	10	20	0.6	1.3	4.5	8.1
(c)	20	20	3.6	6.2	14.1	20.9

Figure E-1. Temperature distributions for error analysis of plume rise, with means and standard deviations as indicated.